DANMARKS OG GRØNLANDS GEOLOGISKE UNDERSØGELSE **RAPPORT 2020/35**

Capture, Storage and Use of CO_2 (CCUS)

Depth conversion of seal and reservoir maps from the Havnsø and Hanstholm areas (Part of Work package 5 in the CCUS project)

Anders Mathiesen, Shahjahan Laghari & Rasmus Rasmussen

GEOLOGICAL SURVEY OF DENMARK AND GREENLAND
DANISH MINISTRY OF CLIMATE, ENERGY AND UTILITIES

GEUS

Capture, Storage and Use of CO_2 (CCUS)

Depth conversion of seal and reservoir maps from the Havnsø and Hanstholm areas (Part of Work package 5 in the CCUS project)

Anders Mathiesen, Shahjahan Laghari & Rasmus Rasmussen

GEOLOGICAL SURVEY OF DENMARK AND GREENLAND
DANISH MINISTRY OF CLIMATE, ENERGY AND UTILITIES

G E U S

Preface

Late 2019, GEUS was asked to lead research initiatives in 2020 related to technical barriers for Carbon Capture, Storage and Usage (CCUS) in Denmark and to contribute to establishment of a technical basis for opportunities for CCUS in Denmark. The task encompasses (1) the technical potential for the development of cost-effective CO_2 capture technologies, (2) the potentials for both temporary and permanent storage of CO_2 in the Danish subsurface, (3) mapping of transport options between point sources and usage locations or storage sites, and (4) the CO_2 usage potentials, including business case for converting CO_2 to synthetic fuel production (PtX). The overall aim of the research is to contribute to the establishment of a Danish CCUS research centre and the basis for 1–2 large-scale demonstration plants in Denmark.

The present report forms part of Work Package 5 (Validation of storage complexes) and focuses on conversion of seismic time-structure and time-isochore maps from the Havnsø and Hanstholm areas into depths and thickness maps.

Content

Preface **2**

Dansk Sammendrag **4**

Summary **6**

1. Introduction to depth conversion methods **8**

1.1 Sources of velocity information 9
1.2 Choice of a depth conversion method....14

2. Database and previous depth conversion in Denmark **15**

3. Depth conversion in the Havnsø and Hanstholm areas **17**

3.1 Depth conversion of maps from the Havnsø and Hanstholm area....22
3.2 Assessment of depth uncertainty 23

4. Suggestions for supplementary investigations and research **25**

References **27**

Tables and Figures **29**

Appendix 1 Time-depth relations **45**

TDR: Stenlille-2....49
TDR: Stenlille-10....50
TDR: Stenlille-12....51
TDR: Stenlille-13....52
TDR: Stenlille-15....53
TDR: Stenlille-18....54
TDR: Stenlille-19....55
TDR: Thisted-1 56
TDR: Thisted-2 57
TDR: Thisted-3 58
TDR: Thisted-4 59

Appendix 2 Time maps (ms TWT) **60**

Dansk Sammendrag

For at opfylde de globale mål om at begrænse CO_2-udledningen til atmosfæren er interessen for geologisk lagring og udnyttelse af CO_2 i Danmark vokset. Herunder også for Hanstholm- og Havnsø-strukturerne som kunne blive potentielle steder til CO_2-lagring.

En nøjagtig afgrænsning af potentielle CO_2-lagringsstrukturer i den danske undergrund er fortsat et komplekst problem. Begrænsninger i den eksisterende database såsom begrænset seismisk dækning, lav seismisk opløsning, misforhold mellem krydsende seismiske linjer, mangelfuld borehuls- eller brøndinformation (wireline logs, kernedata) osv. betyder at der er stor usikkerhed forbundet med geofysiske og geologiske tolkninger af strukturerne i den danske undergrund. Høj-opløselige seismiske data sammen med gode wireline-log-information langs de eksisterende brønde spiller en vigtig rolle for fremtidige CCUS-projekter til brug for CO_2-opsamling og -lagring.

Dybdekonvertering af geofysiske og geologiske modeller tolket i tidsdomænet er blandt de mest kritiske faser i ethvert geologisk modelleringsprojekt. Det er kun gennem dybdekonvertering, vi kan bekræfte eksistensen af de overordnede geometriske rammer og derved bekræfte den rumlige fordeling af segl og reservoir. Den geometriske ramme udgør sammen med den geologiske model et væsentligt input til reservoirmodellen, som kan bruges til dynamisk at simulere ændringer i reservoiret.

Seismiske reflektionsdata registrerer tovejs rejsetid (TWT) fra overflade til en eller flere undergrundsgrænseflader. Dybdekonvertering er den proces, hvor tolkede seismiske horisonter på seismiske tværsnit i tidsdomænet konverteres til dybdeenheder (fra TWT i millisekunder til dybde i meter). Flader, horisonter, forkastninger, seismiske punktdata osv. tolket i tidsdomæne kræver at der kan opstilles den bedst mulige hastighedsfunktion til dybdekonvertering. Dette opnås ved hjælp af et grundlæggende empirisk forhold, som overfører data i tid til data i dybde via Dybde = Hastighed * Tid, hvor hastighederne som udgangspunkt kendes fra brønddata. Konfidencen af en dybdekonvertering aftager derfor væk fra brøndene, hvorfor dybdekonverteringen skal integreres med seismiske hastigheder fra seismiske sektioner og geologiske modeller.

Hastigheden for den seismisk bølge er en geofysisk egenskab for en given bjergart og afhænger af bjergartens hårdhed. Bestemmelse af bjergartens hårdhed er et komplekst problem, som afhænger af en række faktorer såsom bjergartens sammensætning, porøsitet og mikrofrakturer, kemisk sammensætning af matrix osv. Generelt er den seismiske bølgehastighed lave i havvand (~1500 m/s) men øges med dybden efterhånden som bjergarten bliver mere kompakteret og tættere og dermed kan opnå hastigheder på 4000 op til 5000 m/s. Dette er imidlertid ikke altid tilfældet, da hastighedsvariationer også kan variere som følge af lokale geologiske forskelle i lithologi, tektonisk udviklingshistorie m.m.

Denne rapport fokuserer på dybdekonvertering af segl (Fjerritslev Formationen, primært sammensat af skifer) og reservoiret (Gassum Formationen, primært sammensat af meget porøse og gennemtrængelige sandsten) omkring Hanstholm og Havnsø strukturerne.

Dybdekonvertering af disse enheder kan opnås dels ud fra polynomiske og lineære regressionsmetoder eller ved brug af V0_k-metoder, som begge har fordele og ulemper.

Foreløbige analyser viser, at ved lave dybder (under 1000–1500 m) kan både polynomiemetoder og V0_k-metoder anvendes til dybdekonvertering, hvis der findes brønddata tæt på de to strukturer. Ved større dybde under Kridtgruppen og hvor geologien bliver mere kompleks og hastighederne mere variable, bliver V0_k-metoden mere pålidelig og vil kunne reducere usikkerheden på den konverterede dybde.

Studiet viser, at der nu er et bedre grundlag for at kunne opstille et workflow, som integrer hastigheder fra brønde og seismiske data og som er styret af de mulige geologiske aflejringsmodeller. Man må imidlertid acceptere, at man på baggrund af de nuværende data og viden ikke vil kunne fastlægge Havnsø og Hanstholm strukturernes præcise udbredelse (f.eks. dybden til strukturens toppunkt og saddelpunkt), men må acceptere at der kan opstilles udfaldsrum af flere mulige dybdekonverterede scenarier. Dette understreger behovet for, at der skal indsamles nye data.

Der er derfor angivet en række anbefalinger som kan forbedre den eksisterende dybdekonvertering og styrke sikkerheden. For at opnå de mest sikre modeller for områderne omkring Hanstholm og Havnsø, og dermed den bedst mulige udnyttelse som et fremtidigt lagringskompleks, er det nødvendigt at indsamle nye geofysiske og geologiske data. Høj-opløselige 3D seismiske data suppleret med 2D linjer for at opnå en henholdsvis tættere seismisk dækning og for at etablere forbindelse til de nærmeste brønddata. Især 3D seismiske data kan forbedre den rumlige forståelse af de to strukturer, hvilket også vil kunne føre til en mere detaljeret hastighedskortlægning.

Summary

To meet the global goals of restricting the CO_2 emission into the atmosphere, geological storage and utilisation has gained increased interest in Denmark. The Hanstholm and Havnsø structures have among others been identified as potential CO_2 storage sites and operational success and overall storage security of a CO_2 storage project depends to a large extend on the mobility of CO_2 in the reservoir.

Accurate delineation of prospective CO_2 storage structures in the Danish subsurface remains a complex problem. Data limitations such as low density of seismic coverage, low resolution of seismic data, mis-ties among intersecting seismic lines, missing borehole or well information (wireline logs, core data) etc. brings a lot of uncertainty to the geological and geophysical interpretations of Danish subsurface structures. Thus, high-resolution seismic data followed by good wireline-log information along the existing wells will play a vital role in future CCUS (Carbon capture use and storage) projects.

Depth conversions of geophysical and geological models from time domain are the most critical phases of any geological modelling project. It is only through depth conversion we can confirm the existence of overall geometrical framework and thereby confirm the spatial distribution of seal and the reservoir. The geometric framework together with the geological model serves as an important input for the reservoir model, which can be used to dynamically simulate changes in the reservoir.

Seismic reflection data records the two-way travel time (TWT) from surface to a subsurface interface(s). Depth conversion is the process by which interpreted seismic horizons and seismic cross-sections in time domain are converted to depth units (from TWT in milliseconds to depth in meters). Surfaces, horizons, fault interpretations, seismic data, points etc. in time domain require the best possible velocity function for depth conversion. This is achieved by using a fundamental empirical relationship which provides a bridge between time and depth:

$$\mathrm{Depth\ (s)} = \mathrm{Velocity\ (v)} * \mathrm{Time\ (t)}$$

where the velocities are primary are known from well data. The confidence of a depth conversion therefore decreases away from the wells, why that the depth conversion should be integrated with seismic velocities from seismic sections and geological models.

Velocity of seismic wave is an intrinsic geophysical property of a rock and depends on the hardness of the rock. Determination of hardness of a rock is a complex problem as it depends on number of factors such as chemical composition of rock, percentage of pores and microfractures, chemical composition of matrix etc. Generally, for a marine setting, compressional seismic wave speed is slowest in seawater (~1500 m/s) and increases as the seismic wave enters denser compacted sediments or metamorphic rocks reaching velocities from 4000 up to 5000 m/s. However, this is not always the case, as velocity variations can also vary due to local geological differences in lithology, tectonic history etc.

This report focuses on the depth conversion of the seal (the Fjerritslev Formation, primarily composed of shales) and the reservoir (the Gassum Formation, composed of highly porous and permeable sandstones) around the Hanstholm and Havnsø structures. Depth conversion of these units can be achieved through polynomial and linear regression methods or the V0_k velocity estimation method. Both methods have their own advantages and limitations, which are discussed in the report.

Preliminary analyses reveal that for shallow depths (below 1000-1500 m), both the polynomial and the V0_k methods can be used for depth conversion, if wells exist close to the two structures. At greater depth below the Chalk Group and where the geology becomes more complex and velocities more variable, the V0_k method becomes the more reliable method and will reduce the uncertainty on the converted depths.

The study shows that there now is a better basis for setting up a workflow that integrates velocities from wells and seismic data and that is guided by the possible geological deposition models. However, we must accept that based on the current data and information, we will not be able to come up with an exact distribution of the Havnsø and Hanstholm structures (e.g. the depth to the structure's apex and saddle point), but must accept that it is only possible come up with a series of possible depth converted scenarios. This underlines the need for new acquired data.

A number of recommendations are given which can improve the existing depth conversion and strengthen the confidence. In order to achieve the most reliable models for the areas around Hanstholm and Havnsø, and thus the best possible utilization as a future storage complex, it is therefore necessary to collect new geophysical and geological data. High-resolution 3D seismic data supplemented with 2D lines to increase seismic density and to connect to the nearest wells is therefore of the highest priority. Especially 3D seismic data can improve the spatial understanding of the two structures, which also can lead to more detailed velocity mapping.

1. Introduction to depth conversion methods

To estimate the storage potential of CO_2 in the Havnsø and Hanstholm structures, three structural and seismic stratigraphic studies has been carried out (Gregersen et al. 2020; Vosgerau et al. 2020 and Rasmussen & Laghari 2020). In both areas seismic data was used to identify and map three seismic time-structure surfaces important for assessing potential CO_2 storage: top Vinding Formation (or Base Gassum), top Gassum and top Fjerritslev. In the Havnsø study area the Base Chalk seismic time-structure surface is also interpreted and mapped. The time-isochore maps between the Top Fjerritslev and the Top Gassum surface defines the Fjerritslev seal of mainly shales and the time-isochore maps between the Top Gassum and the Top Vinding surface defines the Gassum storage reservoir of mainly sandstones. Both these mapping studies also included a seismic facies analysis of the Gassum Formation to strengthen the geological model and to identify possible sedimentary and erosional features within the Gassum reservoir.

Interpretation and mapping of different formations and stratigraphic units in Havnsø and Hanstholm studies aim at defining the size and type of the CO_2 storage reservoir in time domain i.e. Two-Way-Time (TWT) using available seismic dataset composed of reprocessed 2D seismic lines (Rasmussen & Mathiesen 2020), vintage 2D seismic sections. and Stenlille 3D data. A rock physics study of 3D Stenlille seismic survey, evaluates the rock physics and seismic properties of the Gassum Formation using the Stenlille aquifer gas storage as a reservoir analogue for the Havnsø CO_2 storage prospect (Bredesen 2020).

Most seismic interpretation is done in the time domain, where stratigraphic interpretation is usually acceptable for seismic facies and sequence stratigraphy analyses and mapping, because the seismic facies remains almost same with changing structures. Structural interpretation is more critical because interpreting structures in the time domain explicit means assuming a constant velocity model, and assuming that all possible velocity aberrations are caught during the interpretation process.

This report focuses on conversion of time-structure and time-isochore maps for both Havnsø and Hanstholm into depth structure and thickness maps. The report also includes an introduction to the methods adopted for depth conversions. The final goal is to provide 3D geological models in depth domain that will serve as an input for reservoir simulations studies. The report also focuses on the limitations of the adopted depth conversion methods based on data limitations and thereby provides a list of recommendations for future geological and geophysical studies related to Carbon Capture Use and Storage (CCUS) studies.

Depth conversion is a way to remove the structural ambiguity inherent in time and verify the existence of structures in the subsurface. Here, potential usable structures for storage must be confirmed to determine the spill point and gross thickness to assess volumetrics for storage calculations, and before planning the first exploration well. Different depth conversion methods have their own advantages and disadvantages, and the choice of method is often subjective, dictated by access to reliable velocity data, or by time and cost constraints. No single conversion method is superior in all cases and in all study areas.

1.1 Sources of velocity information

Velocity information plays an important role in all phases of the exploration, storage/production, and development, and is the key parameter for depth conversion, optimal pre-drilling well design, for modelling of rock/fluid prediction, and for post well appraisal. There are several geological controls on velocity e.g. burial history, structural history, lithology (depositional environment, grain size, porosity, fluid content etc.), and temperature gradient, pressure gradient, and abnormal pressure. Thus, there are many pitfalls when the seismic data are interpreted in the time domain (milliseconds or ms TWT); lithologies with anomalously high velocities can produce structural pull-ups in time domain, while anomalously low velocities can produce structural sags.

There are four primary sources of velocity information:

1. Well based velocities
2. Seismic stacking velocities – the DIX conversion/correction.
3. Direct time-depth conversion – the Polynomial method
4. Time-depth conversion – the V0_k conversion method

1. Well based velocities

Wells with sonic logs, give us some information about the velocities. Sonic log velocities are categorized as lowest or least reliable velocities and may lead to poor depth conversion. Check shots (measuring the time it takes a seismic wave to reach a specified depth point) and vertical seismic profiles (VSP) give more reliable velocity information for depth conversions. If we have depth measurements for well-tops in a well and their corresponding seismic times derived through constructing synthetic seismogram, then we can calculate seismic velocities so that depth and seismic time of well-tops are consistent. VSP and check shot derived velocities may be used directly whereas sonic derived velocities require corrections for “drift” during sampling.

The lithostratigraphic subdivision of the Danish onshore subsurface is given in Figure 1. This subdivision is used in Nielsen and Japsen (1991). For all wells the depths and two-way travel times (ms TWT) to the top and base of each unit is given (see example in Table 1). The depths are given both relative to the reference level used while logging (meters or feet below kelly bushing, drilling floor, or rotary table) as well as in meters below mean sea level mbMSL (referred to as Z_t and Z_b), whereas the travel times are given as two-way time in milliseconds (ms TWT) below mean sea level (referred to as T_t and T_b). The thickness of each unit is given in meters (ΔZ) and the two-way time thickness in milliseconds. For units where the necessary QC’ed travel time data exist, the average velocity to the top of the unit is calculated as $2Z_t/T_t$, and to the bottom of the layer as $2Z_b/T_b$. The interval velocity, V_{int}, of each unit is calculated as $2\Delta Z / \Delta T$. The travel times listed have been determined from the available check shot surveys or calibrated sonic logs. The more recent wells both have check shot surveys and sonic logs (see Nielsen and Japsen, 1991).

2. Seismic stacking velocities – the DIX conversion/correction

Seismic data offer a spatially dense, regular, and objective sampling, and cover the entire depth range throughout a survey area. This supports the limitations of only using well data. However, seismic data are a measure of time rather than depth or velocity directly, and the stacking velocity data derived from seismic are imaging velocities, and not vertical propagation velocities such as in wells.

In areas where only very few or no wells are available, the only option usually is to use stacking velocities which by theory are biased towards being too high, even in the case of high-quality seismic data. Furthermore, seismic stacking velocities should only be obtained from relatively horizontally stratified portions of the seismic data. The stacking velocity method can benefit from the availability of a few wells located on the seismic line to assess the amount of bias by which contoured stacking velocity maps should be reduced.

The time-to-depth conversion strategy involves the following steps after the seismic data has been interpreted in the time domain:

a) RMS velocity functions picked at specified analysis locations over the survey area with the time horizons to derive horizon-consistent RMS velocity maps. The RMS velocity functions are preferably picked from gathers derived from pre-stack time migration.
b) Dix conversion of the RMS velocity maps to derive interval velocity maps.
c) Vertical-ray or image-ray depth conversion of the time horizons using the interval velocity maps.

The combination of the interval velocity maps from b) with the depth horizons from step c) constitutes the velocity model that can be used for time-to-depth conversion. This velocity model may then be calibrated to well data. Stacking velocity inversion sometimes may be substituted for Dix conversion to estimate interval velocities.

Thus, depth conversion of time horizons may be performed using a combination of Dix conversion of RMS velocities to interval velocities and image-ray depth conversion of time horizons interpreted from the time-migrated volume of data. This is the usual implementation of map migration.

3. Direct time-depth conversion – The Polynomial method

Direct time-depth conversion using a polynomial function is quick and easy to implement, but ignores the structural and lateral heterogeneity (spatial anisotropy patterns) of velocity and is only successful at known depth points locations (i.e. at well locations) by forcing an exact or minimal error match between actual and predicted depths. Thus, direct conversion only involves seismic times at well locations, while velocity information from seismic and other spatial sources including geological information is not used. The disadvantage of the method is the possible incorporation of large uncertainty in areas without check shots, whereas, an advantage is that the fitted polynomial function can be used to extrapolate a time-depth

relationship for depths below that covered by e.g. check shot data, if there is otherwise good control on velocity data in the available wells.

The direct time-depth conversion method reveals little information of the validity of the time-depth relationship between the wells. Therefore, the confidence is usually weak, as the method prevents the incorporation of velocity data from seismic, which may provide valuable additional information between well control. One of the major causes of error in depth predictions using this method is mis-ties in time between seismic horizons and the corresponding geologic well pick in time. The method hides these errors by forcing the wells to tie, thus altering the velocity provided independently by the well.

4. The V0_k conversion method

Velocity modelling is a more advanced method than direct conversion because velocity information adds two features to the time-depth conversion, 1) the velocity model can be evaluated numerically, visually, and can be tested independently of its ability to predict depth, thus increasing its reliability, something that cannot be done with the direct time-depth conversion method, and 2) velocity modelling enables the use of velocity information from both seismic and wells, providing a much broader data set for critical review and quality control.

Velocity modelling involves building a reliable velocity model using all available velocity data. This may include various types of well velocities including arbitrary calibrated seismic stacking velocities. Modelling may use simple average velocity (single layer), or interval velocity (multi-layer), or instantaneous velocity (variation of velocity with depth) (see sketch below). The goal is to create a model that gives the best results between the known depth points but also match the known data points (i.e. well locations). This method is an independent way to predict depth because it uses velocity functions as the input rather than horizon depth and time at wells, and because it can involve seismic stacking velocities in addition to or even instead of well velocities.

The most reliable velocity model incorporates all available velocity information by weighting different sources (seismic and wells) properly, and therefore are geologically more reliable and consistent. Geologically consistent means building a velocity model that follows the appropriate layering scheme; in hard rock environments this usually means following the true geological structure, taking into account lithological contrasts (e.g., bedding), folding, and faulting; in soft rock environments the layering may simply by parallel to the topography or bathymetry variations, because velocity may be mainly a function of overburden or depth of burial.

Multi-layer depth conversion

In multi-layer depth conversion, the section is divided into separate geological layers, each of which likely has a different, but internally consistent, interval velocity. A separate velocity model is built for each layer, and results in a depth prediction of the base of the layer, given the top of the layer from the previous calculation. The top of the first layer is usually the seismic datum, followed by geological layers where base of each layer serves as top to the next layer. Some layers may not carry any commercial importance but play a vital importance

in overall velocity model as velocity in each preceding (shallower) layer has profound effect on the velocity of next (deeper) layer. This means the overburden above the zone/s of interest constrains the velocity in geologically important layers.

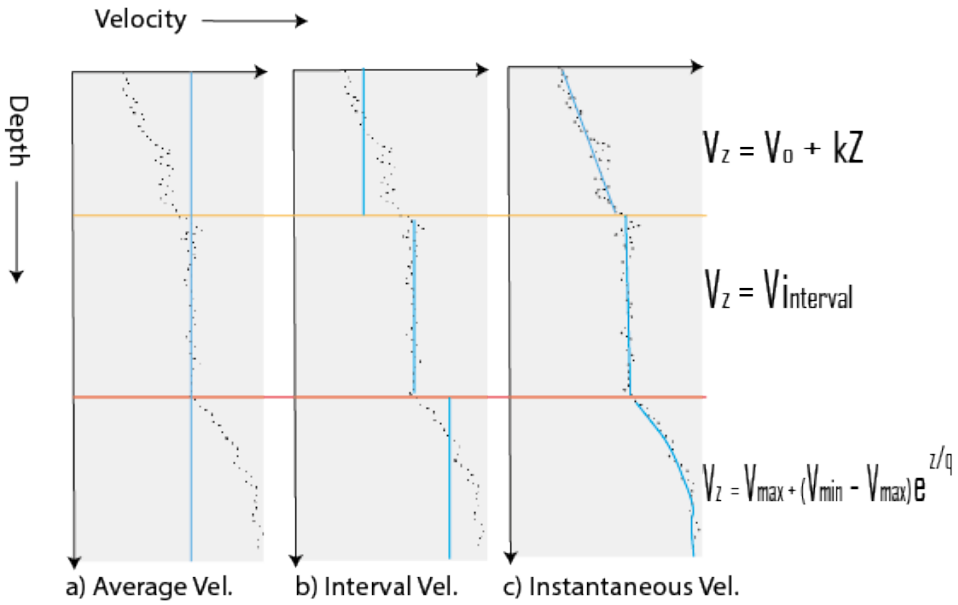

Sketch showing the three levels of detail in velocity modelling. Level 1) or a) uses average velocity, where the subsurface is not described in detail, resulting in a reduced confidence in the predicted depths. Level 2) or b) uses interval velocities with a constant velocity for each layer within a given well. Both using a) and b) allows spatial variation of velocity between well locations. Level 3) or c) the model includes variation with depth e.g. due to overburden. Instantaneous velocities are normally modelled as a linear function of depth.

There are three levels of detail in modelling velocity, depending on how the velocity behaves with depth (see sketch above). Using average or interval velocities allows spatial variation of velocity between well locations. By cross-plotting interval velocity versus midpoint depth or contouring the well average or interval velocities introduces spatial variation by e.g. geostatistically using seismic processing velocities at distances far from the wells (i.e. the kriging algorithm).

Adding still more detail (Level 3 in sketch above), we would like the model layer velocities to include variation with depth in some cases, because velocities often increase with greater degrees of compaction caused by thicker overburden. Here, instantaneous velocity data is included, such as a time-depth curve from a vertical seismic profile, or a check shot survey, or an integrated sonic log. This type of curve provides velocity variation over very small depth increments. The simplest way to describe this variation is to model instantaneous velocity as a linear function of depth: V(z) = V0 + kZ, where V(z) is the instantaneous velocity at depth Z, and V0 and k are the intercept and slope of the line. Numerous other functions, both linear and curvilinear can be used, where the functions are fitted separately for each layer to ensure geological consistency.

Pseudo-velocity-wells

By using seismic stacking velocities, it is possible to compile pseudo-velocity-wells calibrated to true vertical velocities, where time-depth curves (TD curves or velocity-depth functions) are computed at each stacking location. The TD curves can be averaged into pseudo-velocity-wells and used in instantaneous velocity function modelling, just as the TD curves from wells but with a finer time sampling. This can be used to smooth the error inherent in stacking velocity analysis. If neither seismic data nor well data exists pseudo-velocity-wells can be derived to do the instantaneous velocity modelling.

The pseudo-velocity-wells technique can be used as a geological tool and as a velocity modelling tool for time-depth conversion in areas with good seismic coverage, thus creating pseudo-velocity-wells at locations with good geological understanding. The use of discrepancy contouring can then divide study areas into smaller areas with different velocity anomalies, pointing out areas of major facies changes, differences in uplift caused by faulting or anomalously-pressured geological geopressured units that must be handled during drilling.

The discrepancy analysis

The best combination of V(z) function is the one that will effectively predict depths at locations away from the wells. This is where the actual V(z) curve fits over the entire depth range for the given layer and not just the one with the best tie at the well.

Within a given seismic unit, the variation of velocity with depth can be described equally well by a range of V0 and k parameter values. These analytic functions describe a smooth variation of velocity with depth, much smoother than the high frequency fluctuations observed on sonic logs. In practice no analytic function can represent the actual high frequency changes of instantaneous velocity with depth precisely. Thus, the purpose is not to describe the detailed geology signature in that specific well location, but to fit a typical velocity within the geological unit overall, by finding a specific parameter combination that produces a closer adequately fit than any other combination for all wells.

A quantitative method for determining the accuracy of the fit or 'discrepancy' between the well velocity is calculated as function curve based on the two parameters (V_0, k). The '*discrepancy*' is calculated for each pairing (from Al-Chalabi, 1997):

$$F(\mathrm{v}_0, k) = \left[\sum_{i=1}^{m} \frac{(v_i - C_i)^q}{m}\right]^{1/q}$$

where V_i (or V_{int}) and C_i is the i^{th} actual (observed) and function velocity values respectively, m is the number of sampled depth points, and q is the norm (q=2 in this case). '*Discrepancy analysis*' may reveal that there are several different sub-areas within the overall area. These often belong to different fault blocks, or different facies associations.

1.2 Choice of a depth conversion method

The choice of a depth conversion method depends on data availability and data quality, the target structures, and time and cost constraints on the depth conversion process. Direct methods are fast and accurate at the wells, which may be sufficient. Velocity modelling can also be fast and exact, but normally requires significant data resources, modelling expertise, and time to create reliable velocity models, achieving greater confidence in the results, particularly in areas between well control. Choice of correction techniques such as gridding residuals (extrapolating) or tapering with a radius from the well control point can have considerable bearing on the final result. Varying these parameters with consistency between methods is critical to further refine this analysis.

By using suitable conversion methods, it may be possible to translate seismic interpretations from Two-Way-Time (TWT ms) to depth (meter), by integrating the seismic interpretation with geologic, petrophysical, and production data. In velocity modelling, description of the velocities is the focus, while best possible well-ties are the focus in the direct conversion methods where velocity analysis is of minor importance.

Any procedure that combines hard data (i.e. well data with low uncertainty and low sampling density) and soft data (i.e. seismic data with higher uncertainty and high sampling density) is recommended because it is consistent with the well data. Geostatistics or spatial statistics can be used to combine the advantages from hard and soft data ensuring a reasonable weighting of well control and still maintaining the spatial trends. Gridding algorithms such as kriging (including various versions of kriging and cokriging) is a method that uses specially weighted combinations of data observed at known well locations to predict values at other locations away from well control. Furthermore, kriging algorithms also provides estimates of the uncertainty of the predicted values.

2. Database and previous depth conversion in Denmark

Since the 90'ties in-house depth conversion in the Danish onshore and near-onshore areas has been carried out using several conversion methods, some of which have been published:

- A V0_k method was used for the North Jutland Maps, updated in 2007 (Britze & Japsen 1991; Japsen & Langtofte 1991a; Japsen & Langtofte 1991b) (Figure 2)
- An updated V0_k method (GEUS, 2002) based on Japsen (1993) and Japsen and Bidstrup (1999) was developed with focus on the offshore Central Graben area.
- A local Direct time-depth conversion function was used in the Copenhagen area prior to drilling the MAH-1 geothermal well (GEUS report from 2001).
- A regional Direct time-depth conversion function was used for regional mapping of potential geothermal reservoir units (Mathiesen et al., 2009).
- Several local Direct time-depth conversion functions, e.g. used in the Farum and Hillerød areas North of Copenhagen (GEUS, from 2010 to 2014).
- 2D depth migrated sections in depth from the Sønderborg, Farum and Hillerød areas (GEUS, 2013 and 2014).
- An updated V0_k method (GEUS, 2015, in-house depth conversion model) used for the 3D geophysical model used in the Geothermal WebGIS Portal (Figure. 3) and in Hjelm et al. 2020)

Most of the mentioned depth conversion studies have used velocity data from Nielsen and Japsen (1991) and polynomial or V0_k conversion methods (see also Section 1).

The polynomial method

Initially, velocity analysis is carried out using plots of True Vertical Depth Sub-Sea (m TVDSS) vs. two-way-time (ms TWT) based on check shot data or as here velocity data sets from all the available Danish wells, and involves analysing the velocity data sets and the nature of the subsurface layers for consistency (Nielsen and Japsen 1991). The polynomial method is a velocity function that describes the time-depth relationship of a dataset regardless of the number of lithostratigraphic units present in the subsurface as in Figure 1 and Table 1. Normally, it does not consider e.g. local variation of velocities at the shallower lithostratigraphic units and is therefore expected to be more accurate when dealing with shallower objectives below depths of 1000–2000 m (Figure 4 and 5). The higher the order of the polynomial, the more accurate is the equation (see also Section 1). A regional velocity trend line using a third order polynomial equation can be obtained and used for depth conversion (Figure 4).

In this study, the polynomial function method is improved by using calibrated sonic logs to derive an updated local velocity function obtained from the seismic to well tie process to describe the velocity trend in two study areas (see below).

V0_k function and the multilayer velocity method

In the V0_k models velocity increases as a result of burial compaction and the model assumes that velocity changes linearly with depth by describing the time-depth relationship with a straight line. It employs the instantaneous interval velocity of each successive layer, and therefore the cumulative effect of the contribution of local velocity variation in each of the overlying layers influences the velocity profile of deeper layers. The method is expected to be more accurate to ascribe velocity to deeper rock layers than a polynomial function.

The necessary inputs into this velocity modelling technique are the updated TWT (ms) and TVDSS (m) values obtained from the seismic to well tie process. The interval velocities of the layers are calculated and plotted against the corresponding depth to produce an average of the different estimated values of V0 and k (see also Section 1). The equation that defines the velocity function can be described by the equation of a straight-line following V = V0 + kZ, where k is the gradient that reflects the effects of compaction as unconsolidated sediments becoming buried over time.

The multilayer velocity depth conversion method has been adapted to the Danish setting by Japsen in 1993 and 1994. Each layer is assigned a surface velocity (V0) and a depth gradient (k) according to the linear equation: V(z) = V0 + kZ, where V(z) is interval velocity for the layer at depth z. To ensure a reasonable fit at well locations, lateral deviations from the average interval velocity functions are allowed through the application of the DV parameter, which is added to the V0 parameter i.e. V(z) = (V0 + DV) +kZ. At each step a back-interpolation of the depth maps has to carried out in order to match the depth values at well locations. The generated error-grids is then sequentially added to the depth grid.

The V0 and k can be found by application of simple linear regression to cross-plots of interval velocity vs. mean depth for the various sediment packages that are defined by the interpreted seismic reflectors (see also Japsen, 1993 and 1994). It is important to realise that V(z) is not the average velocity of an interval, but the instantaneous velocity at depth z. Variations in DV-values may express lateral variations in geology facies or lithology of a given interval or a case positive anomaly may indicate late uplift of an interval while a negative value may indicate under-compaction (overpressuring) assuming uniform lithologies in a larger area.

3. Depth conversion in the Havnsø and Hanstholm areas

The Hanstholm and Havnsø structures both contain Gassum Formation sandstones sealed by Fjerritslev Formation mudstones. The Gassum Formation in the Hanstholm structure has the top point at c. 900 m depth and spill point at c. 1300 m (Japsen and Langtofte 1991), whereas the Havnsø structure has the top point at c. 1300 m and spill point at c. 1550 m (Figure 3).

The seismic time-structure (ms TWT bMSL) and time-isochore maps (ms) of the Fjerritslev (seal) and Gassum (reservoir) seismic intervals are in the Stenlille-Havnsø and Thisted-Hanstholm areas interpolated as 500x500 m grids using a search radius of 5000 m and smoothing and filtering to produce reliable maps (Gregersen et al. 2020). The irregular seismic coverage and data quality in the mapped areas, together with parameters for the gridding algorithm, may result in unsmoothed maps; especially the thickness maps may show variations in thickness which is geologically not constrained and more irregular than in nature (Rasmussen & Laghari 2020). This may influence the assessment of uncertainty, especially in areas where the thickness is less than 50 ms and where the coverage or data quality is poor. Further discussion and comments regarding the interpretation and mapping and choice of the most appropriated gridding algorithm (cell size, search distance/radius, sensitivity, impact on uncertainty etc). is addressed in the reports covering the interpretation and mapping of the Stenlille-Havnsø and Thisted-Hanstholm areas.

Simple time-depth assessments from well data and time maps

One simple way to assess the thickness of the Gassum Fm in the Havnsø structure is based on the interpretation and mapping in the Stenlille-Havnsø area where the time-thickness (ms TWT) in the Stenlille area is between 80–90 ms (avg. ~85 ms), and that the thickness over the Havnsø structure is between 100–140 ms (avg. ~120 ms) (see Gregersen et al. 2020; Appendix 2). Thus, the increase from Stenlille to the Havnsø is 25–50% on top of the structure, where the time-isochore Gassum map shows a generally westward thickening from ~85 ms TWT (±20 ms) in the Stenlille 3D area to ~120 ms TWT (±30 ms) in the Havnsø structure, which is roughly an avg. of 35 % (±40–50 ms) time-thickness increase. The local thinning on the time-thickness maps may be caused by initial movements of the underlying salt into a salt pillow that later developed and elevated the Havnsø structure and possibly caused removal of the upper parts of the Fjerritslev Formation (Gregersen et al. 2020).

From the deep well database, we know that the Gassum Fm in the Stenlille-1 to -6 has a thickness of ~150 m (Table 1). This gives a thickness of ~150*1.35 = ~200 m (±75 m) at the Havnsø structure.

Simple polynomial method based on well data

Another way is to depth convert the seismic time-structure map (ms TWT bMSL) and time-isochore maps is using polynomial time-depth relationships (Figures 4–5). The regional Danish subsurface relationship can be considered as a good regional approximation to local conditions. Figure 4 shows Two-way-time (ms TWT) velocities vs. Depth (mbMSL) for all Danish onshore and near-shore wells and for all lithostratigraphic units excluding Zechstein and Pre-Permian data. Using local data from the Felicia-1 and Thisted-2 and -4 Figure 5 shows that the time-depth function plots close the regional function in the Thisted-Hanstholm area, especially in the part deeper than 1000 mbMSL (green line, Figure 5). Using local data from the Stenlille-1 to -6. Figure 5 shows that the velocities plot closer to the minimum fitted function, indicating that the velocities In the Stenlille-Havnsø area are lower compared to the Thisted-Hanstholm area. Neither of the two structures have been drilled and the depth conversion is therefore based on information from nearest wells, assuming that the time-depth relationship based on these wells can be used as analogue in the Stenlille-Havnsø and Thisted-Hanstholm areas. In connection with the evaluation of a smaller local area, the relationship will be adapted by using the nearest well data to adjust the polynomial function. Using this method, the uncertainty of the depth conversion is expected to increase with increasing depth and typically being between 5 and 15%, increasing towards away from the areas with well data. A more qualified assessment on the uncertainty range requires a more integrated workflow (see below).

The seismic time-structure map (ms TWT) and time-isochore maps have been depth converted using these local time-depth relations based on information available from the nearest onshore wells using Depth = 0.0003 TWT^2 + 1.25 x TWT (Stenlille-1 to -6) for the Stenlille-Havnsø area and Depth = 0.0003 TWT^2 + 1,0442 x TWT (Felicia-1 and Thisted-2 and -4) for the Thisted-Hanstholm area. The resulting depth maps are thus partly an expression of the depth to the top of the seal (Fjerritslev Fm) and the reservoirs (Gassum Fm) (Figures 9 (lower) for Stenlille-Havnsø and Figures 12 (lower) for Thisted-Hanstholm).

Using a regional multilayer velocity method in the two study areas

The interval velocities V_{int} (or V_i) for the overburden interval including the POST-Chalk and Chalk Group units are plotted against midpoint depth for all Danish wells (**Figure 6)**. There is a considerable scatter and no obvious depth relationships exist. Several outliers in the Cretaceous and Jurassic interval have high V_{int} despite shallow burial depth.

It is noted that V_{int} for the entire Fjerritslev Fm cluster around a value of 2500–3500 m/s in the drilled thickness range up to 2000 m. In contrast V_{int} of the lower part of Fjerritslev Fm below F-III show an inverse relationship with thickness with highest velocity values at small thicknesses. This could be a result of biased sampling but needs to be analysed further. Likewise, most of the data represent wells drilled in the sandstone rich settings and represent intervals with a possible high proportion of high velocity sandstones of the F-I and F-II compared to well sections with a higher proportion of claystones (e.g. the F-III and F-IV).

Furthermore, recorded average velocities to the seismic markers are highly dependent on the nature of the post-Jurassic overburden, i.e. especially the Chalk Group. and the POST-Chalk unit. This can be illustrated if V_{avg} to Top Gassum in each well is plotted on the regional Chalk Group isochore map from Hjelm et al. (2020). It is expected that high V_{avg} corresponds to a thick overlying, high velocity Chalk Group, but this also needs to be analysed further.

Average velocities to all well-picks of the interpreted horizons versus two-way-travel time are shown in Table 1 for the in the Stenlille-Havnsø area. As shown in Figure 2 a large variation an overall general depth-related trend is observed. However, separate trend lines can be isolated depending on the geographical position of the well (Figure 5). Low depth related trend can be distinguished in areas where the wells only penetrated a rather thin chalk section. V_{avg} derived (and extrapolated) from these trend lines can be used to calculate depths below in the two study areas. However, this simple approach gives rise to considerable uncertainty in the deep undrilled parts of the basin taking the sampling bias in consideration. Therefore, in the Stenlille area well-derived average velocities V_{avg} should be compared with a RMS seismic velocity cubes from 3D Stenlille-97 survey, to verify if the RMS velocities are typically about 10% higher than in the wells as normally is expected. Even higher discrepancies up to 15% can be expected at deeper stratigraphic levels and in areas with no well control.

As a simple reference, the Stenlille structural time map of the Top Gassum Fm can be depth converted using a simple layer-cake method where the thickness of the overburden (POST-Chalk and Chalk Gr. and Lower Cretaceous intervals) are added with the Jurassic Fjerritslev Fm and the Upper Triassic Gassum intervals (Figure 1). Generally, the thicknesses of the overburden (POST-Chalk and Chalk Gr. Intervals and Lower Cretaceous intervals) can be calculated using constant V_{int} of 1856 m/s, 3071 m/s and 2903 m/s, respectively (Table 2). The thicknesses of the Fjerritslev Fm and Gassum Fm were calculated using constant V_{int} of 2698 m/s and 3513 m/s, respectively. These values are arithmetic averages of V_{int} of drilled intervals. It is stressed that this simple well-based velocity estimation is biased and show that use of arithmetic means can result in estimations of depth to the top Gassum that differs more that ±75 m compared to the values from the wells.

For large parts of the Danish area a working seismic velocity model is available, but the model is designed for regional geothermal screening purposes and is very rough, does not fully cover the two structure areas. The velocity model does not focus on local areas and is associated with large known uncertainties (GEUS, 2015, in-house depth conversion model). The velocity model uses a V0_k depth conversion model defined in Petrel© (v2017) but does not cover the Hanstholm area (see Figure 3; GEUS, 2015, in-house depth conversion model). Several challenges are present in both the subsurface and the available data (or lack thereof) and it is unclear where the velocity model could have unreal effect on structure definition or if it potentially could kill of smaller real structures. It is therefore recommended that the regional velocity model, including seismic well ties and well-tops, is revised and updated for both the onshore, but also to include the on- and offshore transition i.e. the Hanstholm structure.

Using calibrated sonic logs in the two study areas

To further update the local time-depth relationships, all the Stenlille-1 to -20 wells in the Stenlille-Havnsø and the Felicia-1 and Thisted-2 and -4 wells in the Thisted-Hanstholm area have been revised to obtain the most reliable well velocities (Figure 7 and Appendix 1). All the wells have been analysed with respect to average velocity to the local interpreted horizons and interval velocities between bounding reflectors together with the synthetic seismograms (Tables 3–4 and Appendix 1). It is important to note, that the time-depth relationships depend on the seismic properties of the penetrated rocks at the well location, especially their sonic and density, which may vary greatly with depth and mineral content, e.g. presence of salt.

Even though the fitted polynomial functions in Figure 7 looks smooth the function is based only on well data. It must therefore be expected than the velocity field in areas without well control like the Havnsø and Hanstholm areas may differ. Due to lack of well data in the two areas it is not possible to establish velocity functions to time-depth conversion without assuming a simple layer-cake analogue based on the well velocity data.

Principally time-depth relationship can be generated by calibrating sonic log in the well and multiplying it with the density values along the borehole/interval of interest to extracted a 1D forward model of the surface as a series of spikes know as reflection coefficient series. Reflection coefficient series can be convolved with frequency dependent wavelet to generate a 1D forward synthetic seismogram. Frequency depended wavelet is a model wavelet based on the dominant frequency of the seismic data and the reflection coefficient series along the borehole, or a time varying operator wavelet extracted along the length of the borehole, if check-shot data already exists in the well. Convolution is a fundamental concept in reflection seismology. Seismic data is the record of reflected energy from different layers that have different geophysical properties. Seismic signature results from convolution of input energy source wavelet with the reflectivity of the layers. Thus, generation of synthetic seismogram is a 1D forward modelling process which involves convolving reflectivity series of the rocks derived from sonic and density logs in a well with a seismic wavelet.

Despite the presence of good quality seismic data coverage especially in the Stenlille area, estimating accurate time-depth relationships (TDR) for the Stenlille wells is difficult. Table APP1.1 lists the database used for generating time-depth relationship for the Stenlille and Thisted wells.

The Stenlille-97 3D seismic survey is covered by all the Stenlille wells except for the Stenlille-6 (ST-6) (see basemap in Figure APP1.1). The spatial as well as temporal resolution of Stenlille 3D is excellent with very high signal to noise ratio. The frequency spectrum of Stenlille-3D seismic data indicates a dominant frequency content of 40–70 Hertz (Figure APP1.3). Due to the lack of the check-shot information for all the Stenlille wells, a model phase ricker wavelet of 48 hertz which is consistent with the dominant frequency range of the Stenlille 3D seismic data (Figure APP1.3) has been used. Electrical resistivity acts as a lower degree proxy for the compressional wave velocity and thereby gives an indication of sonic velocities. A complete suite of resistivity information was present for all Stenlille wells and was used to generate computed sonic log and subsequently Gardner empirical relationship to generate computed density log.

The biggest challenge in estimating time-depth relationship was the fact the sonic and density information along the Stenlille boreholes was very limited or in many wells completely missing. If either of density or sonic information for interval between Top Gassum and Base Gassum was present it was used to drive the other, however for many of the Stenlille wells neither sonic nor a density log information was available for the Gassum interval (Table APP1.1).

Local Interval velocities based on synthetic seismograms

For Havnsø area, most of the Stenlille wells is located within the 3D survey area ~30 km SE of the structure (Figure APP1.1). In this area, the Top Fjerritslev Formation, Top Gassum Formation, and Base Gassum Formation is interpreted on reprocessed 2D seismic lines as well as high frequency 3D Stenlille seismic volume (Gregersen et al. 2020; Rasmussen & Mathiesen 2020). Wireline log information in the Stenlille wells and a model wavelet whose frequency component matches that of the 3D seismic volume was used to generate synthetic seismograms (Appendix 1). Synthetic seismogram in each well constrains the interpreted seismic horizons in time domain (ms TWT) to well picks (Base Chalk Group, Top Fjerritslev Fm, Top Gassum Fm, and Base Gassum Fm) in measured units of depth i.e. meters. Table 3 summaries the time-depth relationships of Stenlille wells after generating synthetic seismograms (included in Appendix 1). Associated interval velocities along each layer is derived by using the empirical relationship between measured depth (m) and Two-way-time (ms). Predicted interval velocities are plotted as function of measured depth (m) vs Two-way-time (ms) (Figure 7) and give a reasonable match to interval velocities presented by Nielsen and Japsen (1991) (Table 3 and Figure 5).

For Hanstholm area, the 2D seismic data ties to the Felicia-1, J-1, and Thisted-1 to Thisted-4 wells where the Thisted are located ~45 km SE of the structure (Figure APP1.2). Respective seismic horizons in time domain (Rasmussen & Laghari 2020; Rasmussen & Mathiesen 2020) are correlated to well picks by generating synthetic seismograms in the same manner as described in previous paragraph. Table 4 summarises the time-depth relationships of these wells after generating synthetic seismograms (included in Appendix 1). Associated interval velocities along each layer is derived by using the empirical relationship between measured depth (m) and Two-way-time (ms). Predicted interval velocities are plotted as function of measured depth (m) vs Two-way-time (ms) (Figure 7) and give a reasonable match to interval velocities presented by Nielsen and Japsen 1991 (Table 4 and Figure 5).

3.1 Depth conversion of maps from the Havnsø and Hanstholm area

At present, based on different depth conversion methods and with different focus, there exist several possible depth converted maps in the Havnsø and Hanstholm areas. The top point in the Havnsø structure range between ~1300–1450 m and the spill point between 1550–1750 m. The top point in the Hanstholm structure range between ~800–900 m and the spill point between 950–1300 m.

Previous assessments of the Gassum Formation in the Hanstholm structure estimated the top point at ~900 m depth and spill point at ~1300 m (based on Japsen and Langtofte 1991), whereas the Havnsø structure has the top point at ~1300 m and spill point at ~1550 m (Figure 3 from the WebGIS Portal). However, Hjelm et al. (2020) showed that the current regional V0_k velocity model used for the Geothermal WebGIS Portal is not usable for the Havnsø structure and does not cover the Hanstholm structure.

The new depth converted maps to the top of the seal (Fjerritslev Fm) and reservoir (Gassum Fm) and resulting thickness maps are based on an updated polynomial function derived from the assessment of the time-depth relationships in all nearby wells (see above and Figure 7). This assumes that the time-depth relations defined from the wells can be applied to the Havnsø and Hanstholm structures, which we know from Gregersen et al. (2020) and Rasmussen & Laghari (2020) is too simple a model.

Figures 8, 9 (upper) & 10 shows the depth converted maps for the Havnsø area estimating the top structure point at ~1300 m and spill point at ~1600 m (based on TWT maps by Gregersen et al. 2020 in Appendix 2). By subtracting the top and base surfaces the resulting thickness maps of the seal and reservoir are shown in Figure 8 (lower) and Figure 10 (lower). The thickness of the seal and the reservoir is 300–400 m and 150–300 m, respectively.

The Figures 11, 12 (upper) & 13 shows the depth converted maps for the Hanstholm area estimates the top structure point at ~800 m depth and spill point at ~1000 m (based on TWT maps by Rasmussen & Laghari 2020 in Appendix 2). By subtracting the top and base surfaces the resulting thickness maps of the seal and reservoir are shown in Figure 11 (lower) and Figure 13 (lower). The thickness of the seal and the reservoir is 200–300 m and 100–250 m, respectively.

By using this simple depth conversion method, it is expected that the uncertainty increases away from the wells into the two structure where no well data can support the simple polynomial function method. The use of the polynomial functions also shows the sensitivity of the method and the need for a velocity model that is integrated and constrained by a geological model to ensure reliable depths structure maps and thickness variation maps.

3.2 Assessment of depth uncertainty

Depth uncertainty is one of the major uncertainties associated with assessment and development of potential storage structures. This uncertainty mostly arises due to the complexity of the subsurface, lack and quality of data, seismic picks, well ties, fault identification and positioning and velocity models. Sensitivity analysis of input parameters for storage capacity estimations has shown that the structural gross rock volume e.g. area of the structure and the reservoir thickness are the most important parameters (see also Hjelm et al. 2020; Figure 21). This can be achieved through good seismic well ties and better seismic data to constrain the structural definition.

Seismic data quality affects the structural definition, and thus the reservoir thickness and the understanding of the structural geometry. Processing of seismic data (poor resolution, poor velocity picks and poor migration) may affect how structures are interpreted and can lead to uncertain definition of the areal limit of a structure, the relief and depth to the spill point (Hjelm et al. 2020). Furthermore, seismic interpretation and mapping in an open grid results in uncertainty related to the spatial structural geometry and storage volume (Rasmussen & Laghari 2020). Selection of different gridding algorithms create very different structures and a simple test shows that the area extent of a structure could vary up to 25% depending only on the selected gridding algorithm (Hjelm et al. 2020).

Depth conversion has important influence on the depth converted structural geometry due to the development of the overburden and how the resulting compaction effects the underlying seals and reservoirs. The uncertainty is a result of cumulative uncertainty of the layers above seal and reservoir, uncertainty in data velocities, uncertainty in well ties and the associated velocity approximation. Thus, uncertainty related to depth conversion can obviously have a significant impact on reservoir simulation of e.g. fluid contact and evaluation of storage volume and efficiency.

The more control there is in mapping the subsurface, the greater the accuracy of the maps. Control can be increased by the correlation of seismic data with well data. The synthetic seismogram is the primary means of obtaining this correlation. Velocity data from the sonic log and the density log (if available), are used to create a synthetic seismic trace. This trace closely approximates a trace from a seismic line that passes close to the well in which the logs were acquired. The synthetic then correlates with both the seismic data and the well log from which it was generated (see above).

It is clear from the synthetic seismograms that the top and base Gassum Formation introduce uncertainty both in terms of well tie uncertainty and interpretation uncertainty (see synthetic seismograms in Appendix 1). This is especially important in a geological setting, like the Havnsø and Hanstholm, with significant lateral changes, and where the seismic picking of the well tops is difficult and not can be regarded as a ‘hard data point’. Even though, the updated maps have been generated based on more integration of all neighbouring well data and new synthetic seismograms, the uncertainty on the depth maps are estimated to be up to 10–15% (or 50–150 m), mainly due to lack of high-resolution seismic data and well data near the two structures.

Furthermore, it is expected that the uncertainties associated with the polynomial method used here will be greater in more distal depositional environments and in areas with increased structural complexity. It is possible that the Havnsø structure is located in a more distal setting than the Stenlille wells, thus changing the spatial distribution of velocities towards and around the Havnsø structure. This, however, awaits more detailed integration of the geophysical seismic mapping and the 3D geological model constrained by biostratigraphy and other associated enrionmental studies before a well-constrained reservoir model can be used for CO_2 simulation.

The study shows the importance of a more quantified assessment workflow. It is therefore recommended, that an integrated iterative workflow between the seismic interpretation and the sequence stratigraphy framework is carried out to assess the various types of uncertainty included in depth conversion, e.g. by using various depth conversion models/methods constrained by geological models and with Min. and Max scenarios in order to evaluate uncertainty ranges for e.g. storage capacity estimations.

In summary, as shown in this study acquisition of new 2D/3D seismic data and sonic log information from new wells are very important for derivation of a more accurate structural definition and a more local confined velocity model ensuring a best possible depth conversion.

4. Suggestions for supplementary investigations and research

This study shows that further investigations and research are needed in order to select the best depth conversion method. This will also increase the confidence of the depth conversion of the seismic interpreted time structural and time-isochore maps (Gregersen et al. 2020; Vosgerau et al. 2020; Rasmussen & Laghari 2020; Hjelm et al. 2020).

The Danish deep wells database is normally used for time-depth relations for key surfaces using formation well-picks and velocity calculations established by Nielsen and Japsen (1991) with later adjustments and additions. Even though, only a few of the onshore wells contain original information from seismic check-shots, these well data provide key information for ties to the seismic interpretations and are essential input to time-depth conversion (see Appendix 1).

Following the need for new 3D and 2D seismic data followed by new details interpretation and mapping several possible improvements can strengthen the depth conversion. By integrated the use of seismic stacking velocities it will be possible to build a more robust depth converted geometric framework for the reservoir simulation models constrained by the geological model with focus on lithofacies variation.

The following is therefore suggested:

- **Time-depth conversion** is not an easy process for the Danish onshore, due to limited velocity check shot and VSP data in the well database. At present the Geothermal WebGIS Portal uses a regional seismic velocity model covering the Danish onshore area developed for regional mapping. The model does not cover the on- and offshore transition and is associated with various uncertainties. The model needs to be updated and improved to cover future site-specific areas like the Hanstholm and Havnsø areas, by integrating seismic stacking velocities into the workflow. It is therefore recommended that the existing velocity model is updated for both the onshore, offshore, and in particular for the on- to offshore transition to cover e.g. the Hanstholm structure.
- **Revision of the seismic velocity data and well ties and TD functions** would strengthen depth conversion. The revision of the existing mapping needs to be integrated with shallow seismic data set (below ~1000 ms TWT) to include better the pre-Quaternary, the POST-Chalk and the Chalk Group seismic units, thus ensuring a better depth conversion to the important Base Chalk reflector (see also Hjelm et al. 2020).
- **Correct seismic positioning of all the Stenlille wells** relatively to the 3D seismic data will result in more correct thickness estimations of the Fjerritslev and Gassum Formations. At present the mapping is entirely based on the Stenlille-19 well, being the only well which correlate correctly with the seismic data. The new updated synthetic seismograms have shown that important interpretation uncertainty both in terms of well tie uncertainty and in interpretation uncertainty (well top picking) due to

laterally varying geology. It is therefore recommended, that an integrated iterative workflow between the seismic interpretation and the sequence stratigraphy framework is carried out to examine if this uncertainty can be reduced. Well tie analysis and testing of interpolation methods, including kriging and establishing varigrams should be carried out.

- **Detailed mis-tie analysis** between intersecting seismic lines is critical to improve the structural and stratigraphic uncertainty of the geological models. Mis-ties can be significantly very high >20-30 ms, and it is therefore recommended that the mis-ties between intersecting seismic data is further examined, by creating visual confidence maps of seismic quality, check shot availability and well tie quality. Mis-ties assessment or even stochastic approach can be used to indicate the local or global variability in uncertainty ranges, and thus identify areas where uncertainties are largest and thus focusing towards areas that are most crucial to de-risk. This will also have influence on the reprocessing of the seismic lines ensuring an appropriate static or dynamic shift or a combination of both. Before new seismic data (high frequency 3D seismic volume(s) and wireline logs (especially sonic and density information)) is acquired, it is recommended that reprocessing and possible removal of mis-ties between seismic data is examined further.
- **New modern high-resolution seismic acquisition** is important to build the best possible geological model for the depositional setting of the Fjerritslev and Gassum Formations, and to build the best possible reservoir simulation model. New 3D seismic surveys covering both the Havnsø and Hanstholm area is recommended, as modern high-resolution seismic data will deliver new seismic stacking velocities and more detailed interpretations with spatial variation of lithofacies both important for depth conversion and for reservoir characteristics. Alternatively, a thorough planned dense network of high-resolution 2D seismic data can be acquired in both the Stenlille-Havnsø and Thisted-Hanstholm areas (see also Gregersen et al. 2020; Rasmussen & Laghari 2020).

References

Al-Chalabi, M. 1997: Parameter non-uniqueness in velocity versus depth functions, Geophysics 62*,* 970-979.

Bredesen, K. 2020: Capture, Storage and Use of CO_2 (CCUS): Quantitative seismic interpretation (rock physics models, seismic inversion, AVO and attribute analysis) (Part of work package 5 in the CCUS project). Danmarks og Grønlands Geologiske Undersøgelse Rapport 2020/52, 9 pp.

Britze, P. & Japsen, P. 1991: Geological map of Denmark 1: 400,000. The Danish Basin. ‘’Top Zechstein’’ and the Triassic; two-way traveltime and depth, thickness and interval velocity. Geological Survey of Denmark Map Series 31, 3 maps and 4 pp.

Gregersen, U., Vosgerau, H. Laghari, S., Bredesen, K., Rasmussen, R. & Mathiesen, A. 2020: Capture, Storage and Use of CO_2 (CCUS): Seismic interpretation of existing 2D and 3D seismic data around the Havnsø structure (Part of work package 5 in the CCUS project). Danmarks og Grønlands Geologiske Undersøgelse Rapport 2020/33, 60 pp.

Hjelm, L., Anthonsen, K.L., Dideriksen, K., Nielsen, C.M., Nielsen, L.H & Mathiesen, A. 2020: Capture, Storage and Use of CO_2 (CCUS) – Evaluation of the CO_2 storage potential in Denmark. Danmarks og Grønlands Geologiske Undersøgelse Rapport 2020/46, 60 pp + 2 App.

Japsen, P. & Langtofte, C. 1991a: Geological map of Denmark 1:400,000. The Danish Basin. ‘’Base Chalk’’ and the Chalk Group, two-way traveltime and depth, thickness and interval velocity. Geological Survey of Denmark Map Series 29, 4 maps and 4 pp.

Japsen, P. & Langtofte, C. 1991b: Geological map of Denmark 1:400,000. The Danish Basin. ‘’Top Triassic’’ and the Jurassic–Lower Cretaceous, two-way traveltime and depth, thickness and interval velocity. Geological Survey of Denmark Map Series 30, 4 maps and 4 pp.

Japsen, P. 1993: Influence of lithology and Neogene uplift on seismic velocities in Denmark: Implications for depth conversion of maps. American Association of Petroleum Geologists Bulletin 77, 194–211

Japsen, P. & Bidstrup, T. 1999: Quantification of late Cenozoic erosion in Denmark based on sonic data and basin modelling. Bulletin of the Geological Society of Denmark, Vol. 46, pp. 79–99. Copenhagen.

Mathiesen, A., Kristensen, L., Bidstrup, T. & Nielsen, L.H. 2009: Vurdering af det Geotermiske potentiale I Danmark. Danmarks og Grønlands Geologiske Undersøgelse rapport 2009/59, 59 pp, 23 Figurer & 2 Bilag.

Mathiesen, A., Nielsen, L.H., Bidstrup, T. & Johannessen, P.N. 2001: Geotermiske reservoirer i Storkøbenhavn, Geologisk prognose ved 7 udvalgte lokaliteter. Danmarks og Grønlands Geologiske Undersøgelse Rapport 2001/60.

Mathiesen, A., Rasmussen, R., Bidstrup, T., Kristensen, L., Laier, T. & Nielsen, L.H. 2014: Seismic quality control, interpretation, mapping and assessment of the geothermal potential in the Hillerød area, Northeastern Zealand. Contribution to an evaluation of the geothermal potential. Danmarks og Grønlands Geologiske Undersøgelse Rapport 2014/35.

Nielsen, L.H. and Japsen, P. 1991: Deep Wells in Denmark, 1935-1990: Lithostratigraphic Subdivision, Oplag 31 af DGU series A, ISSN 0901-0270, Danmarks Geologiske Undersøgelse, 1991, 179 PP.

Rasmussen, R. & Mathiesen, A. 2020: Capture, Storage and Use of CO_2 (CCUS) – Seismic data evaluation and reprocessing trials related to the CCUS evaluation project around the Havnsø and the Hanstholm structures structure (Part of work package 5 in the CCUS project). Danmarks og Grønlands Geologiske Undersøgelse Rapport 2020/51, 18 pp.

Rasmussen, E.S & Laghari, S. 2020: Capture, Storage and Use of CO_2 (CCUS) – Seismic interpretation of existing 2D seismic data around the Hanstholm. Danmarks og Grønlands Geologiske Undersøgelse Rapport 2020/45, 26 pp.

Vosgerau, H., Mathiesen, A., Andersen, M.S., Boldreel, L.O., Hjuler, M.L., Kamla, E., Kristensen, L., Pedersen, C.B., Pjetursson, B. & Nielsen, L.H. 2016: A WebGIS portal for exploration of deep geothermal energy based on geological and geophysical data. Review of Survey activities 2015. Geological Survey of Denmark and Greenland Bulletin 35, 23-26.

Vosgerau, H., Gregersen, U. & Laghari, S. 2020: Capture, Storage and Use of CO_2 (CCUS) – Seismic interpretation of existing 3D seismic data around the Stenlille structure within the framework of sequence stratigraphy and with focus on the Gassum Formation. Danmarks og Grønlands Geologiske Undersøgelse Rapport 2020/34, 53 pp.

Tables and Figures

Table 1. Example from the Deep wells database showing relation between depths, thicknesses, and velocity data from the subdivision of Stenlille-1 to -6 wells from surface and down to the base of the Gassum reservoir (Nielsen and Japsen, 1991).

WELLNAME	LITHOSTRAT. UNIT	Top [ft RF.L]	Base [ft RF.L]	Top [m MSL]	Base [m MSL]	THICK [m]	Top [mSec]	Base [mSec]	THICK [mSec]	Top Velo.	Base Velo.	Int.Velo.
Stenlille-1	Post Chalk Group	5,0	192,0	-37,0	150,0	187,0		143,0			2098,0	
Stenlille-1	Chalk Group	192,0	1200,0	**150,0**	1158,0	1008,0	143,0	750,0	607,0	2098,0	3088,0	3321,0
Stenlille-1	L. Cretaceous units	1200,0	1247,0	1158,0	1205,0	47,0	750,0	782,0	32,0	3088,0	3082,0	2938,0
Stenlille-1	Jurassic units	1247,0	1507,0	1205,0	1465,0	260,0	782,0	965,0	183,0	3082,0	3036,0	2842,0
Stenlille-1	Fjerritslev Fm	1247,0	1507,0	**1205,0**	1465,0	260,0	782,0	965,0	183,0	3082,0	3036,0	2842,0
Stenlille-1	Triassic units	1507,0	1664,0	1465,0	1622,0	157,0	965,0	1049,0	84,0	3036,0	3092,0	3738,0
Stenlille-1	Gassum Formation	1507,0	1651,0	**1465,0**	1609,0	144,0	965,0	1042,0	77,0	3036,0	3088,0	3740,0
Stenlille-2	Post Chalk Group	5,0	204,0	-43,0	156,0	199,0						
Stenlille-2	Chalk Group	204,0	1198,0	**156,0**	1150,0	994,0		751,0			3063,0	
Stenlille-2	L. Cretaceous units	1198,0	1239,0	1150,0	1192,0	42,0	751,0	781,0	30,0	3062,0	3051,0	2780,0
Stenlille-2	Jurassic units	1239,0	1511,0	1192,0	1463,0	272,0	781,0	972,0	191,0	3051,0	3011,0	2846,0
Stenlille-2	Fjerritslev Fm	1239,0	1511,0	**1192,0**	1463,0	272,0	781,0	972,0	191,0	3051,0	3011,0	2846,0
Stenlille-2	Triassic units	1511,0	1662,0	1463,0	1614,0	151,0	972,0			3011,0		
Stenlille-2	Gassum Formation	1511,0	1658,0	**1463,0**	1610,0	147,0	972,0			3011,0		
Stenlille-3	Post Chalk Group	5,0	204,0	-43,0	156,0	199,0						
Stenlille-3	Chalk Group	204,0	1197,0	**156,0**	1149,0	993,0		751,0			3061,0	
Stenlille-3	L. Cretaceous units	1197,0	1242,0	1149,0	1194,0	45,0	751,0	783,0	32,0	3061,0	3049,0	2781,0
Stenlille-3	Jurassic units	1242,0	1504,0	1194,0	1456,0	262,0	783,0	967,0	184,0	3051,0	3012,0	2848,0
Stenlille-3	Fjerritslev Fm	1242,0	1504,0	**1194,0**	1456,0	262,0	783,0	967,0	184,0	3051,0	3012,0	2848,0
Stenlille-4	Post Chalk Group	5,0	234,0	-33,0	196,0	229,0						
Stenlille-4	Chalk Group	234,0	1166,0	**196,0**	1128,0	932,0		756,0			2983,0	
Stenlille-4	L. Cretaceous units	1167,0	1225,0	1128,0	1187,0	58,0	756,0	799,0	43,0	2985,0	2970,0	2712,0
Stenlille-4	Jurassic units	1225,0	1514,0	1187,0	1476,0	289,0	799,0	998,0	199,0	2970,0	2957,0	2905,0
Stenlille-4	Fjerritslev Fm	1225,0	1514,0	**1187,0**	1476,0	289,0	799,0	998,0	199,0	2970,0	2957,0	2905,0
Stenlille-4	Triassic units	1514,0	1686,0	1476,0	1648,0	172,0	998,0	1093,0	95,0	2957,0	3015,0	3621,0
Stenlille-4	Gassum Formation	1514,0	1660,0	**1476,0**	1622,0	146,0	998,0	1079,0	81,0	2957,0	3006,0	3605,0
Stenlille-5	Post Chalk Group	6,0	202,0	-50,0	146,0	196,0		138,0			2117,0	
Stenlille-5	Chalk Group	202,0	1210,0	**146,0**	1154,0	1008,0	138,0	752,0	614,0	2117,0	3070,0	3284,0
Stenlille-5	L. Cretaceous units	1210,0	1285,0	1154,0	1229,0	75,0	752,0	801,0	49,0	3070,0	3069,0	3049,0
Stenlille-5	Jurassic units	1285,0	1551,0	1229,0	1495,0	266,0	801,0	981,0	180,0	3069,0	3048,0	2952,0
Stenlille-5	Fjerritslev Fm	1285,0	1551,0	**1229,0**	1495,0	266,0	801,0	981,0	180,0	3069,0	3048,0	2952,0
Stenlille-5	Triassic units	1551,0	1718,0	1495,0	1662,0	167,0	981,0	1079,0	98,0	3048,0	3081,0	3414,0
Stenlille-5	Gassum Formation	1551,0	1692,0	**1495,0**	1637,0	142,0	981,0	1067,0	86,0	3048,0	3067,0	3295,0
Stenlille-6	Post Chalk Group	5,0	173,0	-28,0	140,0	168,0		135,0			2077,0	
Stenlille-6	Chalk Group	173,0	1235,0	**140,0**	1202,0	1062,0	135,0	770,0	635,0	2077,0	3123,0	3346,0
Stenlille-6	L. Cretaceous units	1235,0	1293,0	1202,0	1260,0	58,0	770,0	812,0	42,0	3123,0	3103,0	2743,0
Stenlille-6	Jurassic units	1293,0	1564,0	1260,0	1531,0	271,0	812,0	992,0	180,0	3103,0	3086,0	3007,0
Stenlille-6	Fjerritslev Fm	1293,0	1564,0	**1260,0**	1531,0	271,0	812,0	992,0	180,0	3103,0	3086,0	3007,0
Stenlille-6	Triassic units	1564,0	1722,0	1531,0	1689,0	158,0	992,0	1082,0	90,0	3086,0	3122,0	3520,0
Stenlille-6	Gassum Formation	1564,0	1706,0	1531,0	1673,0	142,0	992,0	1074,0	82,0	3086,0	3115,0	3461,0

Table 2. Velocity data from the Stenlille-Havnsø area and the Thisted-Hanstholm area (modified from Nielsen and Japsen, 1991).

	POST	Chalk	Low.Cret	Jurassic	Fjerrit..	Trias	Gassum
Stenlille-1		3321	2938	2842	2842	3738	3740
Stenlille-2			2780	2846	2846		
Stenlille-3			2781	2848	2848		
Stenlille-4			2712	2905	2905	3621	3605
Stenlille-5		3284	3049	2952	2952	3414	3295
Stenlille-6		3346	2743	3007	3007	3520	3461
MIN		*3284*	*2712*	*2842*	*2842*	*3414*	*3295*
GSN		3317	2834	2900	2900	3573	3525
MAX		*3346*	*3049*	*3007*	*3007*	*3738*	*3740*

	POST	Chalk	Low.Cret	Jurassic	Fjerrit..	Trias	Gassum
Felicia-1		2702		2683	2683	3587	2726
Thisted-1							
Thisted-2	2067	2733	2677	2677	2677	3271	2688
Thisted-3							
Thisted-4		2759	2700	2605	2605	3409	2603
MIN	*2067*	*2702*	*2677*	*2605*	*2605*	*3271*	*2603*
GSN	2067	2731	2689	2655	2655	3422	2672
MAX	*2067*	*2759*	*2700*	*2683*	*2683*	*3587*	*2726*

Table 3. Time, depth, and interval velocity correlation between different well picks in Stenlille wells based on 1D forward modelling. Synthetic seismograms for the Stenlille wells are presented in Appendix 1 for reference purposes.

Wells	Surface	Depth	MD	TWT (ms)	OWT (ms)	Interval velocity
Stenlille-01	Base Gassum	-1609.4	1651	1042	521	1584.452975
Stenlille-02	Base Gassum	-1605.1	1652.8	1069.82	534.91	1544.932792
Stenlille-04	Base Gassum	-1617.14	1655.54	1076.53	538.265	1537.848458
Stenlille-05	Base Gassum	-1638.86	1694.76	1068.68	534.34	1585.844219
Stenlille-06	Base Gassum	-1672.82	1705.82	1073.9	536.95	1588.434677
Stenlille-10	Base Gassum	-1631.11	1672.61	1063.39	531.695	1572.903638
Stenlille-12	Base Gassum	-1707.41	1753.13	1056.06	528.03	1660.066663
Stenlille-13	Base Gassum	-1779.09	1824.81	1056.64	528.32	1726.99311
Stenlille-14	Base Gassum	-1740.08	1785.8	1054.61	527.305	1693.327391
Stenlille-15	Base Gassum	-1624.16	1676.96	1095.69	547.845	1530.505891
Stenlille-18	Base Gassum	-1666.19	1713.79	1062.25	531.125	1613.358437
Stenlille-19	Base Gassum	-1602.99	1706	1062.97	531.485	1604.93711
Stenlille-01	Top Fjerritslev	-1205.94	1247.54	768.85	384.425	1622.60519
Stenlille-02	Top Fjerritslev	-1229.92	1277.62	766	383	1667.911227
Stenlille-04	Top Fjerritslev	-1186.32	1224.72	778.16	389.08	1573.866557
Stenlille-06	Top Fjerritslev	-1260.06	1293.06	775	387.5	1668.464516
Stenlille-10	Top Fjerritslev	-1250.83	1292.33	772.62	386.31	1672.659263
Stenlille-19	Top Fjerritslev	-1284.14	1386.11	765.8	382.9	1810.01567
Stenlille-01	Top Gassum	-1465.4	1507	965	482.5	1561.658031
Stenlille-02	Top Gassum	-1464.03	1511.73	972.5	486.25	1554.478149
Stenlille-04	Top Gassum	-1475.84	1514.24	998.13	499.065	1517.076934
Stenlille-05	Top Gassum	-1494.71	1550.61	980.74	490.37	1581.061239
Stenlille-06	Top Gassum	-1534.29	1567.29	993.9	496.95	1576.909146
Stenlille-10	Top Gassum	-1482.47	1523.97	976.52	488.26	1560.613198
Stenlille-12	Top Gassum	-1530.63	1576.35	970.64	485.32	1624.031567
Stenlille-13	Top Gassum	-1597.09	1642.81	970.64	485.32	1692.501854
Stenlille-14	Top Gassum	-1568.91	1614.63	972.18	486.09	1660.834413
Stenlille-15	Top Gassum	-1470.7	1523.5	1011.97	505.985	1505.479411
Stenlille-18	Top Gassum	-1516.54	1564.14	975.27	487.635	1603.802024
Stenlille-19	Top Gassum	-1458.03	1561	975.62	487.81	1600.0082
Stenlille-01	Top Vinding	-1609.41	1651.01	1042.01	521.005	1584.447366
Stenlille-19	Top Vinding	-1602.99	1706	1062.97	531.485	1604.93711

Table 4 Time, depth, and interval velocity correlation between different well picks in Felicia-1, Thisted-1 to -4 and J-1 based on 1D forward modelling. Synthetic seismograms for these wells are presented in Appendix 1 for reference purposes.

Wells	Surface	Depth	MD	TWT (ms)	OWT (ms)	Interval velocity
Felicia-1	Top Vinding	-1734.71	1775	1273	636.5	1394.344069
Thisted-1	Top Vinding	-835.3	871	676.77	338.385	2573.991164
Thisted-2	Top Vinding	-1254.1	1290	933	466.5	1382.636656
Thisted-4	Top Vinding	-853.9	891	704	352	1265.625
Felicia-1	Top Gassum in DNB	-1504.76	1545	1122	561	1377.005348
J-1	Top Gassum in DNB	-1696.6	1734	1356	678	1278.761062
Thisted-1	Top Gassum in DNB	-710.3	746	580.95	290.475	2568.207247
Thisted-2	Top Gassum in DNB	-1119.1	1155	836	418	1381.578947
Thisted-3	Top Gassum in DNB	-1092.8	1127	831.28	415.64	1355.740545
Thisted-4	Top Gassum in DNB	-739.9	777	615.89	307.945	1261.58892
Felicia-1	Top Fjerritslev	-961.86	1002	732	366	1368.852459
J-1	Top Fjerritslev	-1073.96	1111.3	951	475.5	1168.559411
Thisted-1	Top Fjerritslev	-600.3	636	484.88	242.44	2623.329484
Thisted-2	Top Fjerritslev	-1028.1	1064	768	384	1385.416667
Thisted-3	Top Fjerritslev	-986.8	1021	747.73	373.865	1365.466144
Thisted-4	Top Fjerritslev	-621.9	659	514.07	257.035	1281.926586

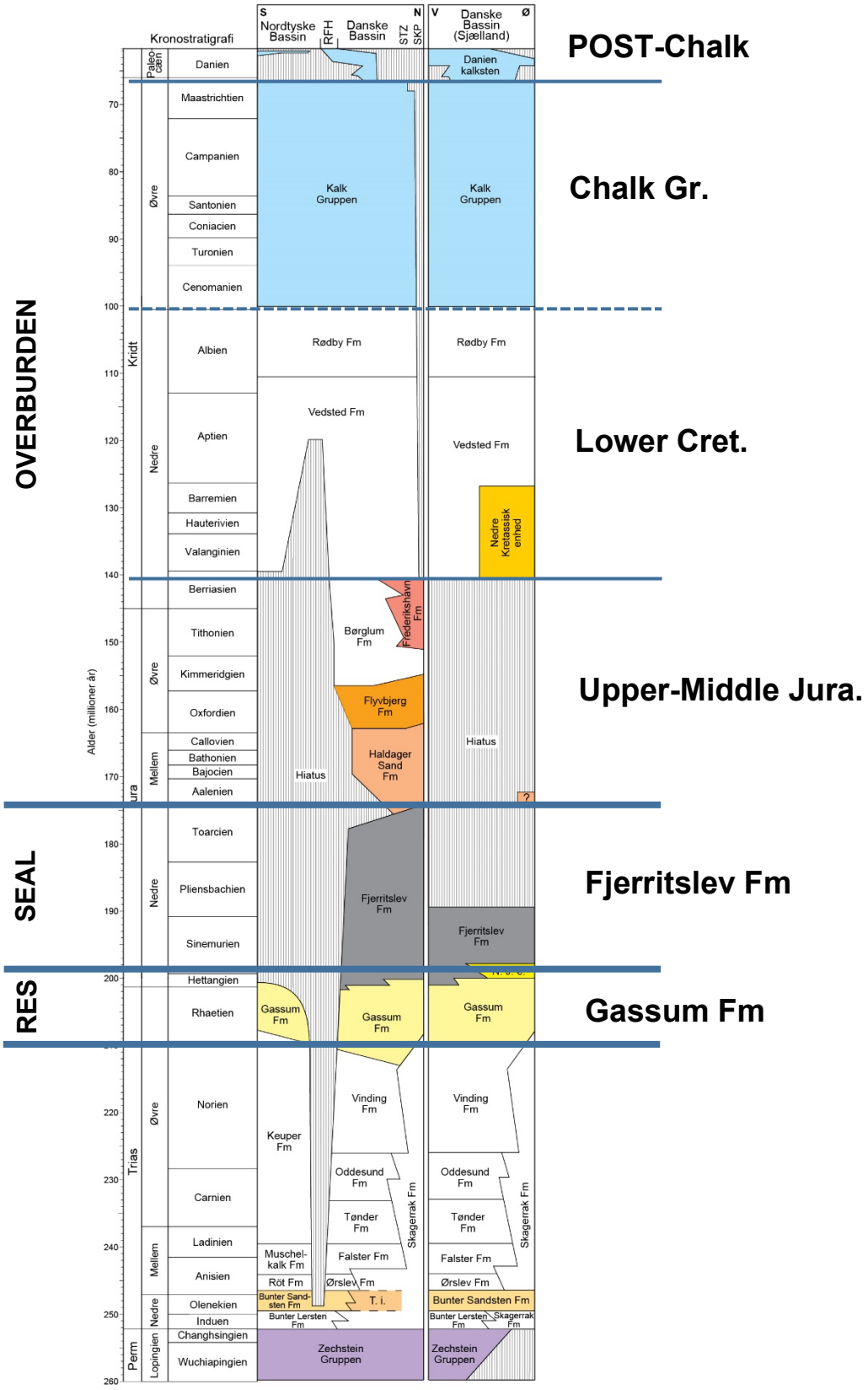

Figure 1. *The Lithostratigraphic subdivision of the Danish onshore area. Notice the stratigraphic position of the seal (Fjerritslev Fm.) and the reservoir (Gassum Fm.).*

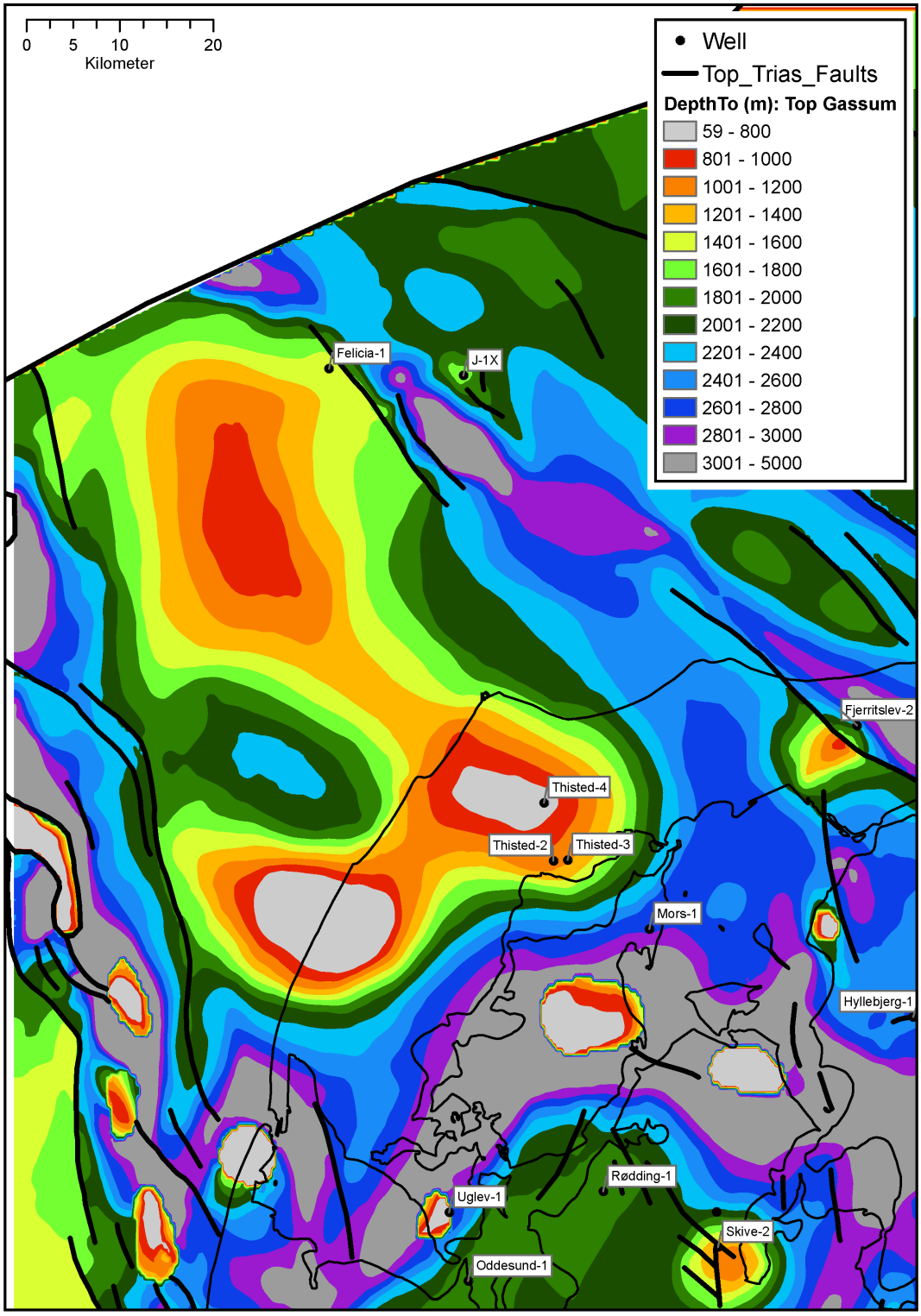

Figure 2. *Depth to top reservoir in the North Jutland area. Depth converted top Gassum Formation depth map (modified map from, Japsen, P. & Langtofte, C., 1991b).*

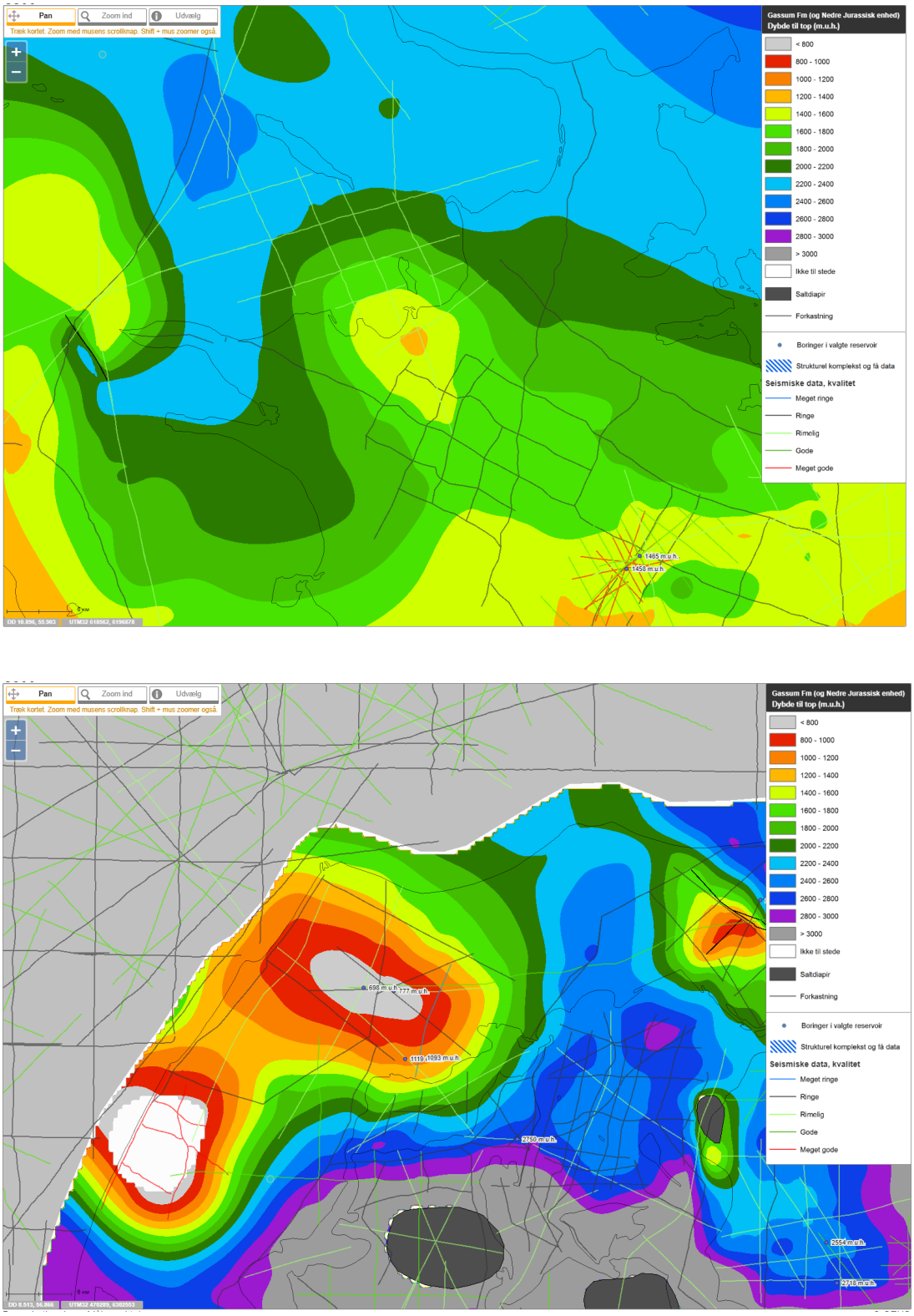

Figure 3. *Depth to top reservoirs in the Stenlille-Havnsø (upper map) and Thisted-Hanstholm area. Notice the coverage of seismic data (black lines), and that the area between the coast and the Hanstholm structure (lower map) was not part of the 2015 3D mapping campaign. The maps modified from the Geothermal WebGIS portal (modified from Vosgerau et al., 2016).*

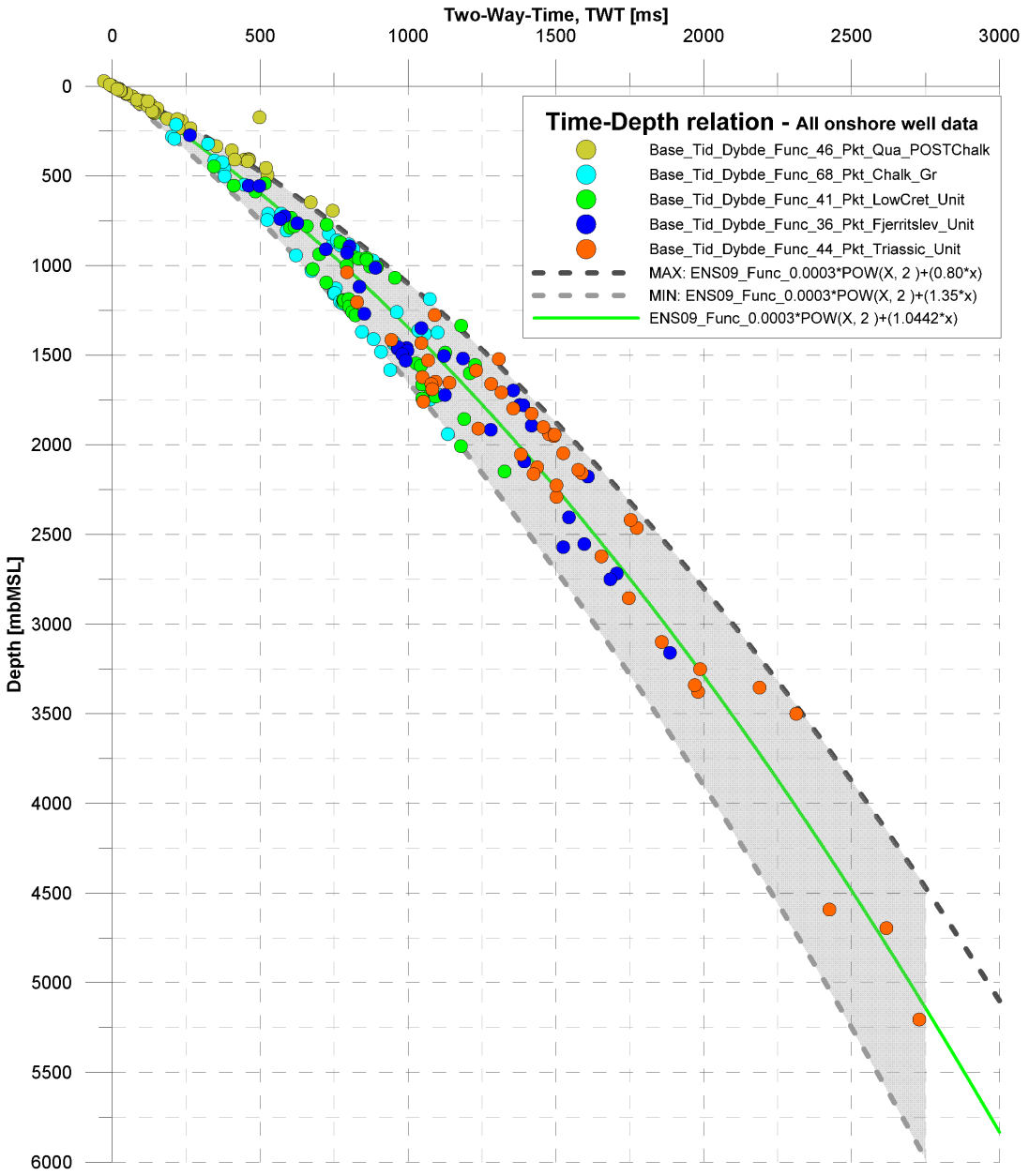

Figure 4. *Time-depth relation based on velocity data for all Danish onshore and near-shore wells and for all lithostratigraphic units. Notice the best fitted polynomial function (green line) and minimum and maximum functions adjusted to cover all data. Notice that there are no clear regional velocity inversions. Data are from Nielsen and Japsen, 1991.*

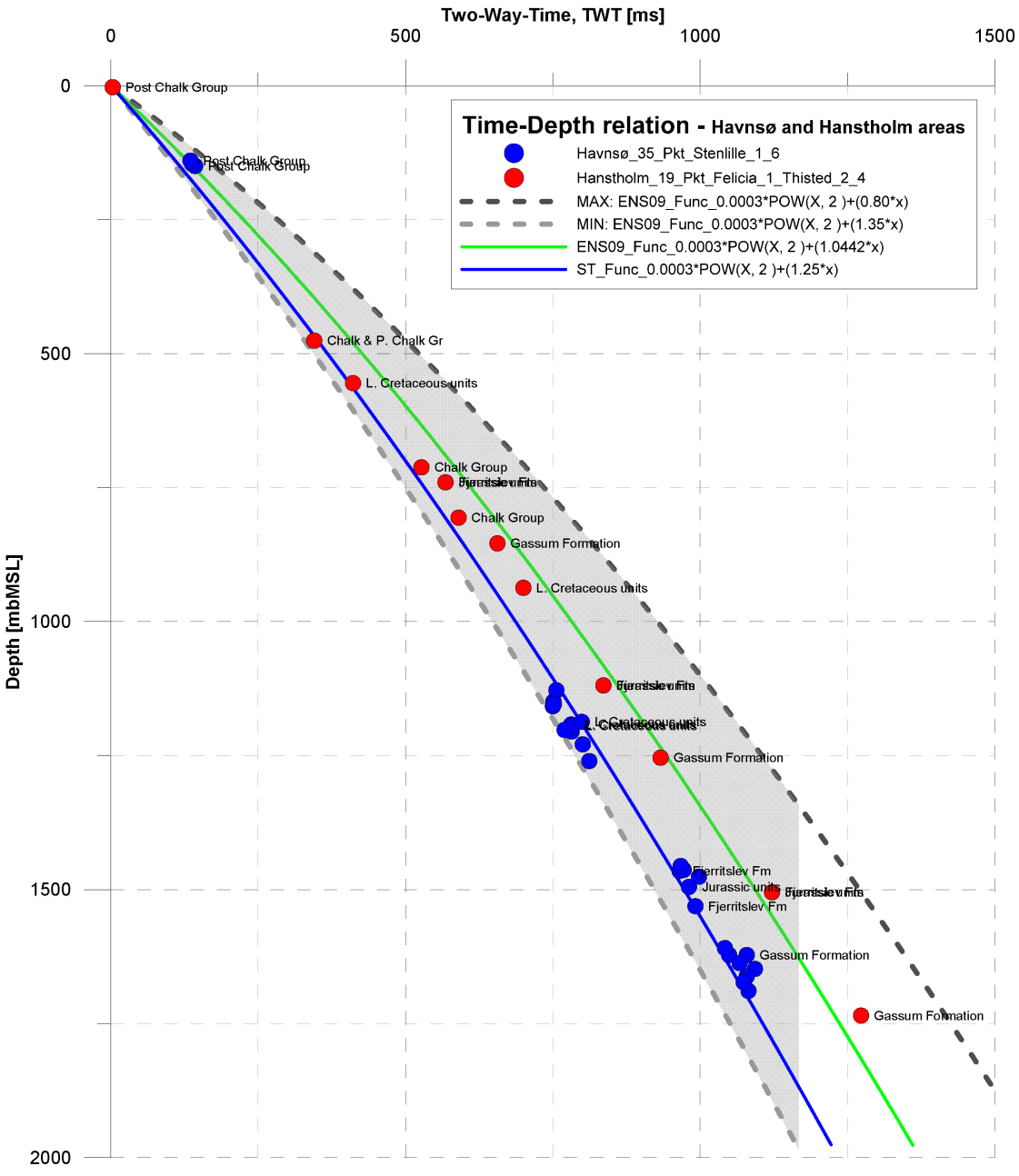

Figure 5. *Comparison of time-depth well velocity data in Havnsø (blue dots) and Hanstholm (red dots) areas. The relations are based on data covering the POST-Chalk down to the Jurassic lithostratigraphic units from the Stenlille-1 to Stenlille-6 wells in the Havnsø area and Felicia-1, Thisted-2 and -4 in the Hanstholm area (see Figure 2 for lithostratigraphic subdivisions) The green line is the best fitted polynomial function in the Hanstholm area, while the blue fitted polynomial function represents the Havnsø area. The two gray dotted curves represent the Min and Max time-depth functions within the two areas. Data are from Nielsen and Japsen, 1991.*

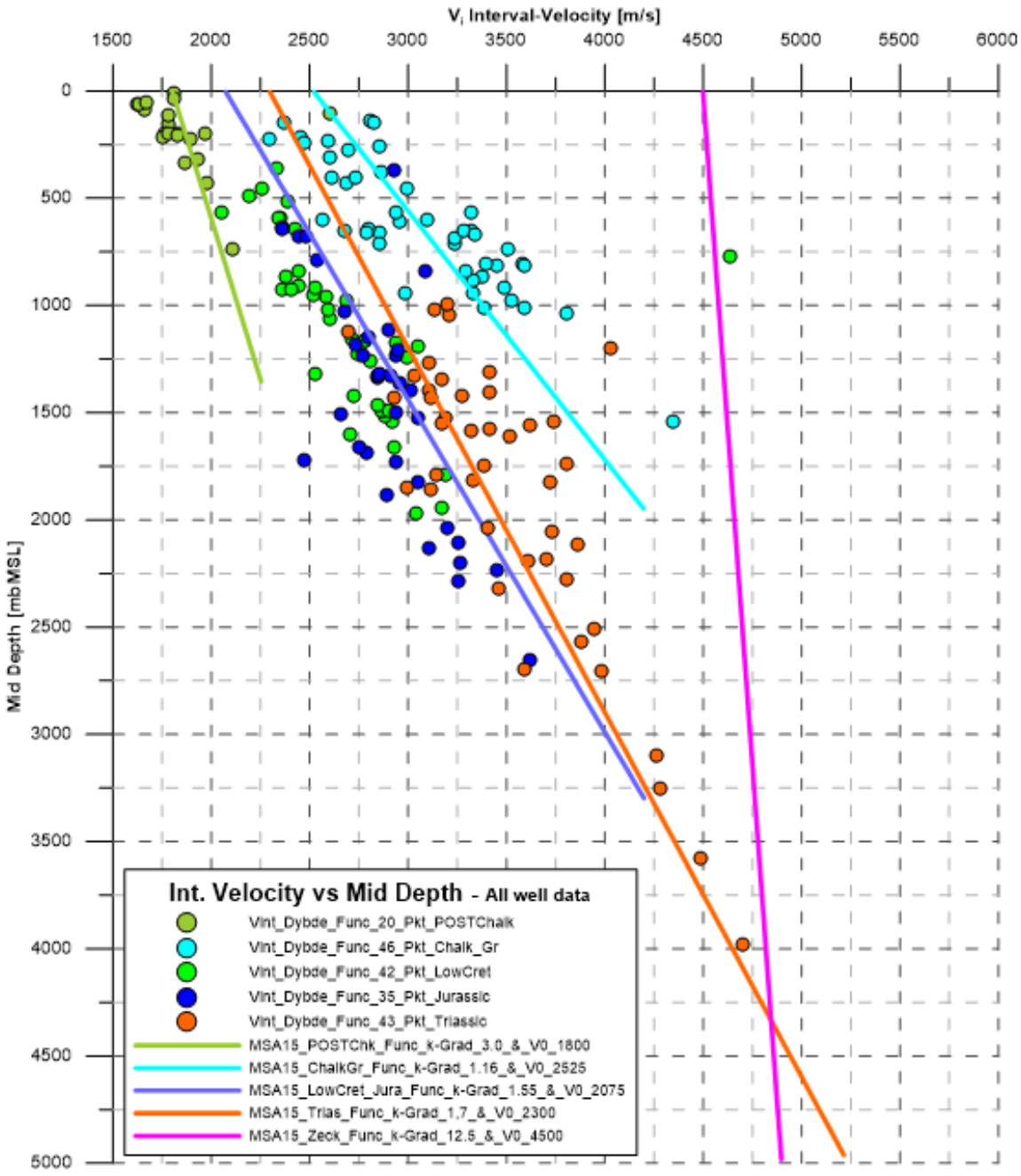

Figure 6. *Comparison of interval velocities vs. mid depth (mbMSL) for all Danish onshore and near-shore wells and for all lithostratigraphic units excluding the Zechstein and Pre-Permian data. Notice the cluster of the lithostratigraphic units and the best fitted linear functions (POST_Chalk, dark green dots and line; Chalk Group, light blue dots and line; Lower Cretaceous and Jurassic units, light green and blue dots and line; Triassic units, orange dots and line). The plot shows the velocity functions for the V0_k velocity model used for the depth converted maps in the Geothermal WebGIS Portal including the function for the Zechstein and Pre-Permian data (magenta line). Data are from Nielsen and Japsen (1991).*

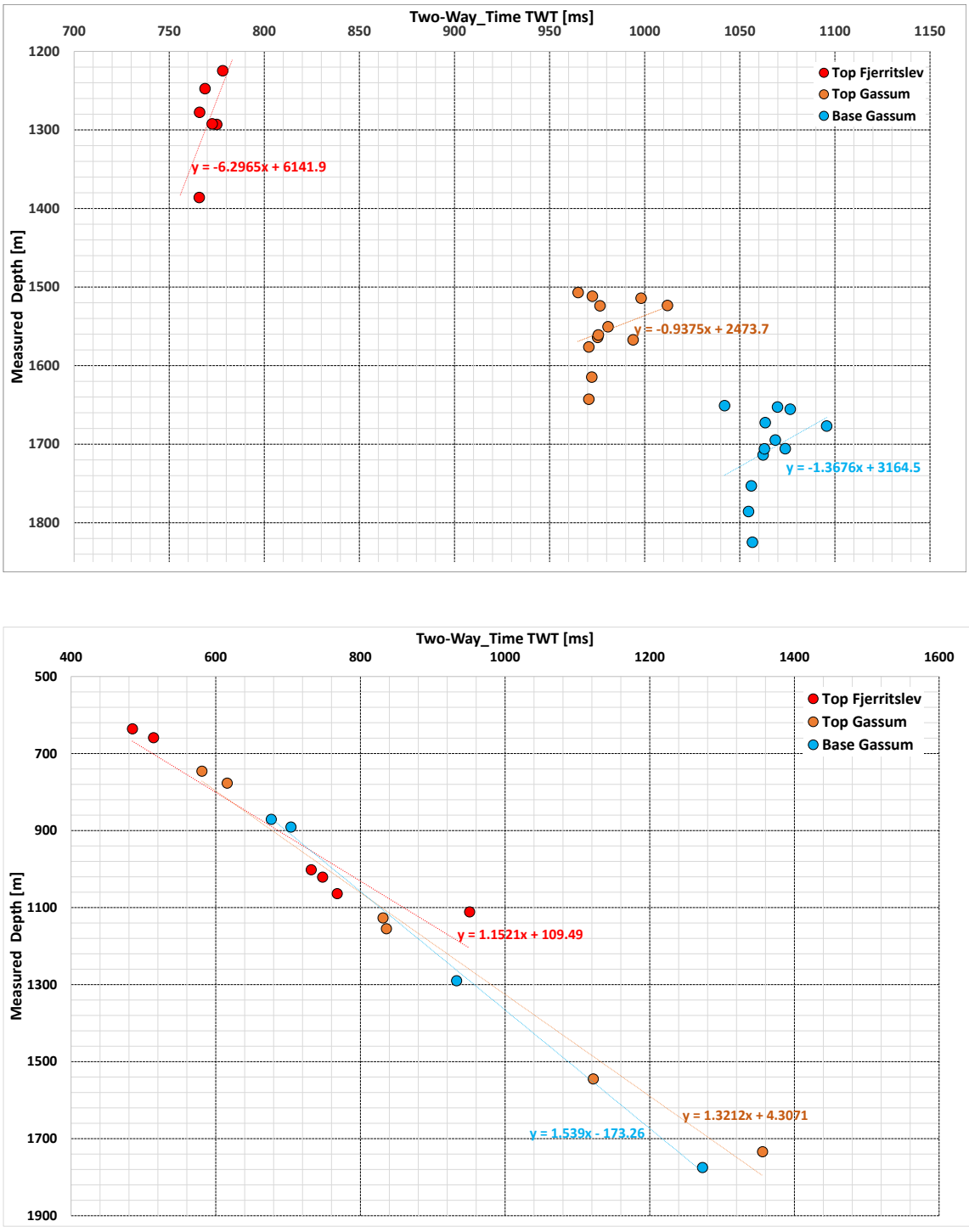

Figure 7. *Comparison of time-depth well velocity data in Havnsø area based on Stenlille wells (upper plot) and in the Hanstholm area based on Felicia-1, J-1 and Thisted-1 to -4 (lower plot). Red, orange, and blue dots represent the interval velocity values for the Top Fjerritslev Fm, Top Gassum Fm, and Base Gassum Fm respectively. The time depth relationships are based on 1D forward modelling where reflection coefficient series for each well is convolved with a model wavelet to generate synthetic seismogram for the well, which is then tied to respective seismic signatures (see also Appendix 1). Notice that the scatter of velocities with depth is less in the Havnsø than in the Hanstholm area, possible due to the closer density of the Stenlille wells in the Havnsø area.*

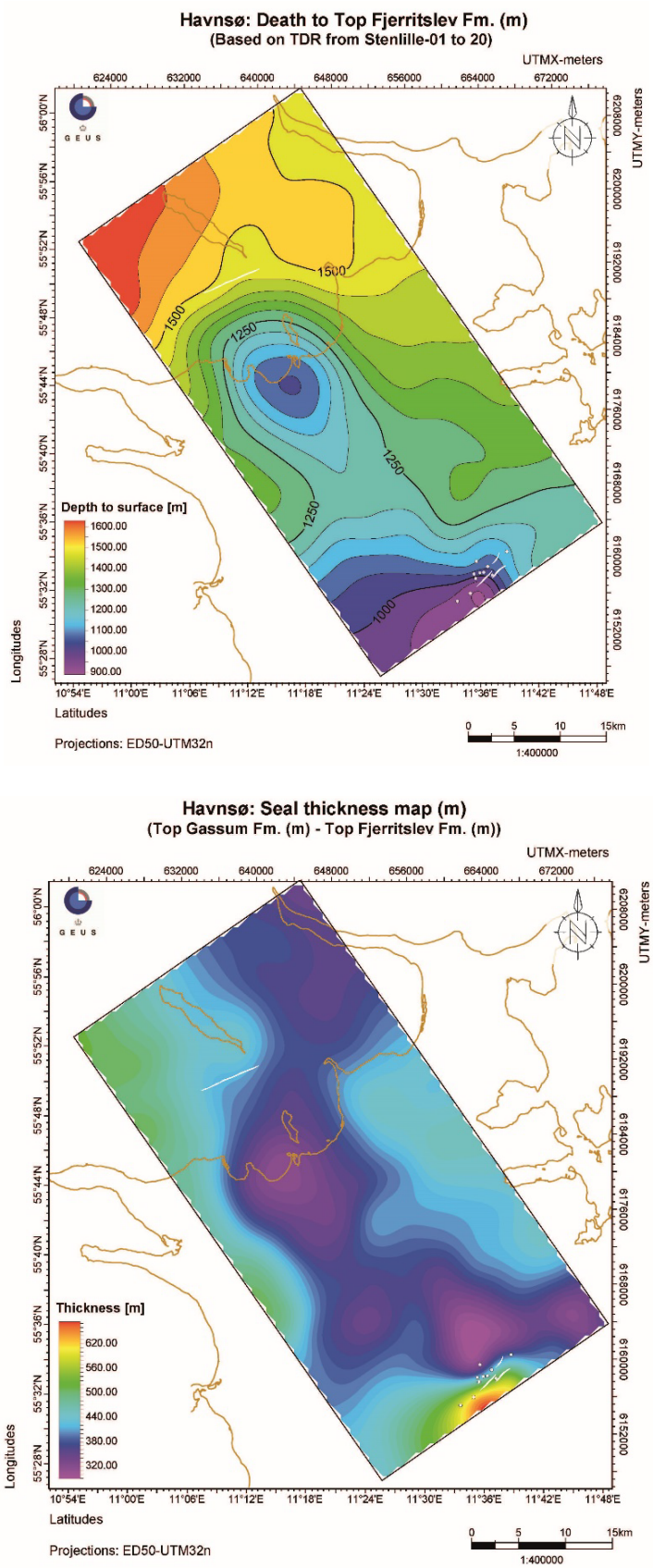

Figure 8. *Depth to top seal and seal thickness in the Havnsø area. Depth converted top Fjerritslev depth map (upper map) and the isochore map of the Fjerritslev Formation (lower map) (based on seismic time-structure and time-isochore map from Gregersen et al. 2020).*

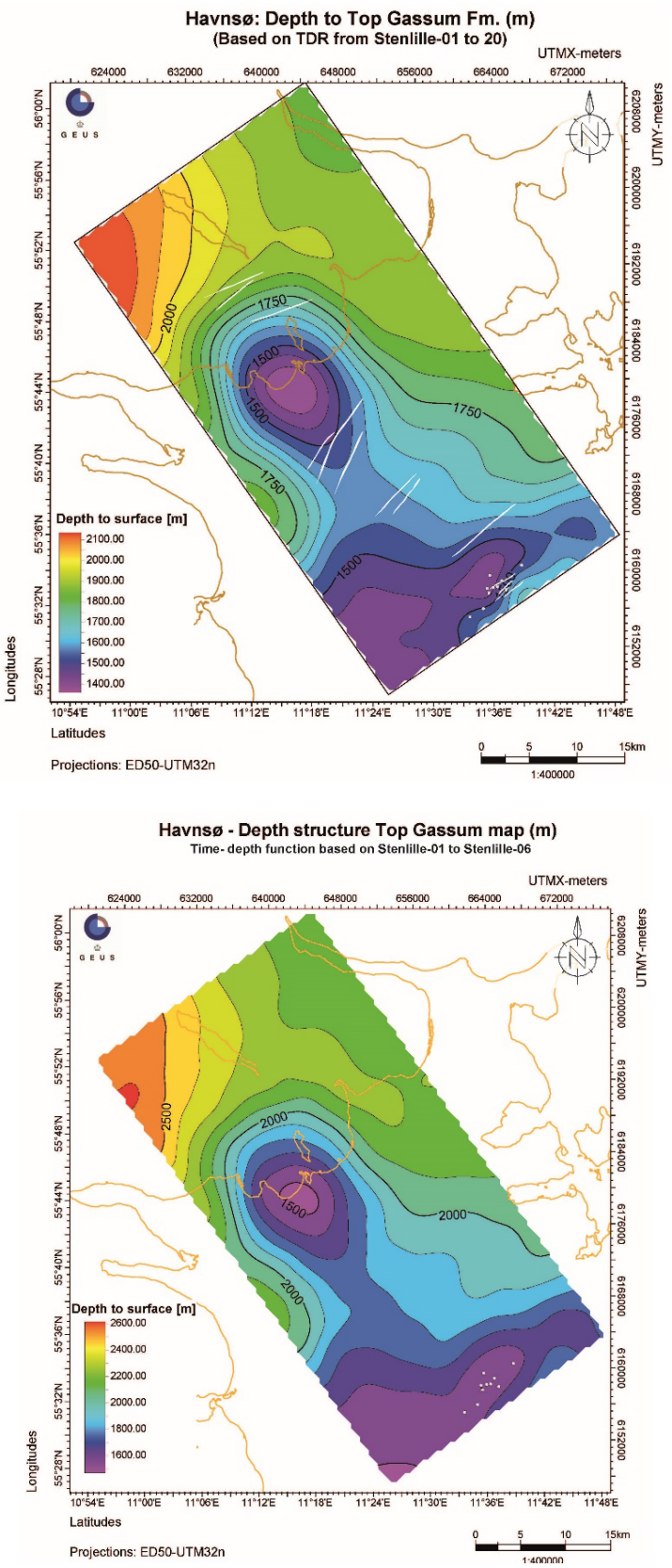

Figure 9. *Depth to top of the reservoir in the Havnsø area. The depth map on the top is based on newly constructed velocity function obtained from time-depth relationships in the Stenlille-1 to -20 wells (see Table 3). The depth map on the bottom is based on velocity function for stenlille-1 to -6 based on deep wells database (see Table 1).*

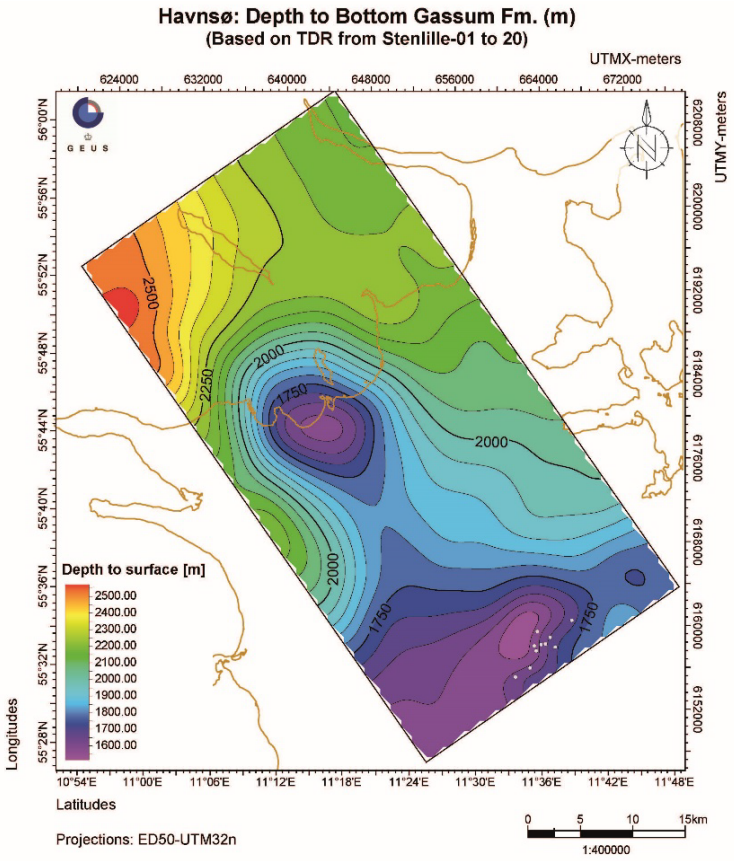

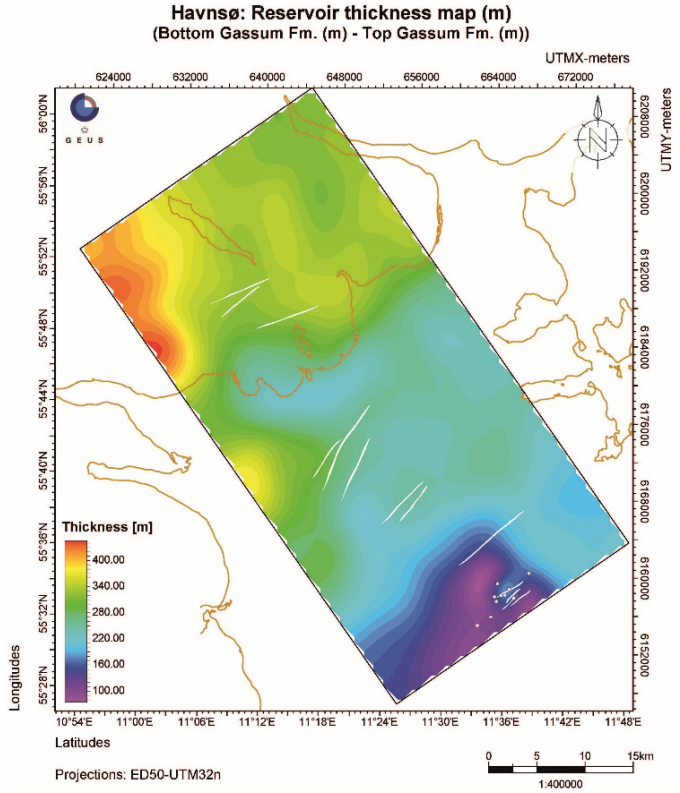

Figure 10. *Depth to base reservoir and reservoir thickness in the Havnsø area. Depth converted base Gassum Formation depth map (upper map) and the isochore map of the Gassum Formation (lower map) (based on seismic time-structure and time-isochore map from Gregersen et al. 2020).*

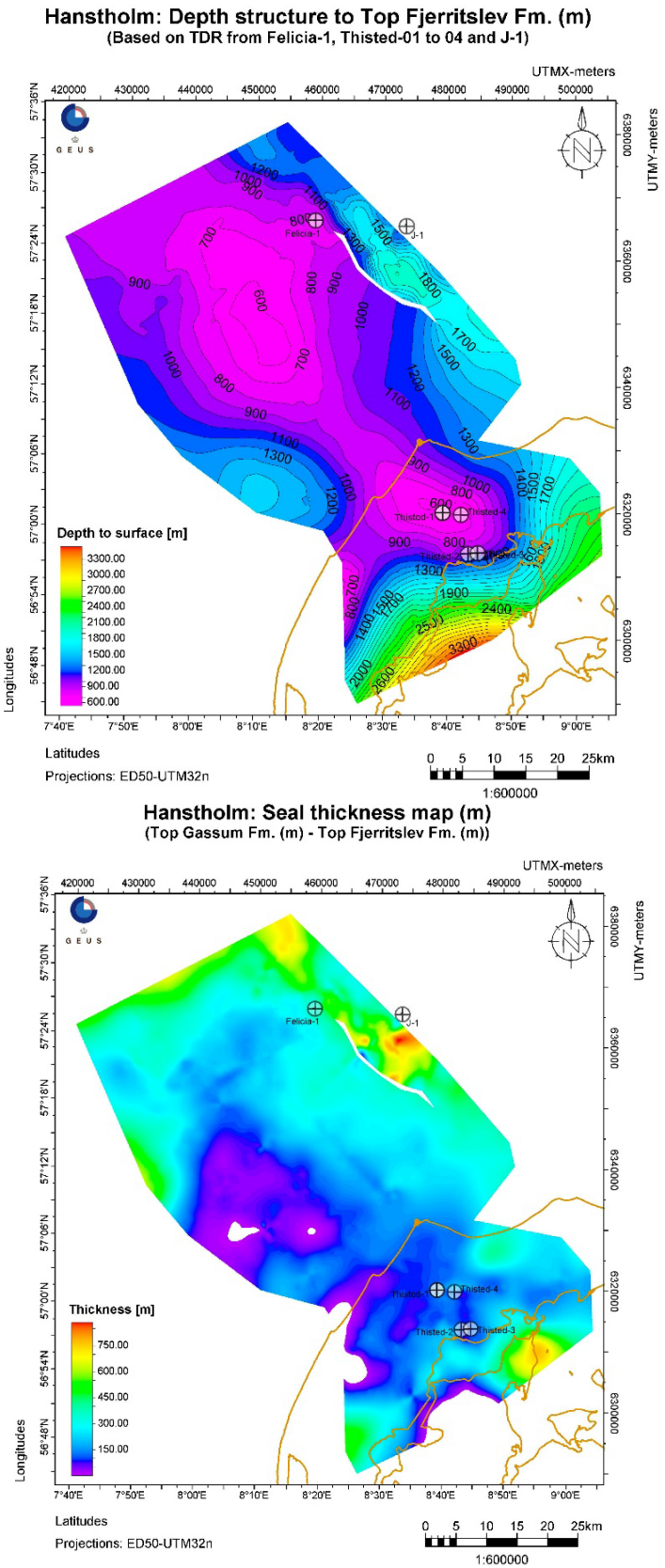

Figure 11. *Depth to top seal and seal thickness in the Hanstholm area. Depth converted top Fjerritslev depth map (upper map) and the isochore map of the Fjerritslev Formation (lower map) (based on seismic time-structure and time-isochore map from Rasmussen & Laghari 2020).*

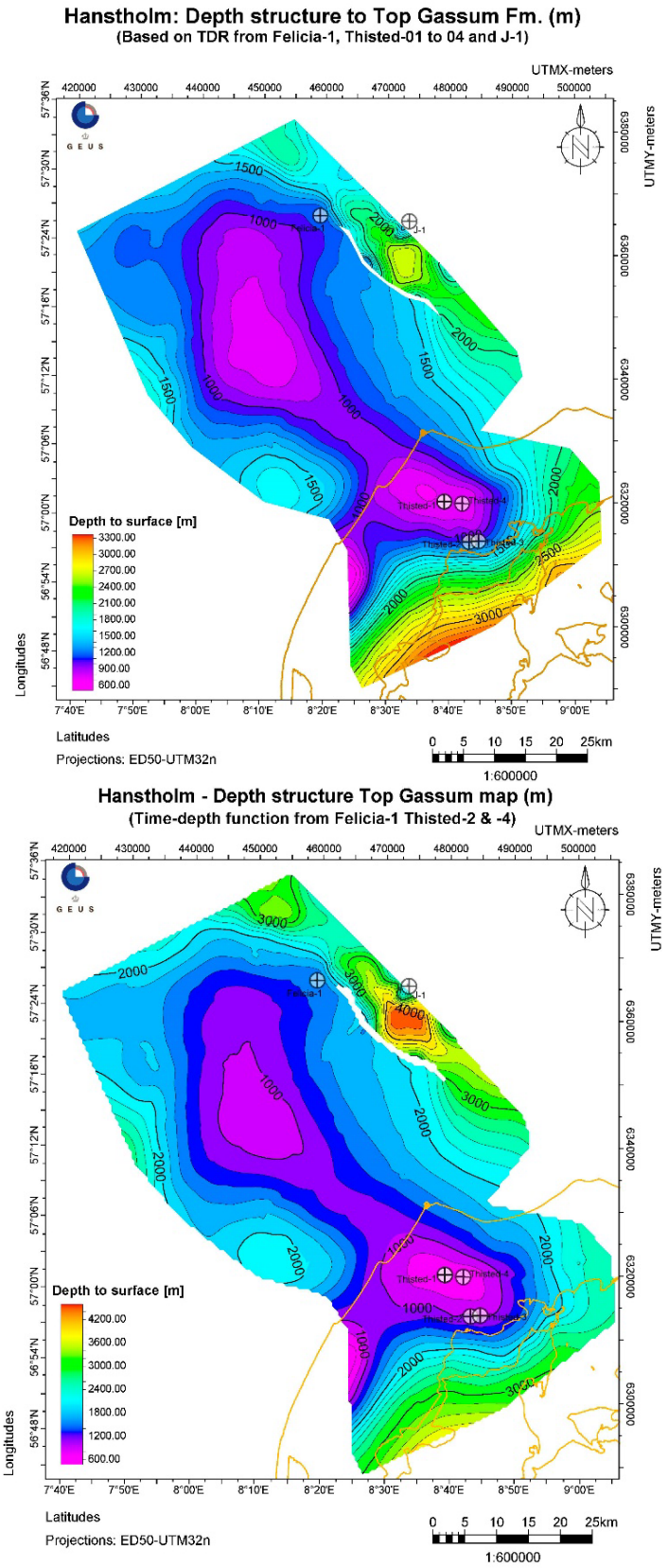

Figure 12. *Depth to top of reservoir in the Hanstholm area. The map on the top is based on newly constructed velocity function obtained from time-depth relationships in the Felicia-1, J-1 and the Thisted-1 to -4 wells (see Table 4). The map of the bottom is based on velocity function for Felicia-1, Thisted-2 and Thisted-4 based deep wells database (see Table 1).*

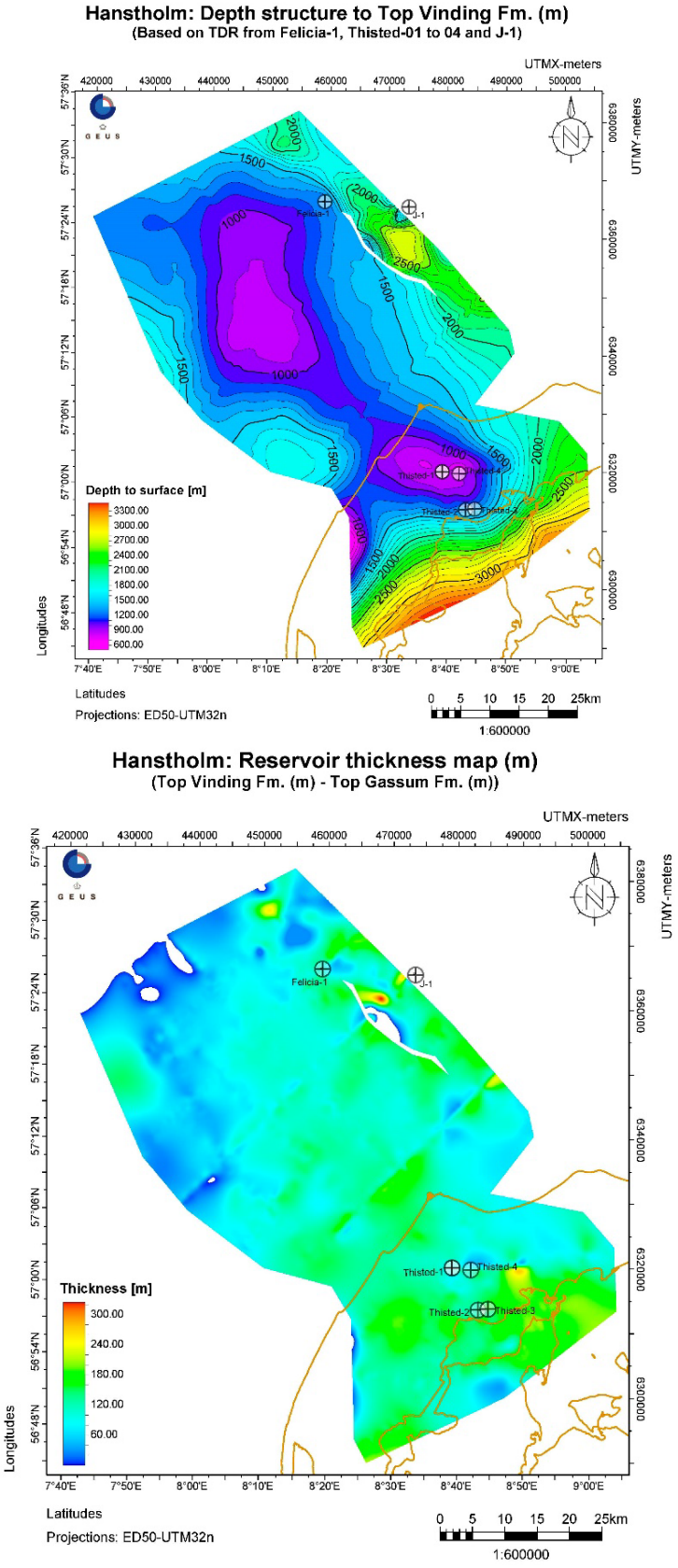

Figure 13. *Depth to base reservoir and reservoir thickness from the Hanstholm area. Depth converted Top Vinding Formation (base Gassum Fm) depth map (upper map) and the isochore map of the Gassum Fm (lower map) (based on seismic time-structure and time-isochore map from Rasmussen & Laghari 2020).*

Appendix 1 Time-depth relations

Table APP1.1: *Data used to create time-depth relationships for different Stenlille wells and Thisted-1 to -4. The red cell with a value of 0 represents non-availability of that wireline-log, whereas the green cell with value of 1 indicates the availability of that log.*

Borehole	Sonic Log	Density log	Computed sonic log	Computed density log
Stenlille - 01	1	0	0	1
Stenlille - 02	1	0	0	1
Stenlille - 04	0	0	1	1
Stenlille - 05	0	0	1	1
Stenlille - 06	0	0	0	0
Stenlille - 10	0	0	1	1
Stenlille - 12	0	0	1	1
Stenlille - 13	0	0	1	1
Stenlille - 14	0	1	1	0
Stenlille - 15	0	0	1	1
Stenlille - 17	0	0	1	1
Stenlille - 18	0	0	1	1
Stenlille - 19	1	0	0	1
Stenlille - 20	0	0	1	1
Thisted-1	1	1	0	0
Thisted-2	1	1	0	0
Thisted-3	1	1	0	0
Thisted-4	1	1	0	0

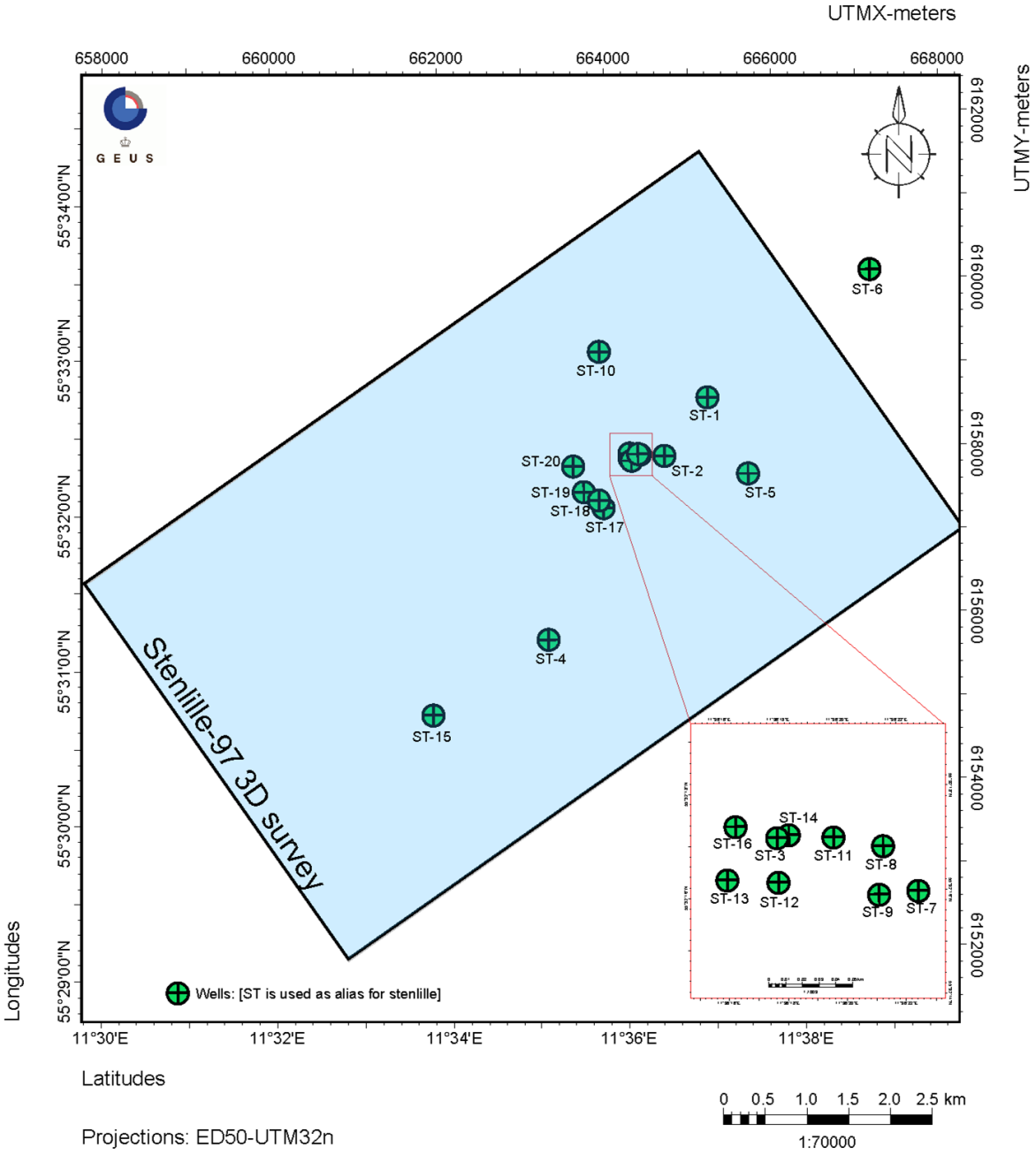

Figure APP1.1: Basemap for the study area showing the spatial distribution of all 20 Stenlille wells over Stenlille 3D seismic volume. Only Stenlille-6 is located outside the limits of 3D seismic volume.

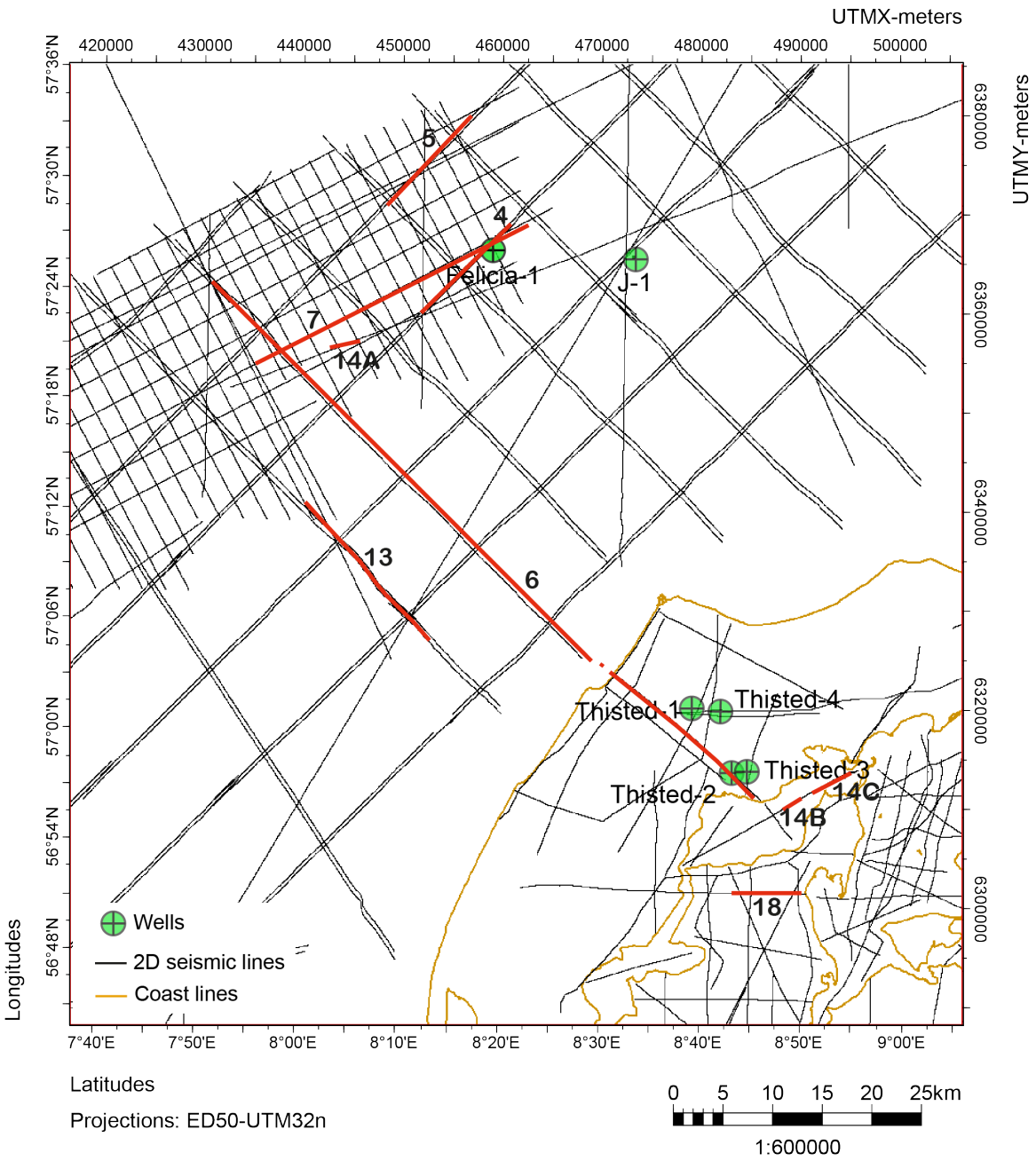

Figure APP1.2: Basemap for the Hanstholm study area showing the spatial distribution of wells covering the Hanstholm structural area.

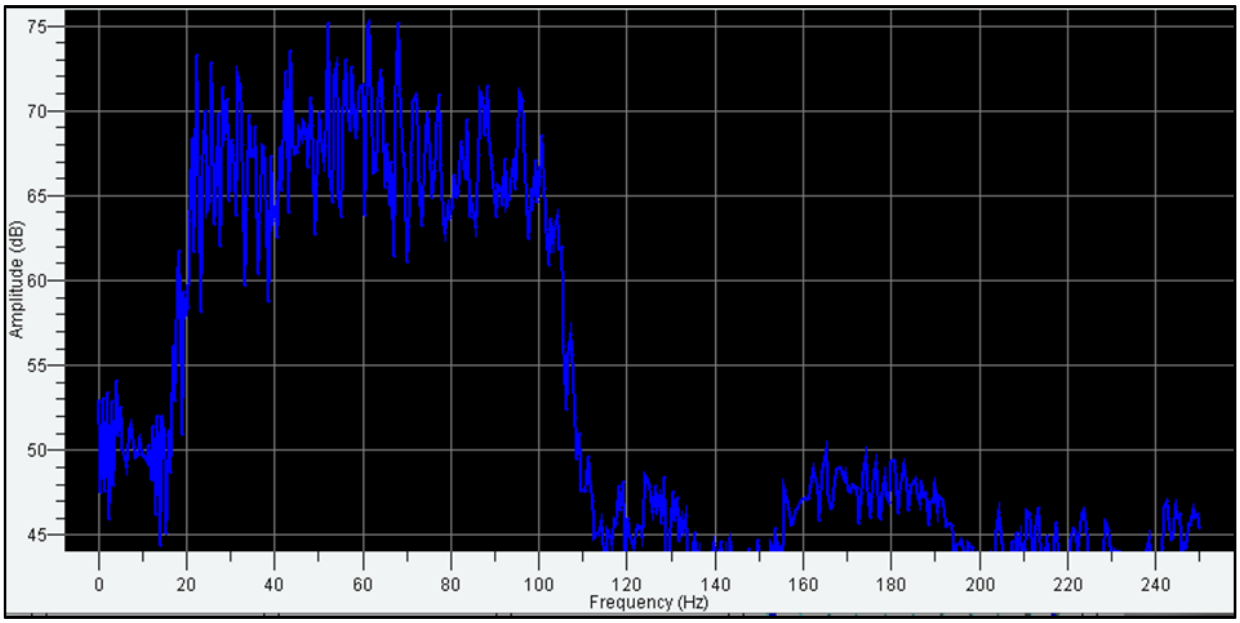

Figure APP1.3: Amplitude spectrum for Stenlille 3D seismic cube. Dominant frequencies throughout the cube are located within the range of 40 to 70 Hertz. Overall, the seismic cube has very high temporal and spatial resolution and a very high signal to noise ratio.

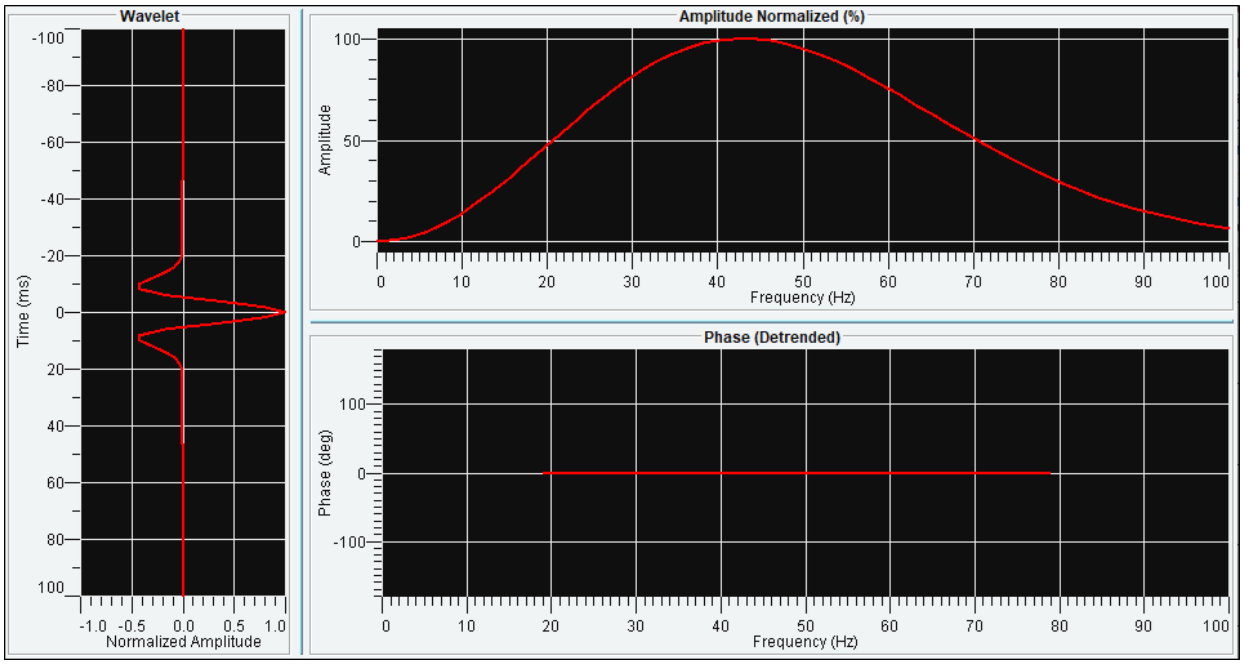

Figure APP1.4: Amplitude spectrum for the model ricker wavelet used to generate synthetic seismograms for Stenlille wells. Ricker wavelet of 45 Hertz was convolved with reflection coefficient series along the Stenlille boreholes to accurately tie Stenlille wells and thereby generate accurate time depth relationships.

TDR: Stenlille-2

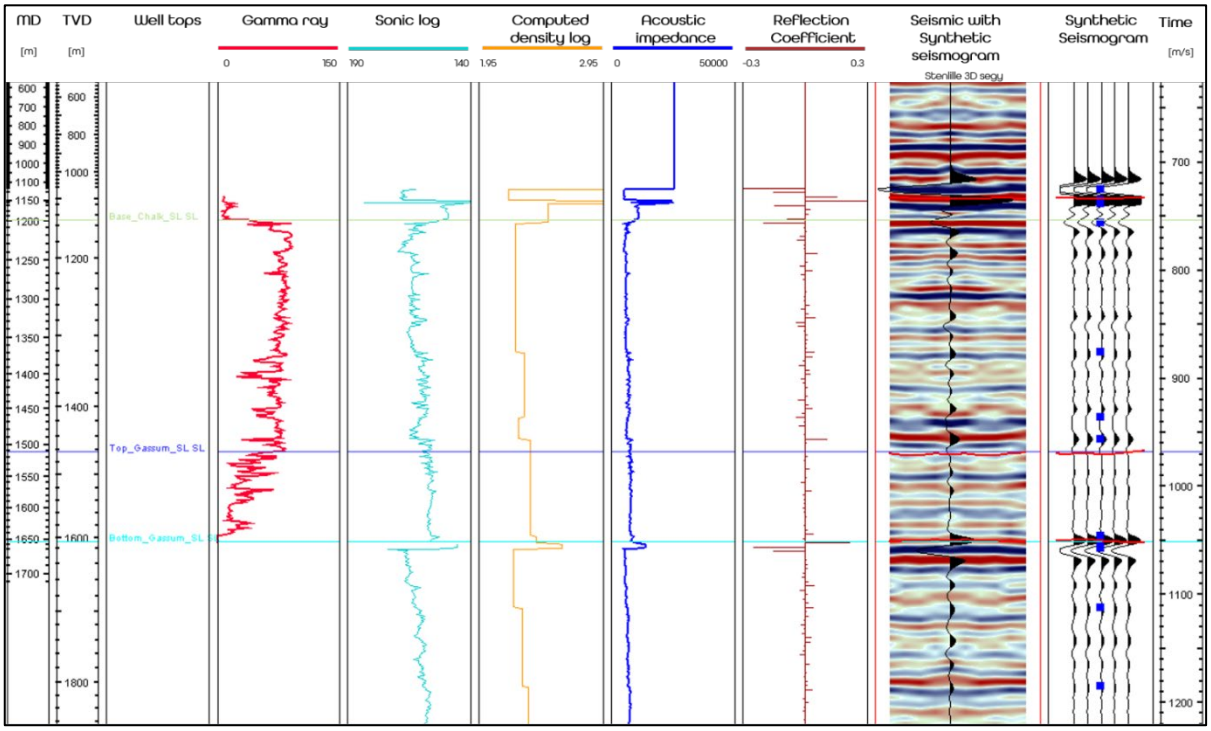

Figure APP1.5: In case of Stenlille-2, sonic log was available, however density log was missing. Sonic log was used to compute the density log using Gardner empirical relationship.

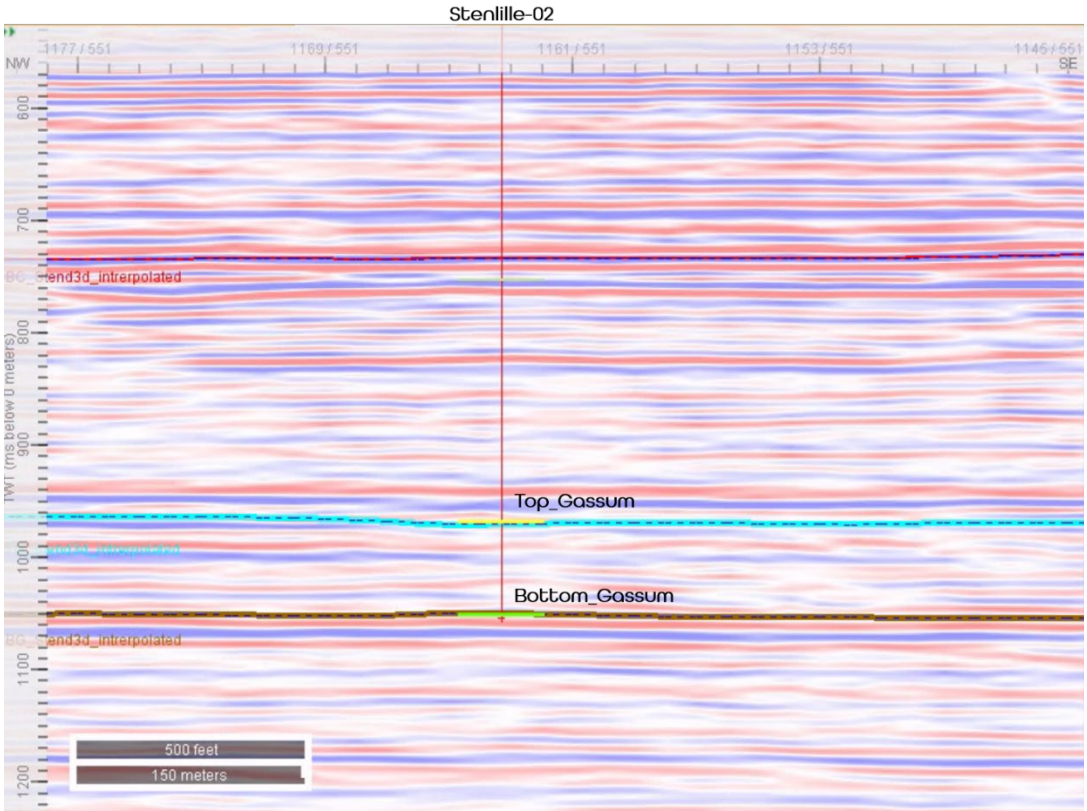

Figure APP1.6: Crossline 551 intersecting Stenlille-2. Both well picks i.e. Top Gassum and Bottom Gassum are tied to interpreted seismic horizons for the top and base Gassum.

TDR: Stenlille-10

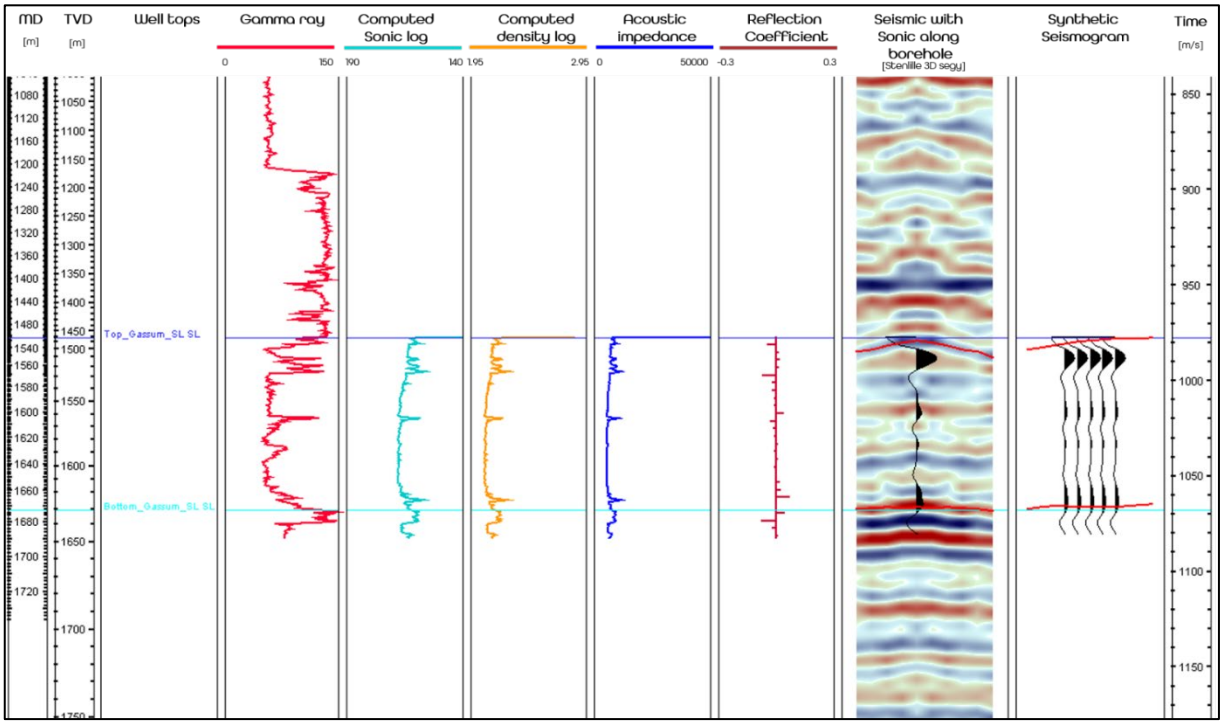

Figure APP1.7: Both sonic and density log were not available for Stenlille-10. Sonic was computed using resistivity log and there after density was computed from computed sonic log and used to computed reflection coefficient series for subsurface along Stenlille-10.

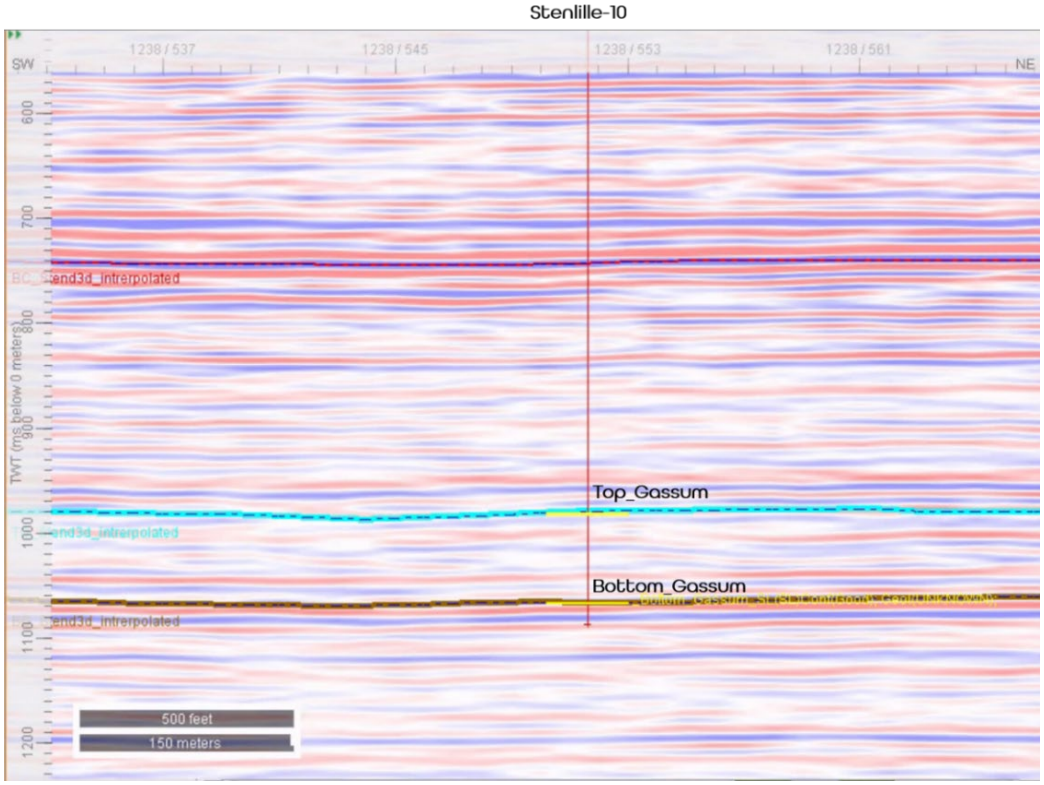

Figure APP1.8: Inline 1238 intersecting Stenlille-10. Both well picks i.e. Top Gassum and Bottom Gassum are tied to interpreted seismic horizons for the top and base Gassum.

TDR: Stenlille-12

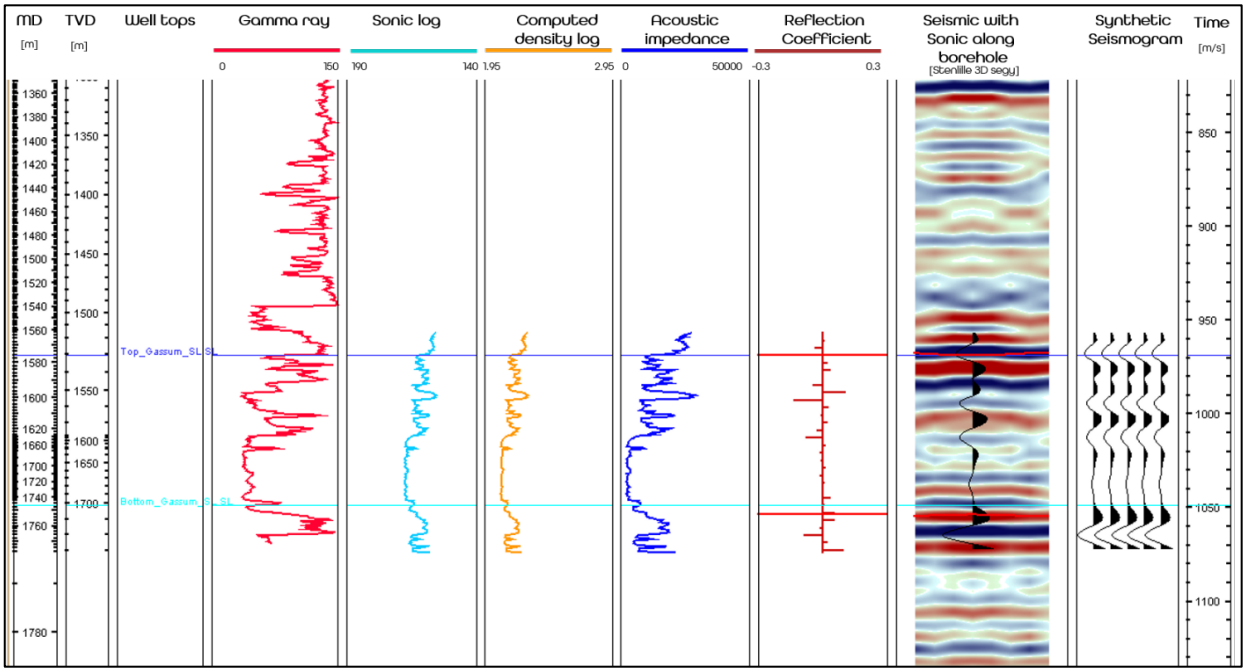

Figure APP1.9: Both sonic and density log were not available for Stenlille-12. Sonic was computed using resistivity log and there after density was computed from computed sonic log. Reflection coefficient series along Stenlille-12 was computed using computed sonic log and computed density log and was convolved with ricker wavelet of 45 Hz to generate synthetic seismogram along the borehole.

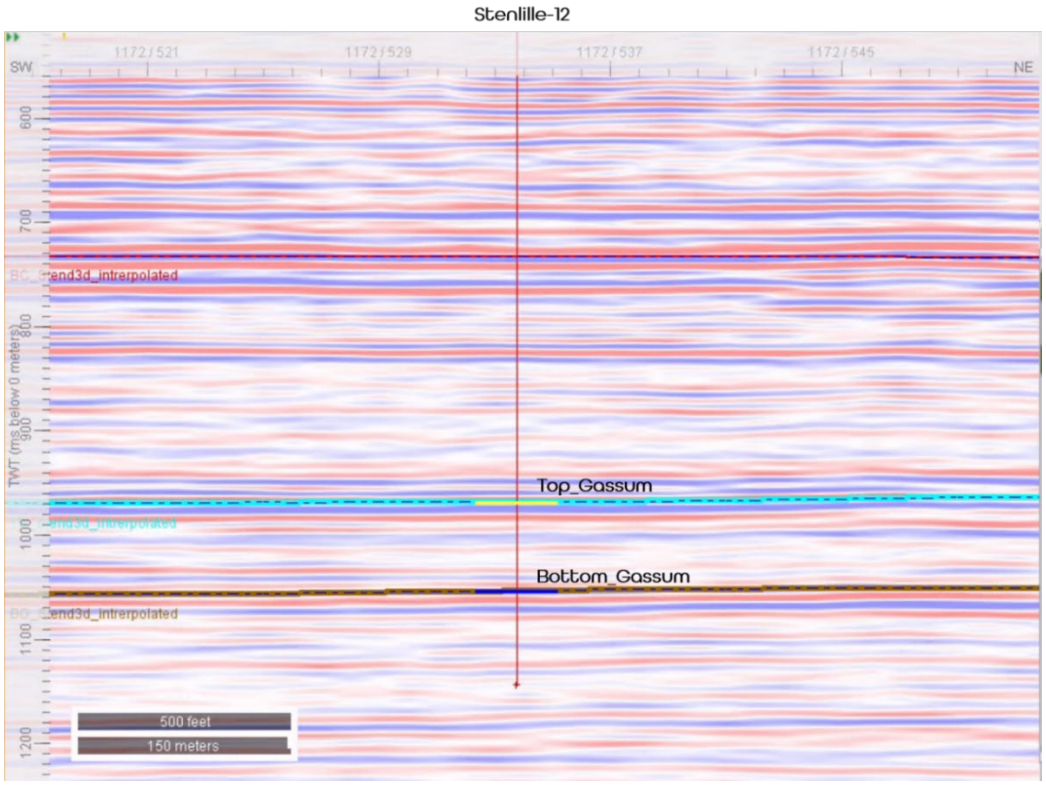

Figure APP1.10: Inline 1172 intersecting Stenlille-12. Both well picks i.e. Top Gassum and Bottom Gassum are tied to interpreted seismic horizons for the top and bottom Gassum.

TDR: Stenlille-13

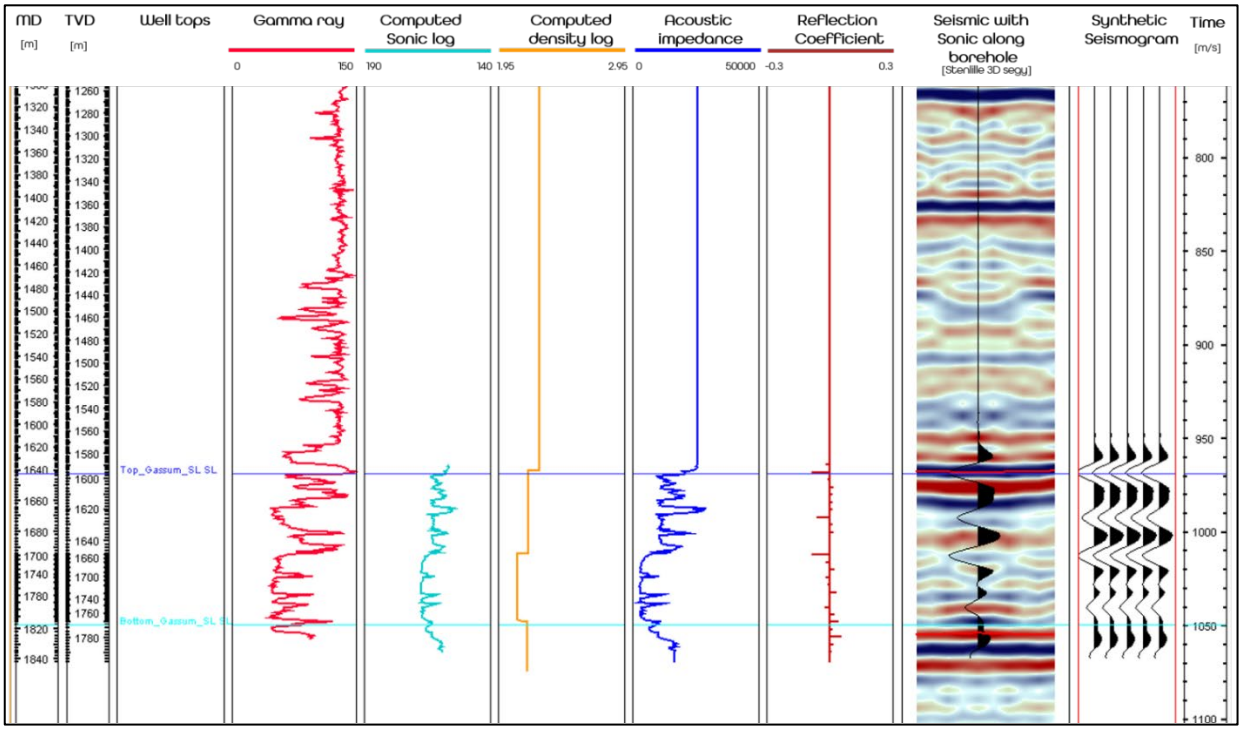

Figure APP1.11: Both sonic and density log were not available for Stenlille-13. Sonic was computed using resistivity log and there after density was computed from computed sonic log. Reflection coefficient series along Stenlille-13 was computed using computed sonic log and computed density log and was convolved with ricker wavelet of 45 Hz to generate synthetic seismogram along the borehole.

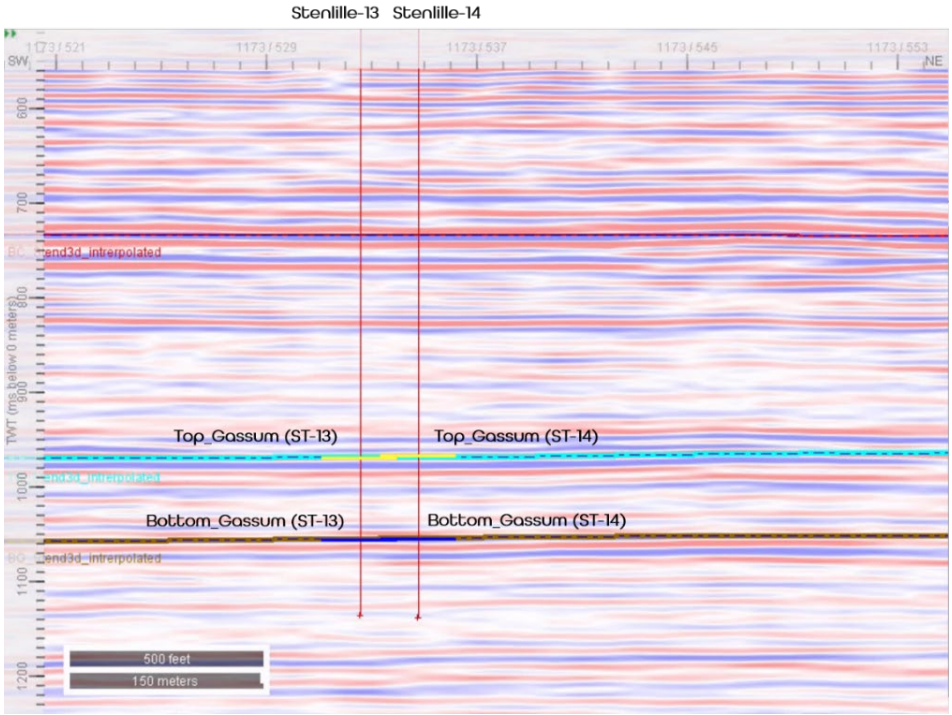

Figure APP1.12: Inline 1173 intersecting Stenlille-13 as well as Stenlille-14. Both well picks i.e. Top Gassum and Bottom Gassum are tied to interpreted seismic horizons for the top and base Gassum.

TDR: Stenlille-15

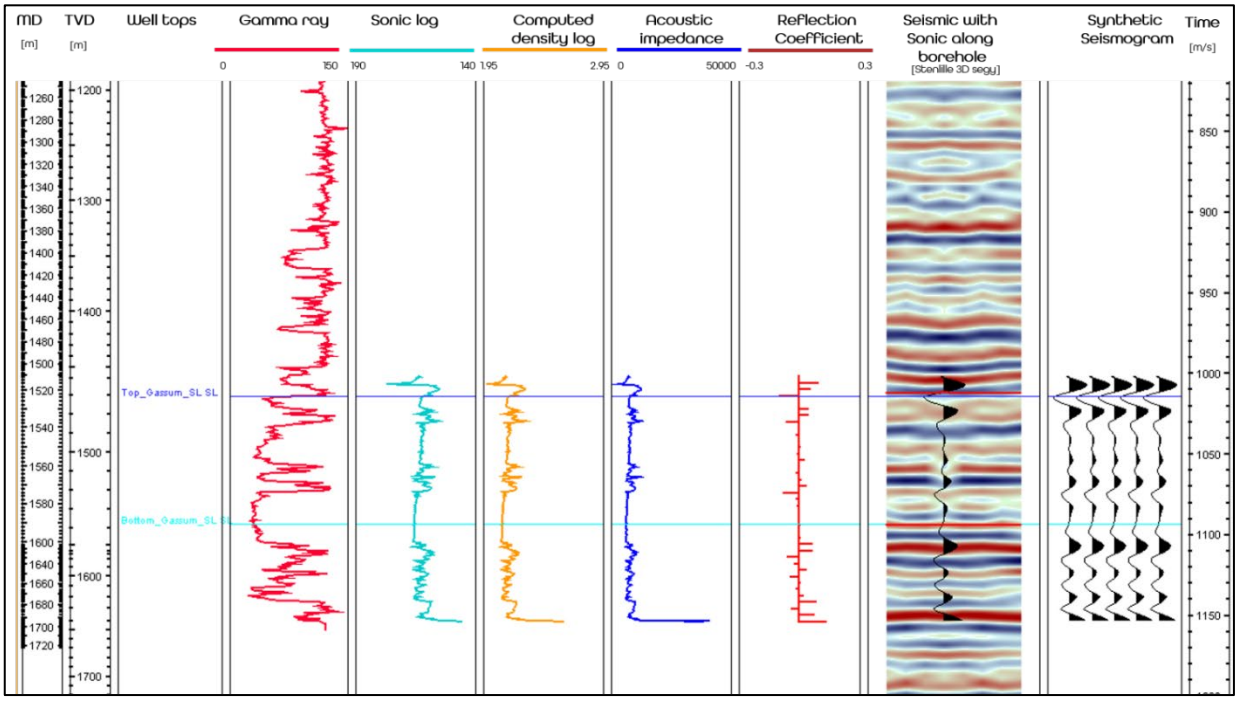

Figure APP1.13: Both sonic and density log were not available for Stenlille 15. Sonic was computed using resistivity log and there after density was computed from computed sonic log. Reflection coefficient series along Stenlille 15 was computed using computed sonic log and computed density log and was convolved with ricker wavelet of 45 Hz to generate synthetic seismogram along the borehole.

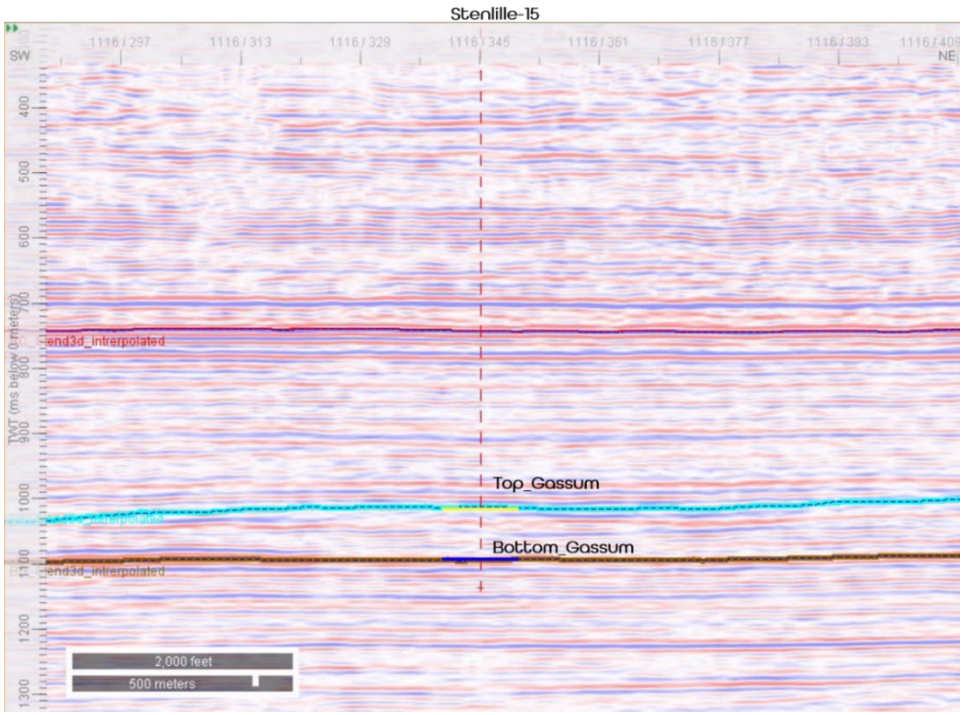

Figure APP1.14: Projection of Stenlille-15 over structural inline 1116 from Stenlille 3D seismic cube. Both well picks i.e. Top Gassum and Bottom Gassum are tied to interpreted seismic horizons for the top and base Gassum.

TDR: Stenlille-18

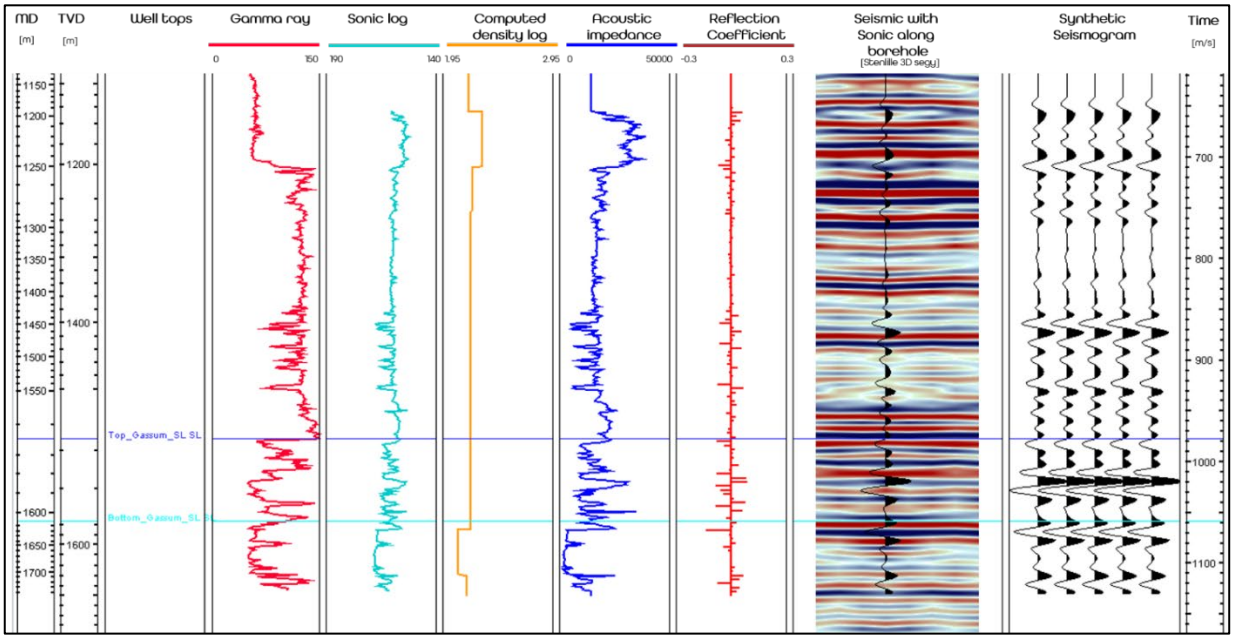

Figure APP1.15: Both sonic and density log were not available for Stenlille 18. Sonic was computed using resistivity log and there after density was computed from computed sonic log. Reflection coefficient series along Stenlille 18 was computed using computed sonic log and computed density log and was convolved with ricker wavelet of 45 Hz to generate synthetic seismogram along the borehole.

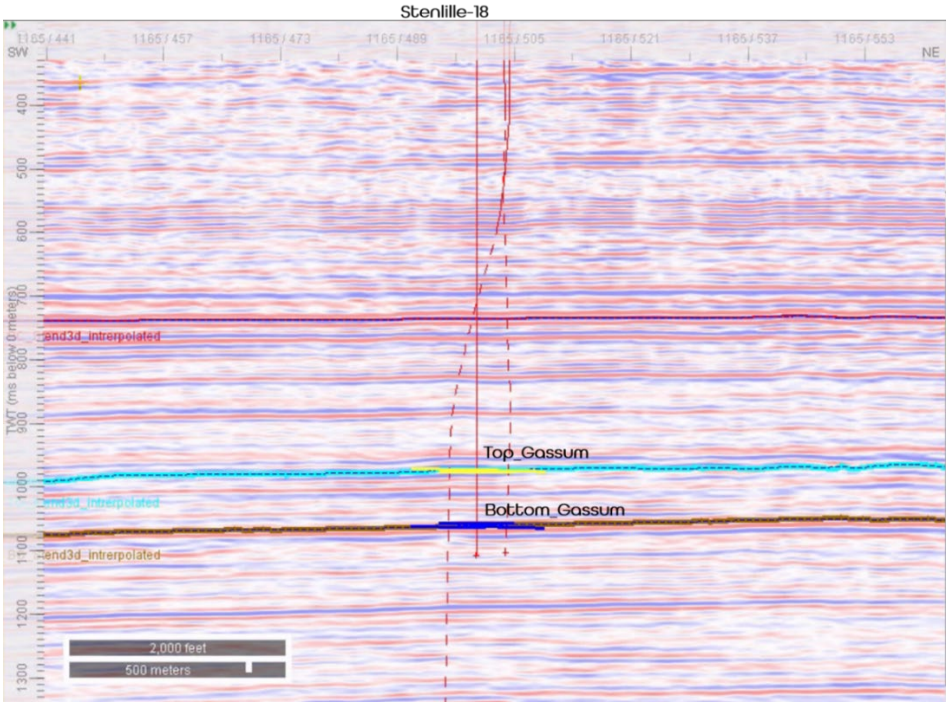

Figure APP1.16: Inline 1165 intersecting Stenlille-18. Projected locations of Stenlille-19 and Stenlille-20 are also visible over the inline. Both well picks i.e. Top Gassum and Bottom Gassum are tied to interpreted seismic horizons for the top and base Gassum.

TDR: Stenlille-19

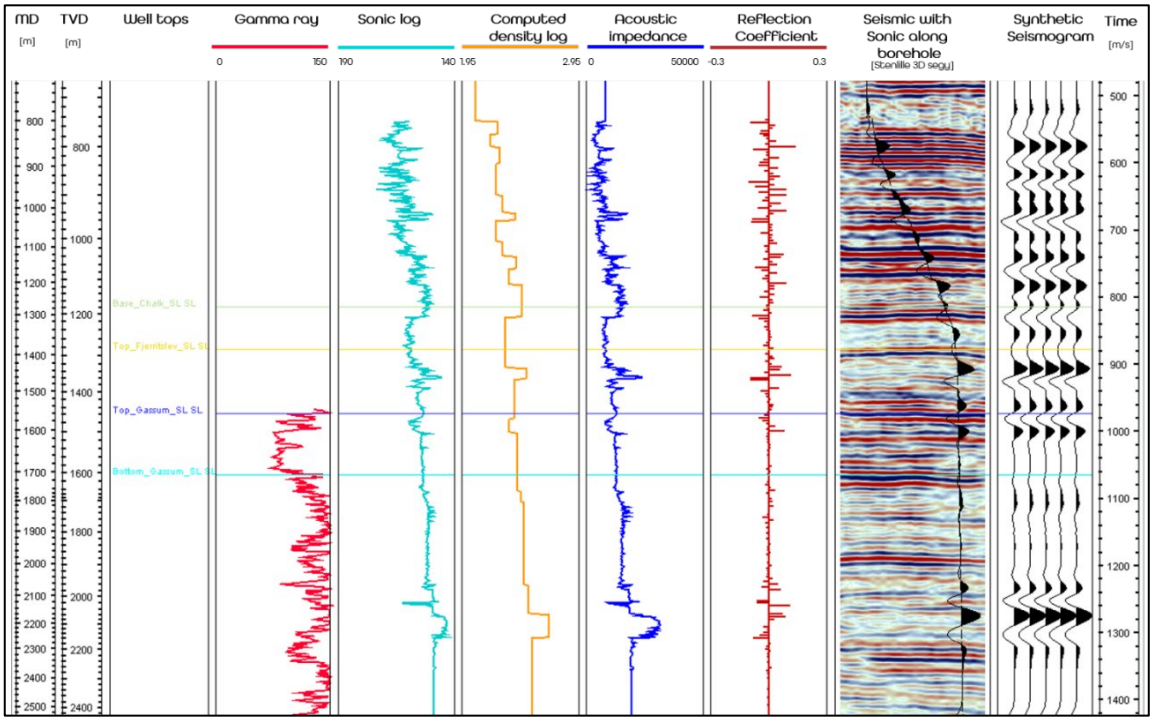

Figure APP1.17: In case of Stenlille-2, sonic log was available, however density log was missing. Sonic log was used to compute the density log using Gardner empirical relationship. Reflection coefficient series along Stenlille-18 was computed using sonic log and computed density log and was convolved with ricker wavelet of 45 Hz to generate synthetic seismogram along the borehole.

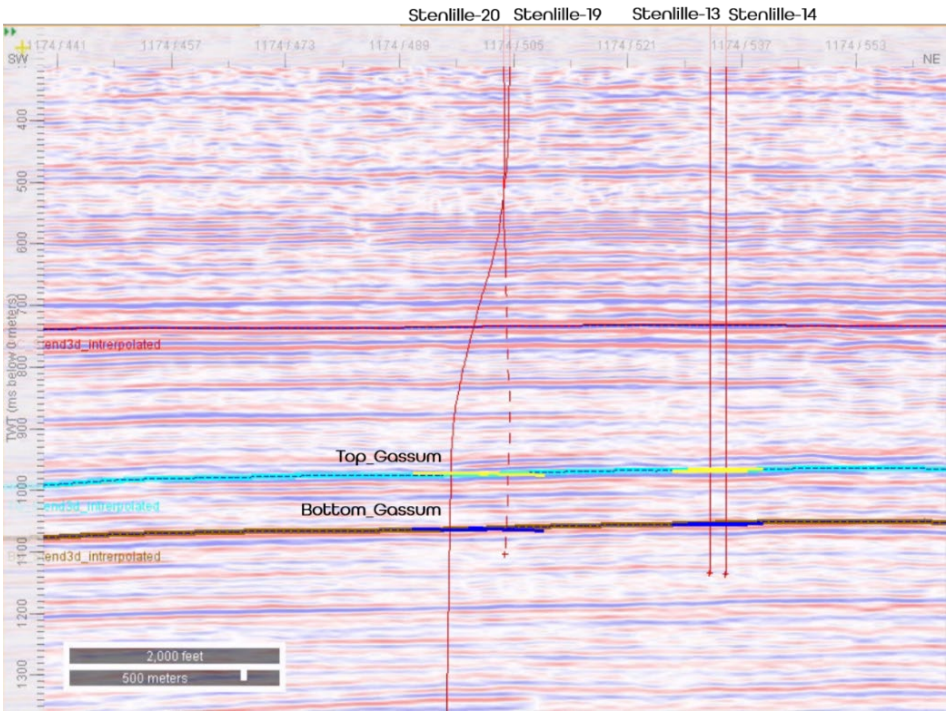

Figure APP1.18: Inline 1174 intersects Stenlille-19, Stenlille-14 and Stenlille-13. The projected location of Stenlille-20 is also visible on this line. Both well picks i.e. Top Gassum and Bottom Gassum seem to have good well tie with their respective interpreted seismic horizons.

TDR: Thisted-1

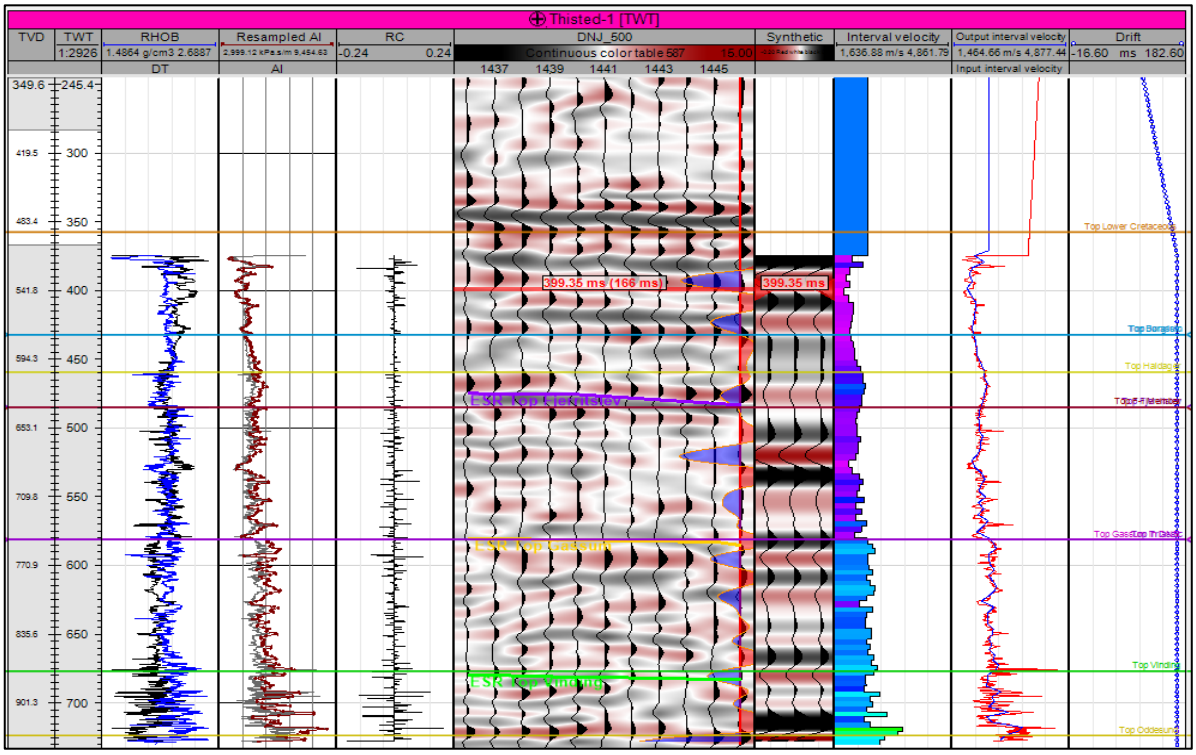

Figure APP1.19: Synthetic seismogram for Thisted-1.

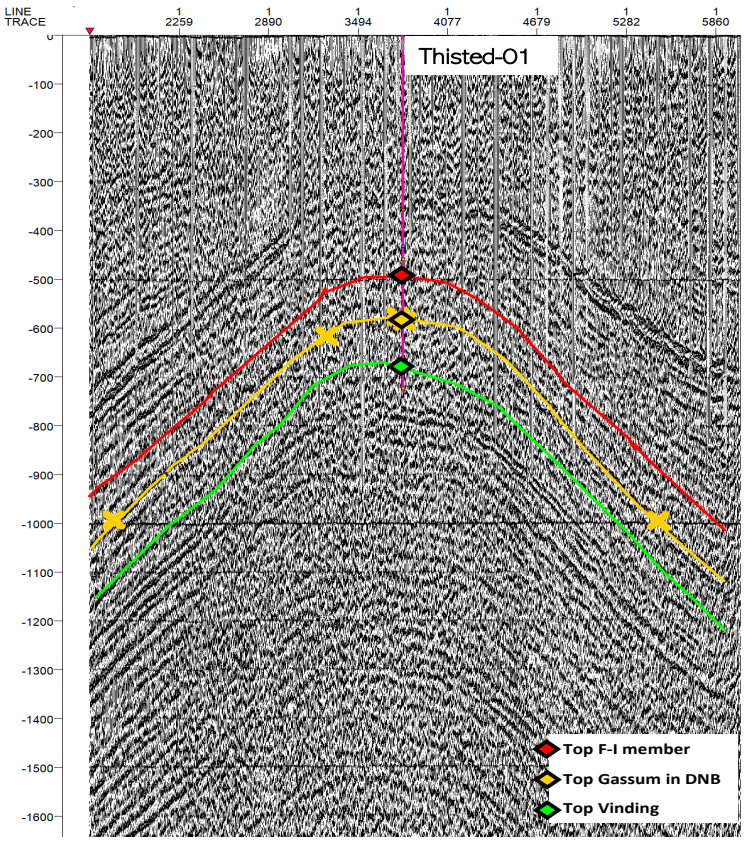

Figure APP1.20: Thisted-1 intersects reprocessed 2D seismic line "ADK85_123 [Realized]". Top F-I-member, Top Gassum Fm. and Top Vinding Fm. all have a very good tie with respective interpreted horizons.

TDR: Thisted-2

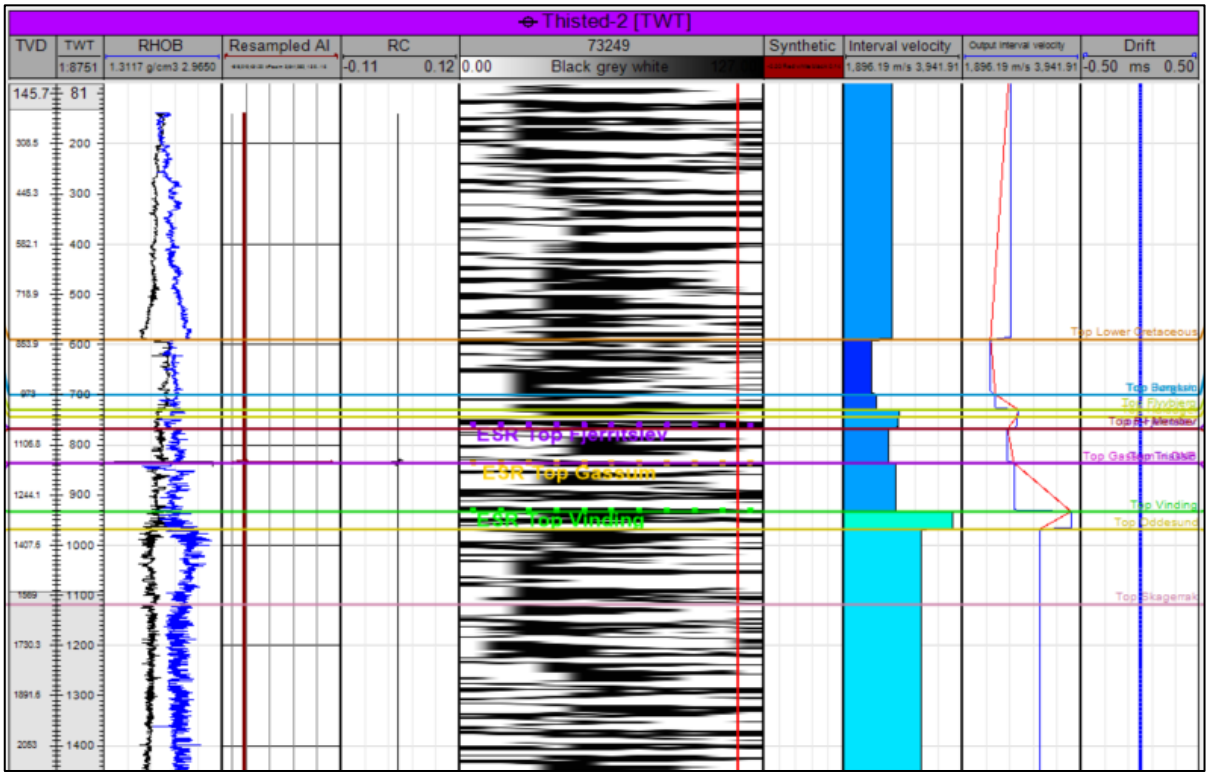

Figure APP1.21: Synthetic seismogram for Thisted-2.

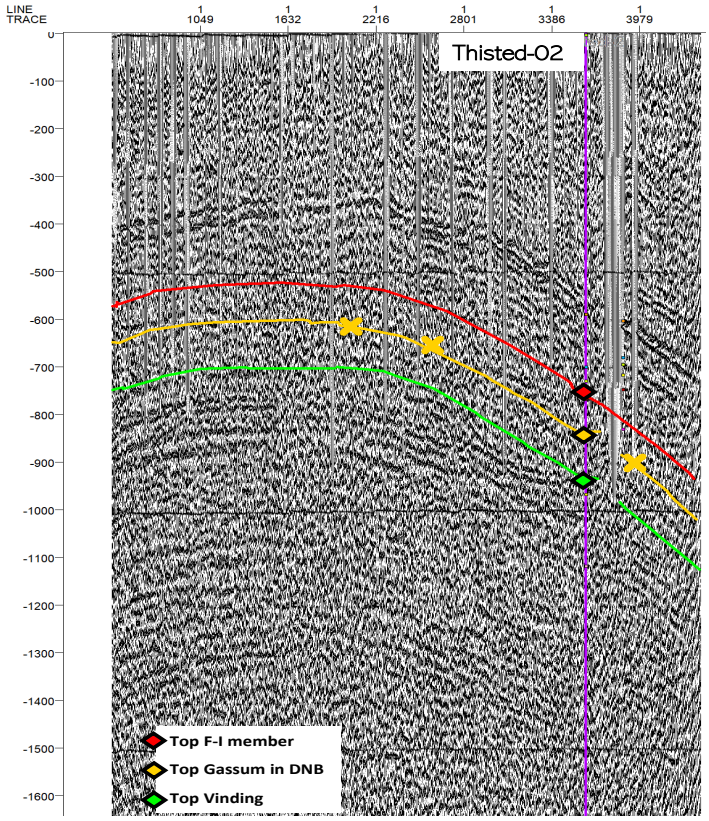

Figure APP1.22: Thisted-2 intersects reprocessed 2D seismic line "73249". Top F-I-member, Top Gassum Fm. and Top Vinding Fm. all have a very good tie with respective interpreted horizons.

TDR: Thisted-3

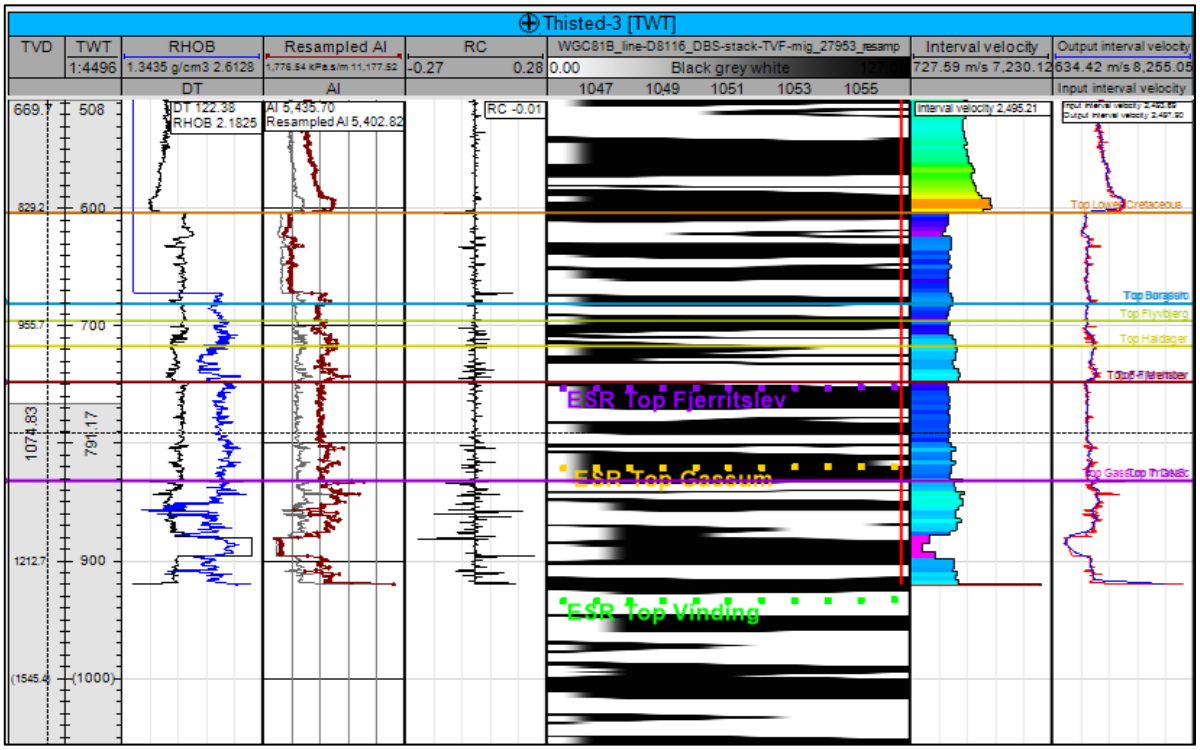

Figure APP1.23: Synthetic seismogram for Thisted-3.

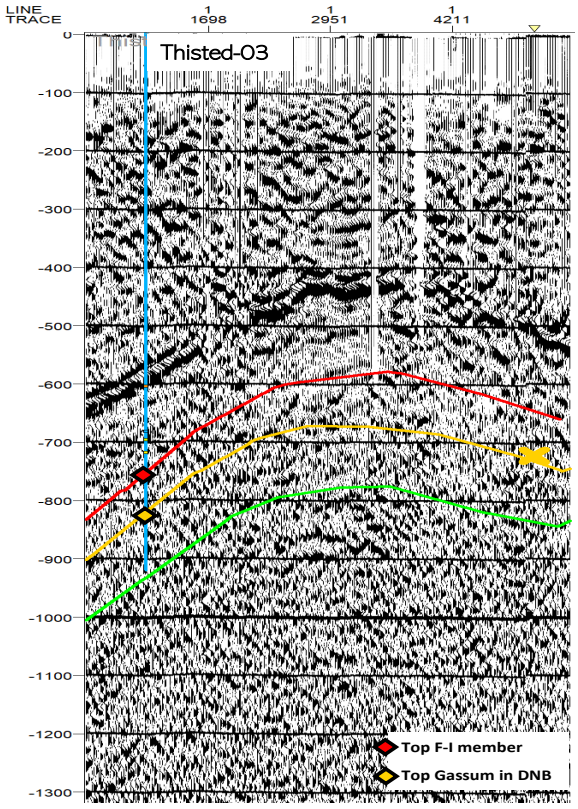

Figure APP1.24: Thisted-3 intersects reprocessed 2D seismic line "WGC81B_line-D8116_DBS-stack-TVF-mig_27953_resamp". Top F-I-member and Top Gassum Fm. have a very good tie with respective interpreted horizons.

TDR: Thisted-4

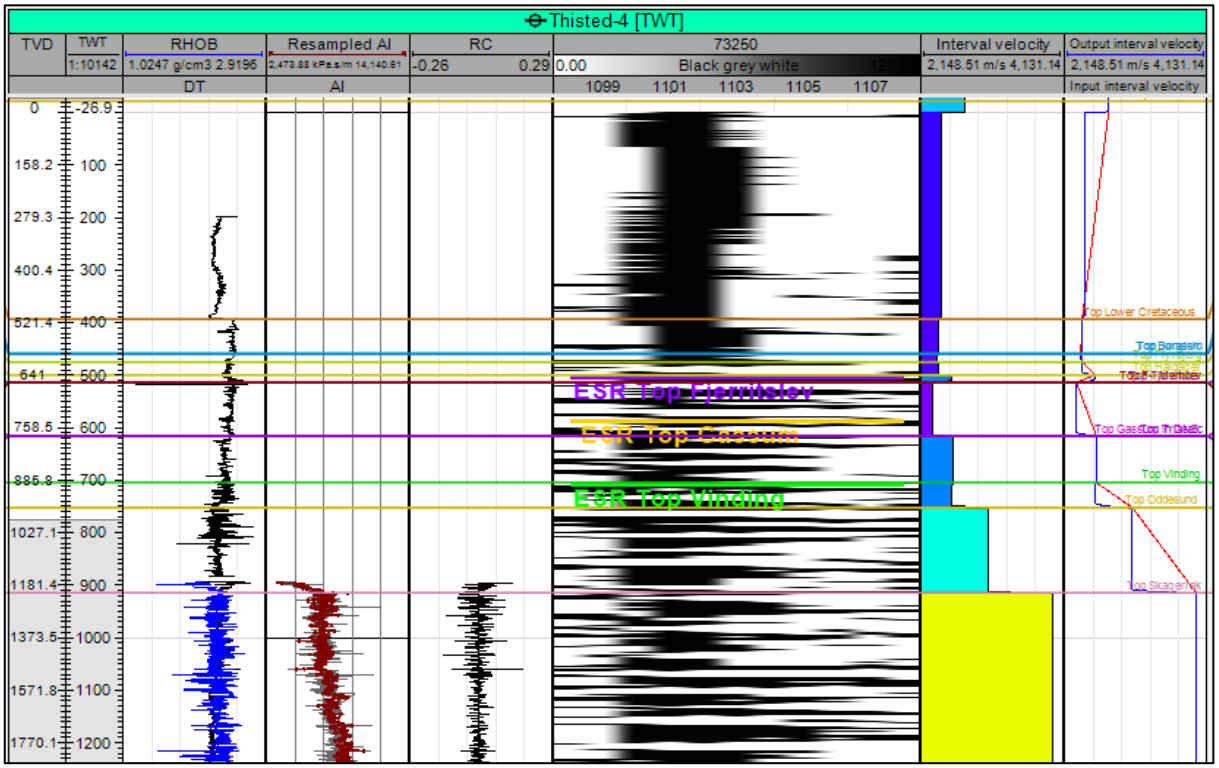

Figure APP1.25: Synthetic seismogram for Thisted-4.

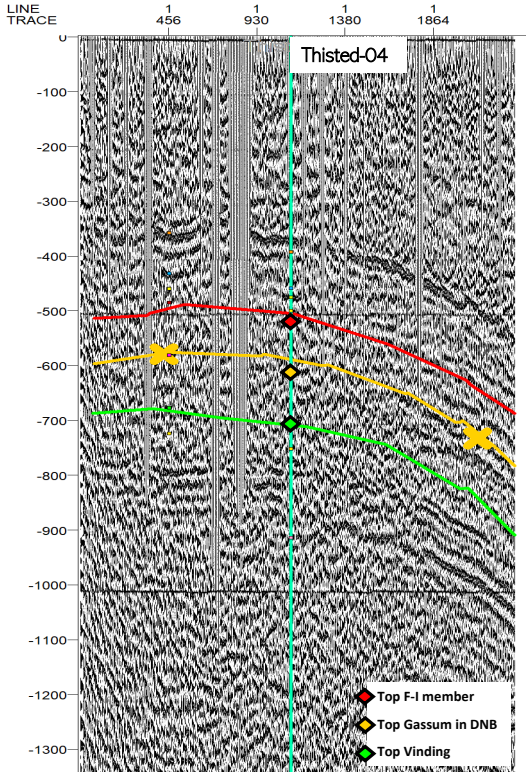

Figure APP1.26: Thisted-4 intersects reprocessed 2D seismic line "73250". Top F-I-member, Top Vinding Fm. has a very good tie with interpreted Top Vinding horizon. Top F-I-member and Top Gassum has slight mis-tie with their respective interpreted horizons.

Appendix 2 Time maps (ms TWT)

Please note that the maps called ‘Depth maps (TWT)’ are Top structure time maps (ms TWT). The maps are from Havnsø area (Gregersen et al 2020) and Hanstholm area (Rasmussen & Laghari 2020), see here for information on gridding algorism and tie to wells.

Base Chalk Group - Depth map (TWT)

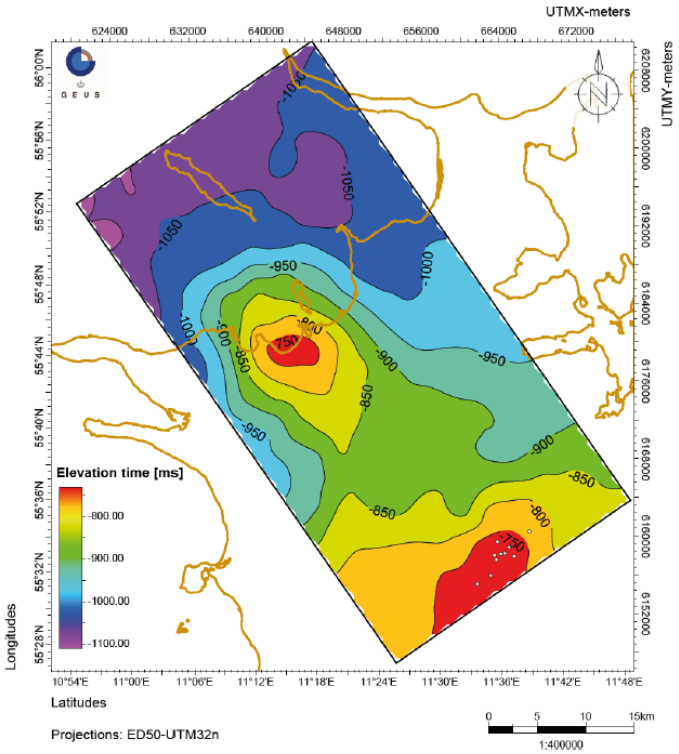

Top Fjerritslev Fm. - Depth map (TWT)

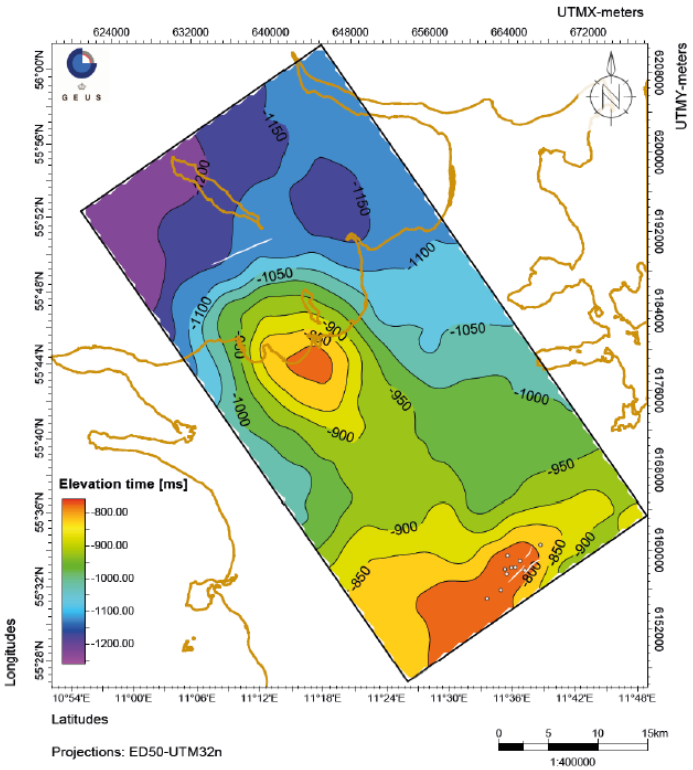

Top Gassum Fm. - Depth map (TWT)

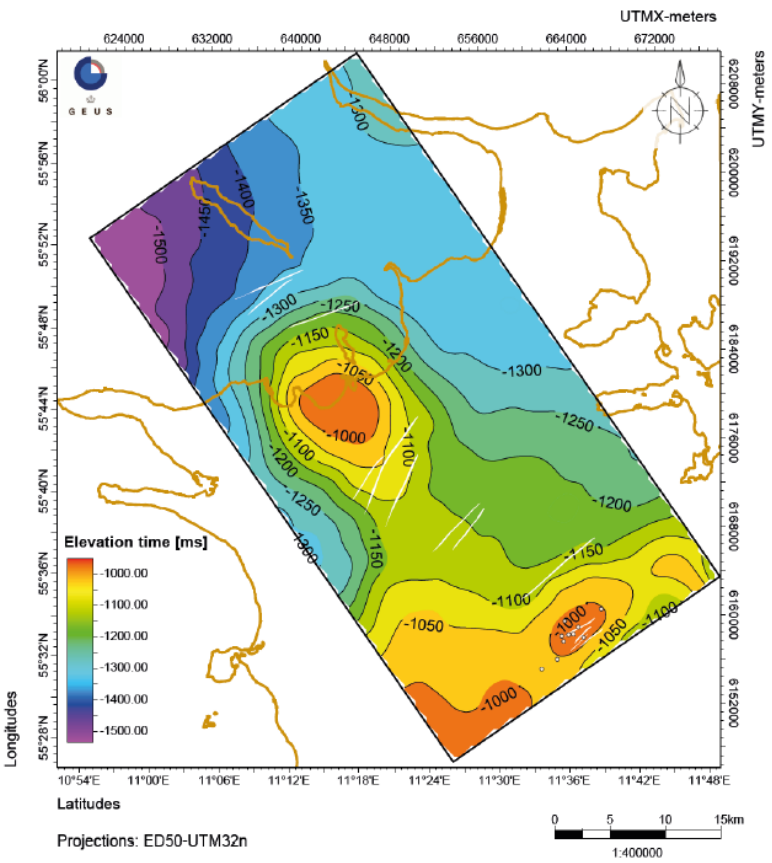

Base Gassum Fm. - Depth map (TWT)

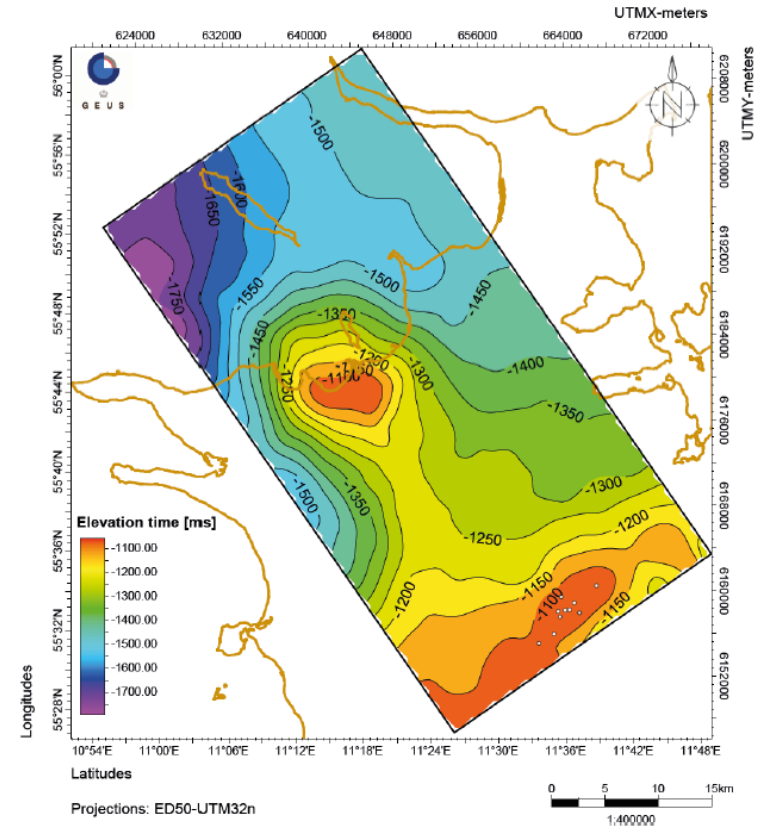

Fjerritslev Fm. - Thickness map (TWT)

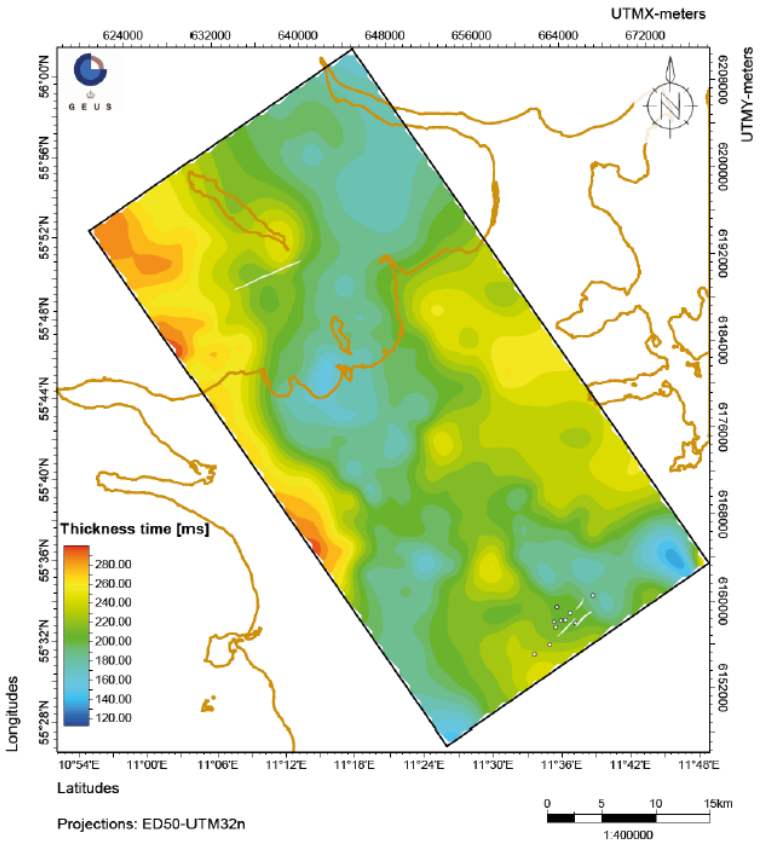

Gassum Fm. - Thickness map (TWT)

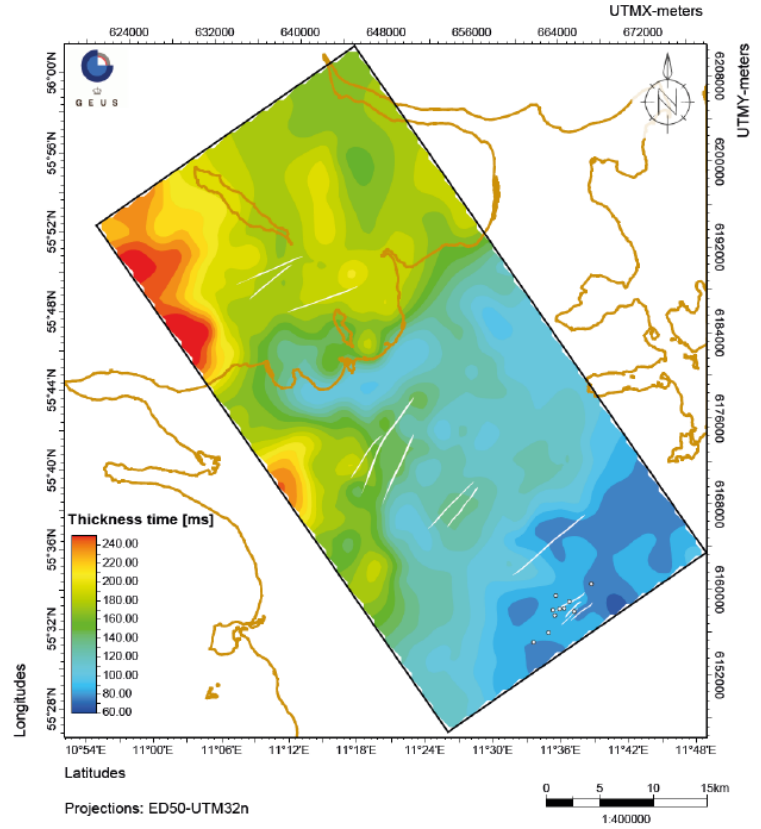

Top Fjerritslev Fm. - Depth map (TWT)

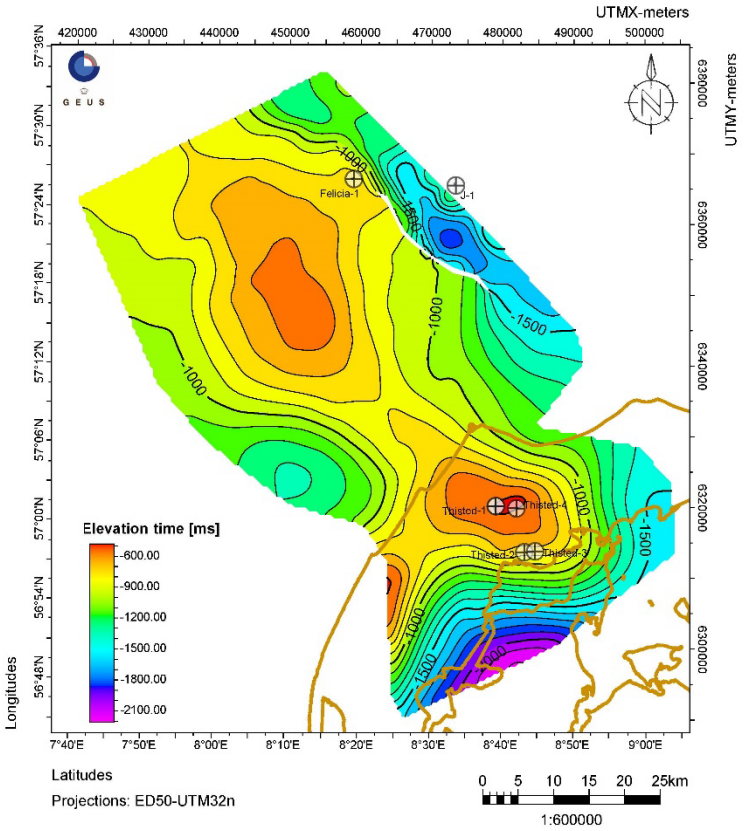

Fjerritslev Fm. - Thickness map (TWT)

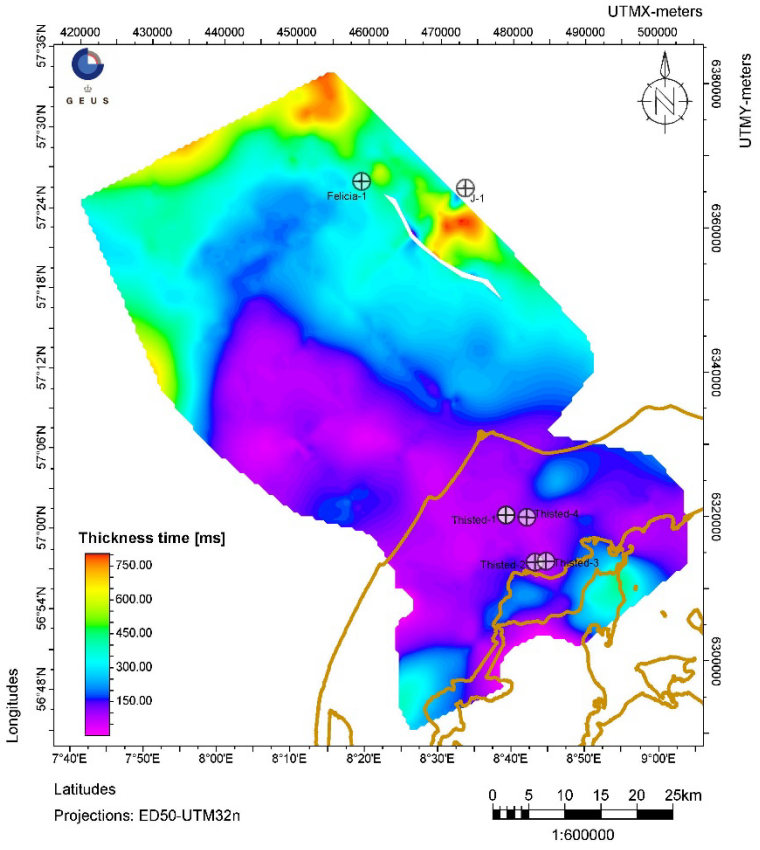

Top Gassum Fm. - Depth map (TWT)

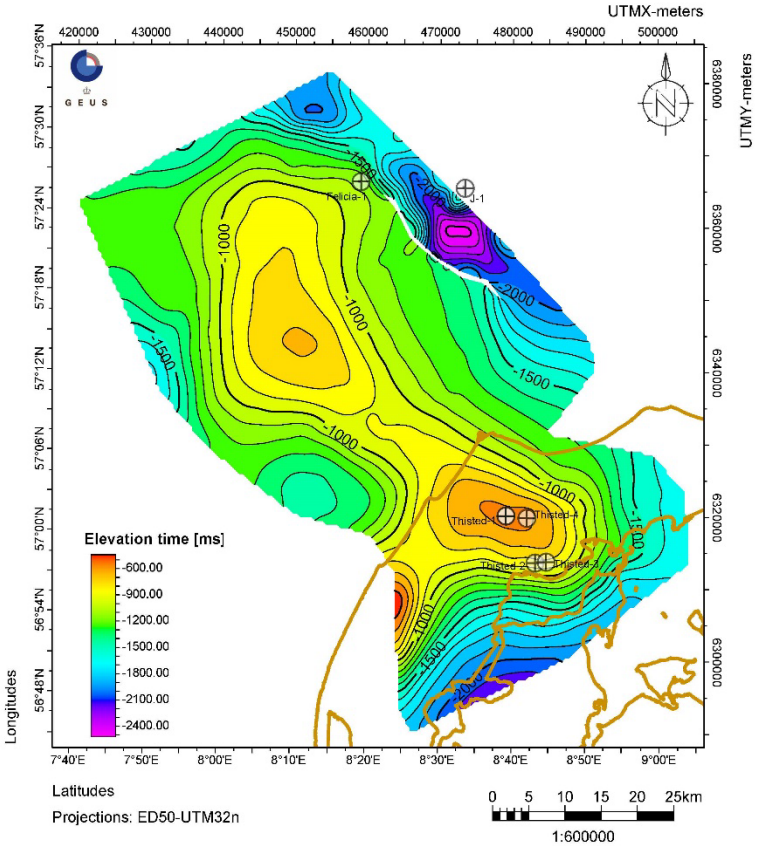

Top Vinding Fm. - Depth map (TWT)

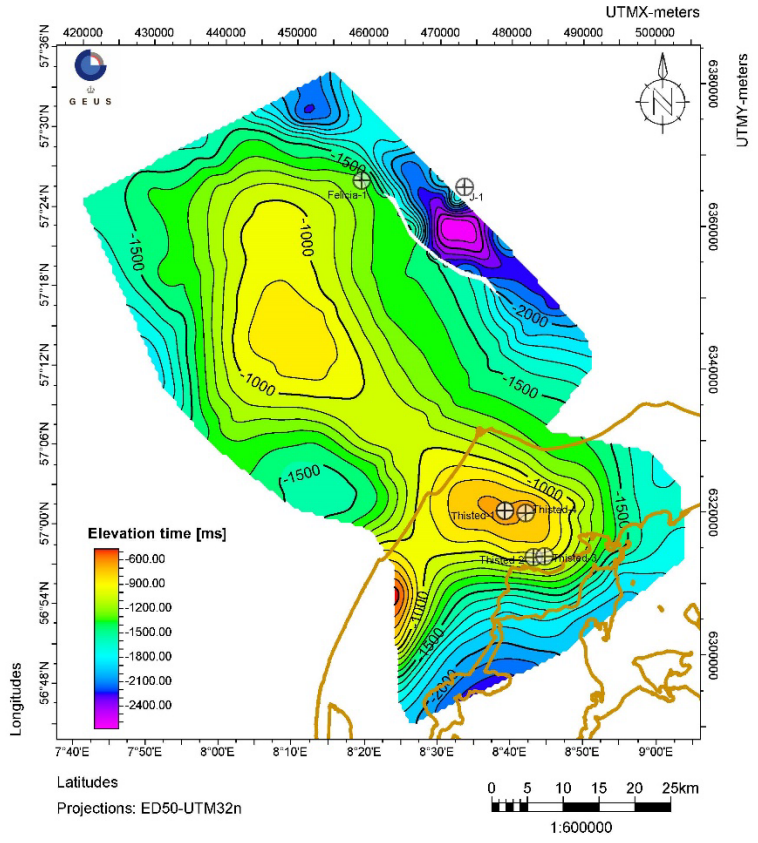

Gassum Fm. - Thickness map (TWT)

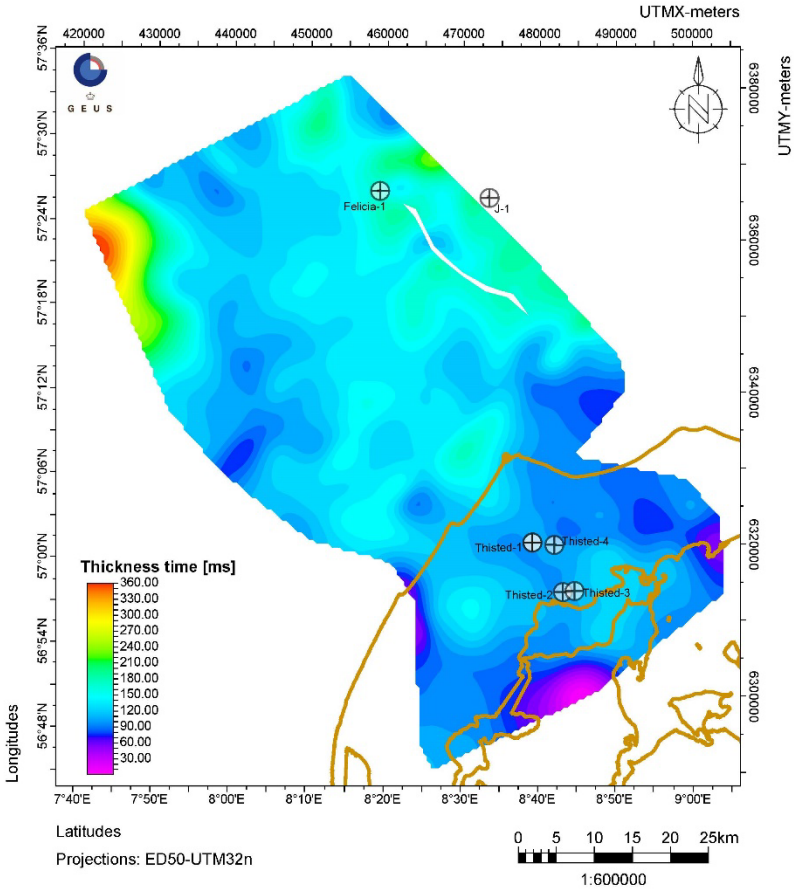

Danish Ministry of Climate,
Energy and Utilities

Geological survey of
Denmark and Greenland (GEUS)

Øster Voldgade 10
DK-1350 Copenhagen K
Denmark

GEUS is a research and advisory
institution in the Danish Ministry
of Climate, Energy and Utilities